RM No. L8H13

NACA

RESEARCH MEMORANDUM

THEORETICAL AND EXPERIMENTAL ANALYSIS OF LOW-DRAG SUPERSONIC INLETS HAVING A CIRCULAR CROSS SECTION AND A CENTRAL BODY AT MACH NUMBERS OF 3.30, 2.75, AND 2.45

By

Antonio Ferri and Louis M. Nucci

Langley Aeronautical Laboratory
Langley Field, Va.

NATIONAL ADVISORY COMMITTEE FOR AERONAUTICS

WASHINGTON

November 10, 1948

Classification cancelled (or changed to UNCLASSIFIED)

By Authority of NASA Tech Pub Announcement #44
(OFFICER AUTHORIZED TO CHANGE)

12 Jan 63

By

(GRADE OF OFFICER MAKING CHANGE)

12 April
DATE

NACA RM No. I8H13

NATIONAL ADVISORY COMMITTEE FOR AERONAUTICS

RESEARCH MEMORANDUM

THEORETICAL AND EXPERIMENTAL ANALYSIS OF LOW-DRAG SUPERSONIC INLETS HAVING A CIRCULAR CROSS SECTION AND A CENTRAL BODY AT MACH NUMBERS OF 3.30, 2.75, AND 2.45

By Antonio Ferri and Louis M. Nucci

SUMMARY

A discussion of inlets having a circular cross section and a central body, designed for high Mach numbers, has been made. The optimum proportion between external and internal supersonic compression has been discussed in relation to the external drag and the maximum pressure recovery. Practical design criteria have been given. Tests of inlet configurations designed with the criteria previously discussed have been presented for Mach numbers of 3.30, 2.75, and 2.45. Values of maximum pressure recovery and shadowgraphs for different combinations of central body and cowling shapes and for different positions of central body relative to cowling have been given. The results of the tests have been analyzed from the aerodynamical point of view. The results show that with the proper selection of geometrical and aerodynamical parameters high pressure recovery and low drag can be obtained. Pressure recoveries of 0.57, 0.67, and 0.78 at Mach numbers of 3.30, 2.75, and 2.45, respectively, have been obtained with very low external drag.

INTRODUCTION

In the design of supersonic inlets for ram jets and turbojets, two parameters are of fundamental importance: the maximum pressure recovery obtainable from the inlet for a given Mach number and the drag due to the aerodynamical phenomena of the inlet.

The relative importance of the two parameters depends on the practical application being considered. Therefore, an exact discussion of the optimum inlet design is not possible. However, in general, it is possible to show that the drag due to the deceleration of flow from high speeds to low speeds becomes more important when the free-stream Mach number increases.

Usually for ram-jet burners and turbojet compressors, the flow must be decelerated to speeds of the order of 0.2 to 0.3, the speed of sound. Therefore, at low free-stream supersonic Mach numbers of 1.4 to 2.0, the

maximum cross section of the stream tube is at the burner or the compressor. (For the turbojet the actual speed in front of the compressor is usually higher, but the total cross section considering also the central part of the compressor corresponds to Mach numbers of the order of those considered.) For this reason, an external shock drag always exists regardless of the type of inlet considered. Thus the external shock drag can be efficiently used for the compression of the flow which goes into the inlet. In the range of Mach numbers between 1.4 and 2.0, it is usually possible to design any particular type of inlet without any large difference in external drag (reference 1). Therefore, the parameter of external drag is not of primary importance in selecting the type of inlet. However, it is important that the aerodynamic design of the inlet be made correctly. This conclusion depends essentially on the fact that, in the Mach number range considered, a given external drag must exist and the supersonic deceleration of the flow can produce only a small increase in pressure along the boundary of the stream tube which goes into the inlet. Therefore, the compression and subsequent shock that can be produced in the flow by the entering stream tube cannot be too large. This compression is of the same order as the increase in pressure and corresponding shock necessary at the lip of the cowling to have an aerodynamically good shape for the body which contains the ram jet or turbojet.

In this lower Mach number range, supersonic inlets with a large part or all supersonic external compression are considered very good because the maximum pressure recovery which can be obtained is higher than for other types of inlets; and with good aerodynamical design, the increase in external drag due to external compression can be reduced or neutralized.

The increase in pressure recovery in this range is useful for two reasons: (1) the thrust per unit mass flow increases; (2) for a constant mass flow the size of the burner decreases because the density in front of the burner is higher. When the size of the burner decreases, the external diameter of the ram jet or turbojet decreases, and thus the over-all drag is less.

As the value of the free-stream Mach number increases, the consideration of drag connected with the inlet becomes more important. Indeed, the external shape of the body tends in many cases to approach a cylinder; therefore, the minimum necessary shock drag produced by the external shape of the body which contains the ram jet or turbojet decreases greatly and can approach zero. However, the drag which can be produced by the aerodynamic phenomena due to the external compression of the flow which enters the inlet increases greatly as the Mach number increases. Therefore, the differences in external drag between different types of inlets can be very large. The increase in drag produced by a large external compression is due to the large increase in pressure and to the correspondingly large deviation of the stream direction at the lip of the cowling. The deviation of the stream requires a large inclination

[redacted]

of the lip of the cowling with respect to the undisturbed stream; therefore, the ratio between the maximum cross section of the body which contains the inlet and the cross section of the free-stream tube must be large. Now, for a constant velocity in front of the burner or compressor and constant cross section of the burner or of the compressor, the free-stream tube increases when the free-stream Mach number increases; therefore, for Mach numbers greater than those previously considered, the maximum cross section of the ram jet or turbojet occurs at the entrance of the inlet and not at the burner or at the compressor. In this case, an increase of pressure recovery no longer permits a decrease in the size of the body that contains the turbojet or ram jet but in some cases requires an increase of body diameter. In this range of Mach numbers, the drag is a fundamental parameter in the selection of an inlet.

In order to give an idea of the changes which occur when the Mach number increases, a comparison has been made between inlets having all external compression and all internal compression for free-stream Mach numbers equal to 1.6 and 3.0. For $M = 1.6$ the pressure recovery which can be expected for an inlet with internal compression is of the order of 0.87 (reference 2), whereas for an inlet with all external compression the pressure recovery can be of the order of 0.94 (reference 1). If the cross-sectional areas of the free-stream tubes are assumed as the areas of reference and are considered equal for both cases, then the maximum cross section of the burner fixing the Mach number in front of the burner at $M = 0.3$ is 1.87 the cross section of the free-stream tube for the case with internal compression and 1.73 the cross section of the free-stream tube for the case with external compression. An 8 percent decrease in maximum cross section of the burner is obtained for the inlet with external compression.

If the frustum of a right circular cone having a 6° half angle is assumed as the external shape of an inlet with internal compression (fig. 1), the pressure coefficient at the lip of the cowling is $P = 0.192$ and becomes of the order of 0.053 at some distance from the lip. Assuming $M = 1$ at the entrance of the inlet, the inclination of the lip for the inlet with external compression becomes of the order of 14°, and, therefore, the pressure coefficient becomes $P = 0.62$. However, along the surface the pressure coefficient decreases very rapidly to zero and the drag of the two inlets is of the same order of magnitude (reference 1).

Assuming a pressure recovery of 0.49 at a Mach number of 3.0 and fixing the Mach number in front of the burner at $M = 0.30$, the cross section of the burner is 0.981 of the cross section of the free-stream tube (fig. 2). Therefore, the external shape of the ram jet or turbojet can be cylindrical of the same diameter as the free-stream tube and for the inlet with all internal compression the shock drag can be zero. If the speed in front of the burner or compressor decreases somewhat, the maximum cross section of the ram jet or turbojet increases but still is of the same order of magnitude as the cross section of the free-stream tube.

[redacted]

When an inlet with all external compression is considered for the same Mach number, the deviation of the lip of the cowling must be of the order of 33° if the external shock is at the lip of the cowling, and, therefore, the pressure coefficient at the lip will be of the order of $P = 1.036$. Therefore even if a very rapid expansion is introduced near the lip, the external drag coefficient will always be very large. Because a deviation of 33° is necessary at the lip, it is apparent that the maximum diameter of the body which contains the inlet (fig. 2) must be larger than the free-stream tube diameter.

For high Mach numbers of the order of 3.0, a compromise must be made between the increase in pressure recovery and the increase in drag. Therefore, it is necessary to determine the pressure recovery for inlets with low external drag in order to have information for the proper selection of inlets.

Directed by these considerations, a preliminary investigation was conducted in the Gas Dynamics Section of Langley Aeronautical Laboratory in order to determine the optimum pressure recovery which could be obtained for low-drag inlets in the range of Mach number between 3.30 and 2.45. This determination permits a comparison of these inlets with inlets designed primarily with the criterion of obtaining very high pressure recovery (references 3 and 4) with no consideration for reducing the external drag. The inlets investigated were nose inlets with partially external and partially internal supersonic compression. They were designed after a preliminary analysis of the conditions required in order to have low external drag. In these inlets, compression through a conical flow is used to obtain external compression. Different values of cone angle, central-body diameter, cowling shape, and central-body position relative to the cowling were included in the tests. The results provide a good aerodynamic design of the inlet for every practical case, because in practical applications the maximum diameter of the body which contains the ram jet or turbojet is given. When the external diameter of the body and the size of the free-stream tube of the entering flow are known, the minimum possible external drag which must be incurred can be evaluated. The proportion between internal and external diffusion used in the inlet can be determined with the criterion of producing a drag of the same order as the minimum drag fixed by the ratio between diameter of the free-stream tube and the maximum diameter of the body.

SYMBOLS

M	Mach number
p	free-stream static pressure
p_1	local static pressure

q	free-stream dynamic pressure
P	pressure coefficient $\frac{p_1 - p}{q}$
p_o	total pressure of free stream
p_f	total pressure after diffusion
p_f/p_o	pressure recovery
D_B	maximum diameter of central body
D_L	entrance diameter of cowling
D_B/D_L	central body diameter ratio
ϵ	shock wave angle
θ_c	semicone angle of central body
θ_l	cowling position parameter (angle between axis of diffuser and line joining apex of cone to lip of cowling)
θ_l^*	cowling position parameter for which conical shock wave attains lip of cowling
θ_{l_c}	cowling position parameter for which the internal contraction ratio corresponds to the value given by one-dimensional theory as the maximum contraction ratio for which the internal diffuser starts at the Mach number at the entrance of the diffuser

AERODYNAMIC CRITERIA USED IN THE DESIGN OF THE INLETS TESTED

In order to obtain high pressure recovery, it is necessary to decelerate the air from the free-stream Mach number to a low supersonic speed with small shock losses and then pass to subsonic velocity with a shock near $M = 1$. The diffusion of the supersonic stream can occur before the stream enters the inlet (external compression) or inside the inlet (internal compression). The external compression is produced by compression waves or shock waves which are generated at the center of the stream and which tend to converge and form only one shock wave. This shock wave can extend beyond the stream tube which enters the inlet, producing a variation of momentum in the external flow, and, therefore, an external drag. In the stream tube entering the inlet, the compression

can be very nearly isentropic, and, therefore, the external compression becomes very efficient.

The internal compression occurs without interference with the outside flow, and, therefore, does not require external drag. The maximum compression which can actually occur depends on the maximum possible contraction of the stream permitted by the starting conditions (reference 2). Inlets with internal compression give very low pressure recoveries for high Mach numbers.

In order to obtain high pressure recovery and low external drag, it is necessary to use external compression. But it is necessary to avoid letting the compression waves produced from the external compression extend to the flow outside the inlet. This condition can be prevented by letting all the compression waves meet the inlet at the lip and then introducing a finite variation in the direction of the stream at the lip (fig. 3(a)). In this case the compression waves are reflected inside the inlet and do not extend to the external flow. This design decreases or eliminates the external drag and permits the use of external compression, which reduces the limitation of the starting condition. However, the maximum value of external compression which can be employed is fixed by the condition of having supersonic flow at the lip of the cowling.

In order to clarify the existence of this limitation, consider the supersonic diffuser shown in figure 3(a). The stream is compressed by compression waves produced along the central body OD. The compression waves meet at A. However, the internal lip angle of the cowling is parallel to the direction of the undisturbed flow; therefore, the compression waves are reflected internally as a shock wave AE from the point A. If the flow at A is supersonic, no interference between the internal and external flow exists, and, therefore, no external shock drag is produced by the internal flow.

Because the reflection that eliminates the deviation of the stream must produce a shock wave of finite strength, the reflection at A is only possible if the maximum deviation corresponding to the Mach number at A behind the compression wave DA is somewhat larger than the deviation which must occur across the shock AE. The maximum possible intensity of the reflected shock at A is determined not only by the condition at A but also by the necessity of reflection of the shock AE at the surface of the central body, point E (fig. 3(a)). Also this condition which will be discussed later requires that the reflected shock AE be of small intensity in order to obtain good pressure recovery. If the lip of the inlet is parallel to the free stream, the maximum external compression which can be used is small because the deviation across the reflected shock at A is equal to the deviation due to the external compression.

The internal compression after the external compression ODA is limited by the starting conditions; therefore, the total compression is far from the isentropic.

In the scheme analyzed, the intensity of the external compression is limited by the intensity of the reflected shock wave at A; therefore, the intensity of the external compression can be sensibly increased if the lip of the cowling is slightly inclined with respect to the free stream (fig. 3(b)). In this case, the intensity of the reflected shock wave AE is reduced. Therefore, the Mach number at A behind the compression waves ODA can be reduced and the external compression increased. A shock wave AG is thereby produced in the external flow which generates external shock drag. Because the external shock drag depends directly on the variation of entropy across the external shock waves, the shock drag can be reduced by producing a rapid expansion along AH in the zone near A that decreases the intensity of the shock AG, thus reducing the drag.

The intensity of the shock which can be accepted practically at A is dependent on external drag considerations, and cannot be fixed with general criteria. In particular, the value selected for the inclination of the lip of the cowling is a function of the ratio between the cross section of the free-stream tube and the maximum diameter of the body which contains the ram jet or the turbojet. Usually in practical applications for free-stream Mach numbers of the order of 3.0 the maximum diameter of the body containing the ram jet or turbojet is slightly larger than the maximum diameter of the body which contains the inlet, and, therefore, an external shock drag must exist. In this case, this external drag can be used in order to increase the intensity of the external compression, and, therefore, the total pressure recovery and a shock wave of some intensity can be accepted at A without increasing the minimum external drag required for the body.

Fixing the lip angle of the cowling so as to permit reflection of the compression waves, it is necessary to design the internal shape of the inlet so that internal supersonic flow can occur.

This condition fixes the value of the maximum contraction ratio which can be used for the internal compression. The contraction ratio which is a function of the Mach number existing behind the external compression can be obtained in the first approximation with one-dimensional criteria given in reference 2.

In order to have supersonic flow inside the inlet independent of the starting conditions, it is necessary that the internal channel be designed with the criteria of permitting the existence of the shock AE (fig. 3(b)). Now the shock AE produced by the lip of the cowling can exist if the shape of the central body at E permits reflection of the shock AE. If the boundary-layer effect is neglected, this condition

can be respected by fixing the lip angle and the shape of the body near E in such a manner that the Mach number and the direction of the flow at E permits the reflection of the shock.

However, the presence of a well-developed boundary layer at E makes the problem more difficult. The reflection at E cannot be exactly determined by theoretical analysis. When the shock AE is strong and the boundary layer before E has undergone a large positive pressure gradient, separation can occur behind the shock which results in a reduction of the geometrical section and choking of the internal diffuser. For this reason, especially when the chosen value of the external compression is small, often it is more convenient to obtain all the compression across a shock wave from the apex of the central body, rather than across gradual compression waves produced along the surface OD, since the compression waves produce a positive pressure gradient that increases the thickness of the boundary layer. The possibility of the reflection can be assured by introducing a local expansion in front of the point of reflection E.

In figure 4 the design of an inlet using this criteria is shown. The figure also gives the flow analysis obtained with the characteristics theory (reference 5). The central body of the inlet has a semicone angle of 25°, and for the design Mach number of 3.301 the shock generated by the cone is reflected at the lip of the cowling. The lip of the cowling has an internal inclination of 4° with respect to the free stream. The Mach number behind the conical shock is 2.3 and the deviation across the conical shock is 17° 51'; therefore, the reflected wave corresponds to a deviation of 13° 51'. The maximum possible deviation for a Mach number of 2.3 is the order of 27°. The difference between maximum deviation of 27° and the deviation used at A is large because the inlet has been designed to have internal supersonic flow also for large angles of yaw for which the assurance of reflection of the shock from the lip at the surface of the central body becomes more critical. The maximum internal diameter of the cowling is 1.052 of the free-stream tube diameter.

The Mach number behind the reflected wave at the lip is 1.76. The reflected wave tends to become stronger near the axis; therefore, in order to permit reflection of the shock from the central body and in order to avoid too large an internal contraction ratio, an expansion is introduced along the central body which accelerates the flow along the surface. A throat of almost constant cross section was added in order to decrease the effect of separation behind the strong shock.

Considering all shock losses of the internal flow, an average theoretical pressure recovery of 0.62 was obtained for this configuration. The experimental values can be expected to be near this value if boundary-layer separation is avoided.

The boundary layer increases the actual internal contraction ratio increasing the efficiency of the internal supersonic compression, but

the losses due to the friction that are not considered in this analysis decrease the efficiency and tend to produce some instability in the flow. In order to eliminate this instability, the shock cannot be at the throat of the internal diffuser, and, therefore, the efficiency of the supersonic compression decreases.

The external shock drag for this inlet has been determined analytically for the same Mach number. The external shape selected and the external shock configuration and pressure distribution are shown in figure 4. The ratio between the maximum external cross section and the free-stream tube cross section is 1.160. The drag coefficient referred to the maximum area of the body which contains the inlet is 0.0081 and becomes 0.0095 if the free-stream tube area is used. The drag of the cowling is small in comparison to inlets with larger external compression. For example, for an inlet with very large external compression (diffuser no. 3, reference 4), using a similar analysis Oswatitsch found for a Mach number of 2.9 an external drag coefficient of 0.43 if the maximum cross section of the inlet is considered and 0.90 if the maximum free-stream tube area is considered. This inlet has a very high pressure recovery but a very high drag, especially if referred to the free-stream tube area, because the ratio between the area of the maximum cross section of the body to the free-stream tube area is of the order of 2.1. This ratio cannot be much smaller since the deviation required at the lip is very large (of the order of 35°).

When the free-stream Mach number in front of the inlet shown in figure 4 is reduced and the internal contraction ratio becomes too large, a strong shock must be expected near the entrance of the inlet, as shown in figure 5. For this condition, the pressure recovery does not decrease greatly because the Mach number behind the conical shock is low, but the external drag increases. However, also in this case the external drag cannot be very large if the diameter of the free-stream tube of the cowling is not much less than the maximum possible diameter of the free-stream tube for the design condition because the external shock decreases in intensity very rapidly due to the expansion around the cowling.

THE MODEL TESTED AND THE EXPERIMENTAL SYSTEM

In order to have some experimental values of pressure recovery which can be obtained with inlets of this kind, models with different geometrical parameters were constructed and tested in an intermittent flow jet. For comparison, an inlet with very large external compression has also been tested.

The general scheme of the model tested is shown in figure 6. The models tested have a central body supported by three equally spaced streamlined struts placed in the subsonic diffuser. The pressure recovery has been determined by nine total-head tubes which permitted a survey

[redacted]

along two radii in the maximum cross section of the diffuser. The static pressure was also determined at two radii in the maximum cross section of the diffuser. The local Mach number at this section in which the pressure recovery was measured was of the order of 0.15 for $M = 3.30$ and 0.2 for $M = 2.45$. The average pressure recovery was obtained by the equation:

$$p_{f_{average}} = \frac{1}{S}\int_{r_1}^{r_2} 2\pi p_{f_{local}} r \, dr$$

where S is the area of the measuring plane, r_1 the radius of the central body, and r_2 the internal radius of the cowling. The back pressure was regulated during the tests by means of a movable plug which was placed on the end of the central body.

The test model was so designed that the shape of the cowling, the shape of the central body, and the position of the central body with respect to the cowling (given by the cowling position parameter θ_l) could be easily changed. The position of the central body was varied by moving the central body axially. Tests were made fixing the position of the central body before the tests (constant geometry diffuser) and a few tests were also made changing the position of the central body and, therefore, the internal contraction ratio during the tests (variable geometry diffuser). This part of the test was not extended because no gains in pressure recovery were obtained by varying the geometry at a fixed Mach number.

All the cowlings tested are shown in figure 7. Four cowling shapes were considered. Three cowlings had internal and external lip angles of $0^\circ,2^\circ$; $4^\circ,7^\circ$; and $7^\circ,10^\circ$; respectively. Because no external drag measurements were considered in this series of tests, only the lip angles and the internal cowling shapes were designed with aerodynamic criteria. The fourth cowling is the cowling used in the inlet with large external compression and was taken from reference 4. The actual shape of the $7^\circ,10^\circ$ cowling tested and given in figure 7 is slightly different from the original design. This difference, due to construction, is localized at the lip and is small. Therefore, the cowling was not remade.

The central body shapes considered are shown in figure 8. The two fundamental parameters considered in the design of the central bodies were the semicone angle θ_c and the maximum diameter of the central body D_B/D_L. The cone angle fixes the intensity of the external compression, and the ratio D_B/D_L together with the cowling position parameter θ_l fixes the internal contraction ratio. The central body of the model with large external compression given in figure 8(d) was

derived also from the data in reference 4. The dimensions of the model in reference 4 were not exactly given; therefore, tests were made for different cowling position parameters.

The models were tested at three Mach numbers of 3.30, 2.75, and 2.45 at zero angle of attack. Some values of internal contraction ratio as a function of cowling position parameter θ_l were calculated in order to obtain an experimental check on the one-dimensional theory for the starting conditions and are shown in figures 9 to 11. The internal contraction ratio has been calculated considering a section perpendicular to the average direction of the stream in the zone considered. In figures 9 to 11, the starting contraction ratio given by one-dimensional theory has been indicated. The corresponding value of the cowling position parameter has been called θ_{l_c}. The cowling position parameter θ_l^* that corresponds to the condition at which the conical shock is at the lip of the cowling has also been indicated.

The models tested had a maximum diameter of approximately 1.83 inches, and the corresponding test Reynolds numbers referred to the maximum diameter were about 3.5×10^6 for $M = 3.30$ and between 3 and 3.5×10^6 for Mach numbers of 2.45 and 2.75. This Reynolds number corresponds to that of a body having a diameter of 2.3 feet at an altitude of 70,000 feet. The test-section jet dimensions were 3×4 inches, approximately. All tests were made in an open jet, using low-humidity air from a large pressurized tank. The pressure readings were recorded photographically from a precision pressure-gage manometer. The maximum possible errors of the measured values are estimated to be of the order of 1 percent.

ANALYSIS AND DISCUSSION OF THE RESULTS

The Maximum Pressure Recovery as a Function of the Cowling Position Parameter

For every cowling and central-body combination considered the figures 12 to 23 give the maximum pressure recovery obtained for different cowling position parameters for the three Mach numbers tested. In order to distinguish the flow configurations for which the flow at the entrance is still supersonic from the configurations for which the flow at the entrance is subsonic (fig. 5), two different symbols have been used in all the figures. The circles indicate points corresponding to configurations having supersonic flow at the entrance of the diffuser, whereas the square symbols indicate points for which the flow in front of the inlet becomes subsonic. The second condition corresponds to a larger external drag. The existence of supersonic or subsonic flow at the entrance of the diffuser was determined by an analysis of the schlieren or shadowgraphs taken during the tests.

[redacted]

In all the figures giving the value of the maximum pressure recovery as a function of the cowling position parameter θ_l, two special values of θ_l are indicated. They are θ_l^* and θ_{l_c} previously defined. The two parameters are important because for values of θ_l less than θ_l^* the conical shock is ahead of the lip of the cowling; therefore, an additive drag exists because the free-stream tube diameter corresponding to the internal flow is smaller than the diameter of the intake (reference 1). This drag must be added to the external cowling pressure drag for determining the total drag. For values of θ_l equal to or larger than θ_l^* for points indicated by the circle symbols the internal flow does not interfere with the external flow, and, therefore, the total drag is equal to the drag along the external surface of the cowling and is small.

The value of θ_{l_c} indicates the position for which the starting conditions of the internal diffuser given by the one-dimensional theory are obtained. Therefore, for values of θ_l larger than θ_{l_c} and smaller than θ_l^* all external supersonic compression (square symbols) is predicted by the one-dimensional theory.

The value of θ_{l_c} has been determined by using the average Mach number between the lip of the cowling and at the surface of the cone, and, therefore, loses significance when the shock is inside the lip. In a few configurations expansion waves are produced in front of the entrance of the inlet by the central body. In the determination of the value of θ_{l_c} the expansion waves for these few cases have not been considered.

For all the tests if the mass flow is decreased somewhat below the maximum possible value by throttling in the rear of the diffuser, an unstable condition is attained and strong vibrations are found in the flow. These types of vibrations exist in all types of models tested when the flow is choked in the rear of the diffuser and have also been found previously by references 3 and 4.

The vibration regime corresponds to a fluctuation of the frontal shock and a variation of the internal mass flow. These vibrations do not exist when the flow at the entrance of the diffuser is subsonic for starting reasons and the mass flow is the maximum possible, but appear also in this case when the mass flow is decreased by a large amount. Some variation of Reynolds numbers does not affect the phenomenon of vibration.

Figure 12 gives the values of the maximum pressure recovery as a function of θ_l for $\frac{D_B}{D_L} = 0.733$, 0.834, and 0.867 for $\theta_c = 20^\circ$. For $\frac{D_B}{D_L} = 0.733$ (fig. 12(a)) the internal contraction ratio is small, and, therefore, internal supersonic flow can exist for all Mach numbers. Therefore, the external drag is small, and the additive

drag is zero for θ_l equal approximately 33° or larger for all the test Mach numbers. The value of the pressure recovery is low. If the diameter of the central body increases (figs. 12(b) and 12(c)) the pressure recovery increases until the internal contraction ratio becomes too large and supersonic compression is all outside.

The maximum pressure recovery obtained for the 20° cone and 4°,7° cowling is about 0.71 for M = 2.45; 0.63 for M = 2.75; and 0.54 for M = 3.30.

Figure 13 gives the maximum pressure recovery obtained for $\theta_c = 20°$ and the 7°,10° cowling for $\frac{D_B}{DL} = 0.719$, 0.817, and 0.850. The results are similar to those obtained for the 4°,7° cowling. The maximum pressure recovery obtained for M = 3.30 for $\frac{D_B}{D_L} = 0.850$ is 0.54 (fig. 13(c)). The internal flow is supersonic for a contraction ratio slightly higher than the maximum contraction ratio considered by one-dimensional theory.

Figure 14 gives some results for $\theta_c = 22°$ and the 0°,2° cowling for $\frac{D_B}{D_L} = 0.733$ and 0.767 for M = 2.45. The compression occurs outside of the inlet. The contraction ratio of the configuration tested is larger than the contraction allowed by the starting conditions so that the diffusers do not start.

Figure 15 gives the maximum pressure recovery as a function of the cowling position parameter for $\theta_c = 22°$ and the 4°,7° cowling for $\frac{D_B}{D_L} = 0.733$, 0.767, 0.800, 0.834, and 0.867. The flow at the lip is supersonic for $\frac{D_B}{D_L} = 0.733$ and 0.767 (figs. 15(a) and 15(b)) for the range of all Mach numbers, and maximum pressure recovery values of 0.77, 0.64, and 0.42 are obtained for Mach numbers of 2.45, 2.75, and 3.30, respectively, with very low external drag in all the range tested. If the diameter of the central body increases, the maximum pressure recovery for higher Mach numbers increases, but the range of Mach numbers for which the flow at the lip is supersonic decreases. For $\frac{D_B}{D_L} = 0.80$ pressure recovery values of 0.67 and 0.49 are obtained for Mach numbers of 2.75 and 3.30, respectively (fig. 15(c)), whereas for $\frac{D_B}{D_L} = 0.834$ (fig. 15(d)), the pressure recovery for M = 3.30 is 0.56. If the mass flow is decreased (of the order of 8 percent), a strong shock occurs in front of the lip of the diffuser and the pressure recovery decreases slightly. The values of pressure recovery corresponding to a decreased mass flow are given in figure 15(d) (M = 3.30, square symbols). Increasing the diameter does not increase the pressure recovery (fig. 15(e)).

[redacted]

Figure 16 gives the values of the maximum pressure recovery for $\theta_c = 22^\circ$ and the $7^\circ,10^\circ$ cowling for central-body-diameter parameters of 0.719, 0.752, 0.784, 0.817, and 0.850. For $\frac{D_B}{D_L} = 0.719$, 0.752, and 0.784 (figs. 16(a) to 16(c)) the flow in front of the inlet can be supersonic for all the range of Mach numbers considered. For $\frac{D_B}{D_L} = 0.784$ for supersonic flow at the entrance, maximum pressure recovery values of 0.75, 0.67, and 0.45 are obtained for the three Mach numbers (fig. 16(c)); whereas for $\frac{D_B}{D_L} = 0.850$ (fig. 16(e)), a maximum pressure recovery of 0.57 is obtained for $M = 3.30$. The pressure recovery for $M = 2.45$ for $\frac{D_B}{D_L} = 0.850$ is less than for $\frac{D_B}{D_L} = 0.752$. The flow in front of the inlet is subsonic in both cases, but for $\frac{D_B}{D_L} = 0.850$ θ_l is far from $\theta_l{}^*$ and, therefore, some expansion waves are produced by the central body in front of the lip.

Figures 16(a), 16(b), 16(d), and 16(e) also give some values of pressure recovery for reduced mass flow. The corresponding decrease of mass flow is of the order of 9 percent. For $\frac{D_B}{D_L} = 0.752$ and $M = 2.45$ (fig. 16(b)) the maximum pressure recovery is obtained when the mass flow is reduced and the shock is outside. This and similar data obtained in all the tests show that the losses due to boundary layer and the necessity of internal flow stability are very important from the point of view of pressure recovery. Practically, it is not possible by increasing the back pressure to put the normal shock near the throat, but it is necessary to have supersonic flow in some extent at the divergent diffuser. Tests have been made without varying the back pressure after the internal diffuser has started for inlets having high internal contraction ratios. The maximum pressure recovery that can be obtained in this condition for a Mach number of 3.3 is only slightly less (of the order of 2 or 3 percent) than the maximum that can practically be obtained by increasing the back pressure after the diffuser has started, while the theoretical gain is of the order of 10 percent or larger. The data shown in figures 16(a), 16(b), and 16(e) confirm these results.

Figure 17 gives the results for $\theta_c = 25^\circ$ and $0^\circ,2^\circ$ cowling for $\frac{D_B}{D_L} = 0.733$, 0.767, and 0.800. The flow is subsonic in front of the diffuser in all the range of Mach numbers and cowling position parameters tested because the deviation across the shock is very large ($\delta = 18^\circ$ for $M = 3.3$) and the reflection of the shock from the lip at the surface of the central body is not possible.

[redacted]

Figure 18 gives the results for $\theta_c = 25°$ and $4°,7°$ cowling for $\frac{D_B}{D_L} = 0.733$, 0.767, 0.800, 0.834, 0.847, and 0.867. For $\frac{D_B}{D_L} = 0.733$ and $M = 2.45$ the flow is supersonic in the region of $\theta_l = \theta_l{}^*$. For larger values of D_B/D_L the flow is supersonic only for values of θ_l very far from $\theta_l{}^*$. The maximum pressure recovery in these cases is 0.76 (figs. 18(a) and 18(b)), whereas for subsonic entrance flow a value of 0.80 was obtained (figs. 18(c) and 18(d)).

For $M = 2.75$ the maximum pressure recovery of 0.67 occurs with subsonic flow in front of the inlet for $\frac{D_B}{D_L} = 0.867$ (fig. 18(f)), whereas for supersonic flow at the entrance for $\frac{D_B}{D_L} = 0.800$ the pressure recovery is 0.64. For $\frac{D_B}{D_L} = 0.847$ the supercritical condition has not been determined.

The results of $\theta_c = 25°$ and the $7°,10°$ cowling are given in figure 19 for $\frac{D_B}{D_L} = 0.719$, 0.752, 0.784, 0.817, 0.830, and 0.850. For $M = 2.45$ and $\frac{D_B}{D_L} = 0.719$ a pressure recovery of 0.78 has been obtained for supersonic flow at the entrance. The corresponding values for $M = 2.75$ and 3.30 are 0.60 and 0.42, respectively. At a Mach number of 2.75 and for $\frac{D_B}{D_L} = 0.752$ and 0.784 (figs. 19(b) and 19(c)) the pressure recovery is larger for subsonic flow in front of the inlet than for supersonic flow in front of the inlet. For $\frac{D_B}{D_L} = 0.817$ the maximum pressure recovery at $M = 3.30$ is 0.53. When the mass flow is decreased, the shock jumps outside and the recovery drops to 0.51. As was previously explained, for all cases in which reduced mass flow data are given, the reduction of mass flow must be small and of the order of 10 percent. For larger variations of mass flow, unsteady flow conditions have been found.

Figure 20 gives the results for $\theta_c = 30°$ and the $0°,2°$ cowling for $M = 2.45$ for $\frac{D_B}{D_L} = 0.767$ and 0.800. For these conditions the flow in front of the inlet is subsonic. The contraction ratio is greater than the starting contraction ratio.

The values of pressure recovery for $\theta_c = 30°$ and the $4°,7°$ cowling for $\frac{D_B}{D_L} = 0.733$, 0.767, and 0.800 are given in figure 21. For Mach numbers

[redacted]

of 2.45 and 2.75 the reflection of the shock inside the inlet cannot occur and, therefore, the flow in front of the inlet is subsonic. The reflection can occur for $M = 3.30$. The maximum pressure recovery obtained for $M = 2.45$ is 0.82 and the maximum recovery for $M = 3.30$ is 0.46 (fig. 21(c)).

The results obtained for $\theta_c = 30^\circ$ and the $7^\circ,10^\circ$ cowling are given in figure 22 for $\frac{D_B}{D_L} = 0.719$, 0.752, and 0.784. Because of the smaller intensity of the reflected shock at the lip of the cowling, the inlet can have internal supersonic flow for $M = 2.75$ (fig. 22(b)). At this Mach number the pressure recovery is higher with subsonic flow at the entrance.

Figure 23 shows the maximum pressure recovery as a function of the cowling position parameter for the inlet with large external compression. The inlet never has internal supersonic flow. The maximum pressure recoveries obtained are 0.84, 0.72, and 0.54 for $M = 2.45$, 2.75, and 3.30, respectively.

The analysis of all the curves shows that for θ_l larger than θ_{l_c} and smaller than $\theta_l{}^*$ usually the flow in front of the inlet becomes subsonic in agreement with one-dimensional theory. (See figs. 12(b), 12(c), 13(b), 13(c), 15(b) to 15(e), 16(c) to 16(e), 18(b) to 18(d), and 18(f).) Only in a few cases has a higher contraction ratio than given by one-dimensional theory been found. See, for example, figures 12(b) ($M = 2.75$), 13(c) ($M = 3.30$), 15(c) ($M = 2.75$), 15(d) ($M = 2.75$), and 15(e) ($M = 3.30$). The differences are very small and can be justified by the inaccuracy of determining the stream-tube areas and the Mach number in front of the entrance. For example, the increase in Mach number due to the expansion waves from the central body has not been considered. For some configurations, subsonic flow in front of the entrance has been found when the contraction ratio is less than the starting contraction ratio. In these cases, subsonic flow is due to the impossibility of reflecting the conical field at the lip of the cowling or at the surface of the central body, as was previously discussed. For example, for $\theta_c = 25^\circ$ and the $0^\circ,2^\circ$ cowling (figs. 17(a) to 17(c)) for Mach numbers of 2.45, 2.75, and 3.30, the reflection of the shock is not possible.

Another example is given by the data in figure 19. The diffuser starts at $M = 2.45$, 2.75, and 3.30 for $\frac{D_B}{D_L} = 0.719$, 0.752, and 0.784, while subsonic flow occurs in the zone of θ_{l_c} for $\frac{D_B}{D_L} = 0.817$, 0.830, and 0.850. For these large diameters the diffuser starts for lower

[redacted]

values of θ_l. This phenomena can be explained by the following consideration. For larger values of D_B/D_L the Mach number and the direction of the stream in front of the inlet are closer to the conditions on the surface of the cone. Therefore, the reflection becomes more difficult. However, when the value of θ_l is small, expansion waves are produced by the central body in front of the inlet, thereby increasing the possibility of reflection. The pressure recovery obtained when the flow in front of the lip is subsonic is in some cases larger than the maximum given theoretically by compression across the conical shock and a normal shock in front of the cowling. This result seems strange because also the subsonic diffuser produces some losses. The shadowgraphs of the phenomena discussed later give an explanation of the results. The compression in front of the inlet occurs across a lambda shock produced by the boundary layer at the surface of the cone. Therefore, the shock losses for the compression in front of the inlet are much smaller than across a single normal shock. For supersonic flow in front of the inlet the maximum pressure recovery increases when θ_l increases because the internal contraction ratio increases. When θ_l is larger than θ_l*, the conical shock enters the inlet and expansion waves are produced locally at the lip of the cowling; therefore the increase of θ_l produces an increase of Mach number in front of the inlet together with an increase in contraction ratio. The two variations have opposite effects on pressure recovery. Therefore by increasing θ_l beyond θ_l*, an increase or decrease in pressure recovery can be found. For subsonic flow in front of the inlet when θ_l increases, the pressure recovery tends to decrease because the strong shock moves in the direction of the apex of the cone.

A few variable geometry tests have been made by moving the position of the central body after the supersonic flow into the inlet had been established. The motion of the central body permitted a variation of the internal contraction ratio because the diameter of the entering stream tube, and therefore, the internal contraction ratio, changed. Tests were performed for cone angles of 20°, 22°, and 25° for the 4°,7° and 7°,10° cowlings at Mach numbers of 2.45 and 3.30 for different central body diameters. No difference in the value of the maximum pressure recovery has been found. The impossibility of obtaining higher pressure recovery with this scheme can be attributed to the disturbances in the subsonic region, which fixes the value of the practical minimum Mach number in the divergent region of the diffuser in order to have stable conditions.

However, the possibility of a small regulation of the position of the central body can be very important in practical applications for two reasons. The motion of the central body permits the changing of the internal contraction ratio, and, therefore, permits the use of the best possible configuration at every Mach number. The best configuration can be the configuration of minimum drag or highest pressure recovery. For

example, in figure 16(e) the optimum θ_l for $M = 3.30$ is about 31°, whereas for $M = 2.45$ and 2.75 the optimum θ_l is 29.5°.

For a given Mach number a movement of the central body permits a regulation of the dimension of the internal stream tube diameter and thus permits supersonic flow at the entrance also for reduced mass flow. For example, from figure 19(f) by changing θ_l from 33.4° to 31.5°, a 14-percent reduction in mass flow can be obtained with internal supersonic flow. The motion of the central body would be 0.015, the diameter of the cowling. Such a regulation of mass flow can be very useful in order to meet the desired flight requirements. Some of the configurations have been tested at small angles of attack (1° and 2°) and no changes have been found in the values of pressure recovery.

The Effect of the Cone Angle Parameter on the Maximum Pressure Recovery Obtained

The figures 12 to 22 give the maximum pressure recovery obtained for the Mach numbers considered for every central body diameter and cowling tested. The maximum values obtained for given values of D_B/D_L, Mach number, and cowling have been plotted in figures 24 to 26 as a function of the cone semiangle. Every point on the curves corresponds to a different cowling position parameter whose values can be determined from figures 12 to 22.

Figure 24 gives the value of the highest pressure recovery obtained as a function of the cone semiangle for a Mach number of 3.30 for the 4°,7° and 7°,10° cowlings. A maximum pressure recovery of 0.56 has been obtained for $\theta_c = 22°$ and $\frac{D_B}{D_L} = 0.834$ for the 4°,7° cowling. For this condition θ_l is larger than θ_l*; therefore, the external drag is low. If the value of D_B/D_L decreases, the maximum internal contraction decreases and, therefore, the value of the maximum pressure recovery for a given cone angle decreases. The maximum value of pressure recovery for low values of D_B/D_L increases as the cone angle increases. This variation is logical because as the value of θ_c increases the Mach number at the inlet decreases and the contraction ratio required in order to obtain high recovery decreases. The highest pressure recovery is obtained for a semicone angle of about 22°. The corresponding internal contraction ratio is the maximum value of contraction ratio permitted by the starting conditions (fig. 10).

If the inclination of the cowling lip angles is increased, the shapes of the curves do not change.

The corresponding values of highest pressure recovery obtained as a function of the semicone angle for a Mach number of 2.75 for the $4^\circ,7^\circ$ and $7^\circ,10^\circ$ cowlings are shown in figures 25(a) and 25(b) for supersonic entrance flow. For some conditions the highest pressure recovery obtained has been obtained for subsonic entrance flow. Therefore, two diagrams have been plotted for each cowling (figs. 25(c) and 25(d)).

Figure 25(a) gives the highest pressure recovery obtained for supersonic entrance flow for the $4^\circ,7^\circ$ cowling. The highest pressure recovery obtained is 0.67. The value occurs for $\theta_c \approx 22^\circ$ at an internal contraction ratio near the maximum possible for the starting conditions. Figure 25(b) gives similar results for the $7^\circ,10^\circ$ cowling.

Figure 25(c) gives the values of highest pressure recovery obtained as a function of the cone semiangle for the $4^\circ,7^\circ$ cowling with subsonic entrance flow. The highest pressure recovery obtained is 0.68 for $\theta_c = 22^\circ$ and 30°.

The highest pressure recovery obtained for subsonic flow seems to occur for large values of semicone angle because no internal supersonic compression is used.

Figure 25(d) shows results similar to figure 25(c) for the $7^\circ,10^\circ$ cowling. The highest pressure recovery obtained is of the order of 0.69.

Figures 26(a) and 26(b) give the highest values of pressure recovery obtained at $M = 2.45$ as a function of the cone semiangle for different body diameter parameters for the $4^\circ,7^\circ$ and $7^\circ,10^\circ$ cowlings and supersonic entrance flow. The maximum pressure recovery obtained for the $4^\circ,7^\circ$ cowling is 0.77 for $\theta_c = 23^\circ$ to 24°. For the $7^\circ,10^\circ$ cowling the maximum pressure recovery is obtained for $\theta_c = 25^\circ$. For $\theta_c = 30^\circ$ supersonic flow at the entrance is not possible. Probably slightly higher values of pressure recovery could be obtained for $\theta_c = 26^\circ$ to 27°. The maximum pressure recovery obtained is about 0.78.

Figures 26(c) and 26(d) give the highest pressure recovery obtained with subsonic flow at the entrance. A pressure recovery of 0.82 has been obtained for $\theta_c = 30^\circ$ and the $4^\circ,7^\circ$ cowling and 0.80 for $\theta_c = 25^\circ$ for the $4^\circ,7^\circ$ and $7^\circ,10^\circ$ cowlings. The results show that the optimum cone angle decreases slightly when the Mach number increases, and in the range of Mach numbers considered, is in the range of 22° to 25° for supersonic entrance flow.

[redacted]

The Highest Pressure Recovery Obtained as a Function of the Central-Body-Diameter Parameter

The figures 12 to 22 have been cross-plotted and the highest value of the pressure recovery obtained for every semicone angle and cowling combination has been plotted as a function of the central-body-diameter parameter for a given Mach number tested (figs. 27 to 32). In order to have an idea of the value of the pressure recovery for Mach numbers different from the Mach number considered, the maximum pressure recovery obtained for the same cone angle, cowling, and cowling position parameter at Mach numbers other than the Mach number considered have also been plotted. Therefore, every figure gives the highest possible pressure recovery obtained as a function of the central-body-diameter parameter for the Mach number considered and the maximum pressure recovery obtained for the same configuration (same θ_l or constant geometry) for the other Mach numbers. These values are not the highest possible values for the central-body-diameter parameter considered.

The points indicated in the figures are not necessarily experimental points. However, the square and circle symbols are still used in order to distinguish the conditions for which the flow is supersonic at the entrance of the diffuser (circle symbols) from the conditions for which the flow at the entrance is subsonic (square symbols).

In the figures the central-body-diameter parameter for which the conical shock is at the lip of the cowling is also shown $(\theta_l = \theta_l^*)$.

For values of the central-body parameter equal to or less than this value, the conical shock is inside the cowling and, therefore, the external drag is small and the internal mass flow is the maximum possible because the free-stream tube that enters the cowling is equal to the cross section of the entrance of the inlet. When D_B/D_L is larger than the value corresponding to the condition $\theta_l^* = \theta_l$, the conical shock is in front of the lip and, therefore, the external drag is larger because an additive drag exists (reference 1), and the mass flow is less than the maximum possible for the entrance cross section considered. The entering mass flow for the supersonic entrance conditions can be easily determined from the analysis of conical flow.

Figure 27 gives the highest pressure recovery obtained at a Mach number of 3.30 as a function of the central-body-diameter parameter for the $4^\circ,7^\circ$ cowling and semicone angles of 20°, 22°, 25°, and 30°. The maximum value of pressure recovery for $M = 3.30$ and the 20° or 22° cones is obtained around $\frac{D_B}{D_L} = 0.84$ for which $\theta_l = \theta_l^*$. The maximum value of pressure recovery obtained is for $\theta_c = 22^\circ$ for which $\frac{p_f}{p_o} = 0.56$.

[redacted]

When the value of D_B/D_L decreases the pressure recovery decreases, but supersonic flow can be established in the diffuser also for lower Mach numbers.

Figure 28 gives similar results for the 7°,10° cowling. For this cowling the maximum pressure recovery also occurs around values of $\frac{D_B}{D_L} = 0.84$.

Figure 29 gives the highest pressure recovery obtained as a function of the central-body-diameter parameter at a Mach number of 2.75 for the 4°,7° cowling and for $\theta_c = 20°$, 22°, and 25°, respectively. For $\frac{D_B}{D_L} \approx 0.80$ and $\theta_c = 22°$ a pressure recovery of 0.67 is obtained together with low external drag. At a Mach number of 3.30 for the same configuration the pressure recovery is 0.50 (fig. 29(b)).

Similar results at a Mach number of 2.75 for the 7°,10° cowling are given in figure 30. At a Mach number of 2.75 and $\theta_c = 22°$, a pressure recovery of 0.68 is obtained for $\frac{D_B}{D_L} = 0.80$ and at a Mach number of 3.30 the pressure recovery for the same configuration becomes 0.50.

A similar analysis has been made for a Mach number of 2.45. Figure 31 gives the highest pressure recovery obtained as a function of the central-body-diameter parameter for the 4°,7° cowling and semicone angles of 20°, 22°, 25°, and 30°. For $\theta_c = 22°$ and $\frac{D_B}{D_L} = 0.77$, the pressure recovery for $M = 2.45$ is 0.77 and the corresponding recoveries at $M = 2.75$ and 3.30 are 0.65 and 0.47, respectively, with very low external drag. With subsonic flow in front of the inlet for $\frac{D_B}{D_L} \approx 0.800$, pressure recoveries of 0.80 and 0.82 have been obtained with semicone angles of 25° and 30°, respectively.

Figure 32 gives similar results of the 7°,10° cowling for semicone angles of 20°, 25°, and 30° at a Mach number of 2.45. At $\frac{D_B}{D_L} \approx 0.80$ and supersonic entrance flow, pressure recoveries of 0.77, 0.67, and 0.51 have been obtained for Mach numbers of 2.45, 2.75, and 3.30, respectively.

The Maximum Pressure Recovery as a Function of Mach Number

A typical variation of pressure recovery as a function of Mach number for a constant geometry inlet is shown in figure 33. The typical configuration has a semicone angle of 22°, the 4°,7° cowling, $\frac{D_B}{D_L} = 0.834$,

and $\theta_l = 32.2^\circ$. Part of the curve corresponds to subsonic flow in front of the inlet and part of the curve corresponds to supersonic flow in front of the inlet.

The highest values of pressure recovery obtained from all the configurations tested are shown in figure 34. For comparison the pressure recovery for the inlet with all internal compression is also shown. The information for the inlet with all internal compression has been taken from reference 2.

Figure 35 gives the optimum values of kinetic energy recovered by all the configurations tested and the diffuser from reference 2. The values have been calculated by using the information in figure 34 and the expression (reference 2):

$$\eta = 1 - \frac{5}{M^2}\left[\left(\frac{p_o}{p_f}\right)^{\frac{1}{3.5}} - 1\right]$$

Optical Observations of the Flow Phenomena about the Inlets

The shadowgraphs taken for every test point give a further indication of the flow phenomena about an inlet. Thus a comparative analysis of the external drag of the different configurations can be made. In figures 36 to 39 some shadowgraphs of the configurations tested are shown.

Figure 36 gives the shadowgraphs for $\theta_c = 25^\circ$, the 7°,10° cowling and $\frac{D_B}{D_L} = 0.817$ for different values of θ_l at the condition of maximum pressure recovery for $M = 3.30$. The shadowgraph in figure 36(a) shows the supersonic flow configuration at $\theta_l = 31^\circ$, whereas figure 36(b) shows the subsonic flow configuration (reduced mass flow) for the same θ_l (fig. 19(d)). The differences in the curvature of the external shocks in the external flow shows that the drag is large for subsonic entrance flow conditions. When θ_l becomes 34.1° the conical shock enters the cowling and the external drag becomes very small. Figure 36(d) corresponds to a θ_l of 35.4° with the conical shock still farther in the inlet. Figures 36(e) and 36(f) correspond to a θ_l of 35.9°. Both photographs have a strong shock in front of the lip. Figure 36(d) corresponds to the maximum possible mass flow in the inlet, whereas figure 36(e) corresponds to a slightly reduced mass flow, before the flow vibrations start. When the mass flow is reduced, the strong shock increases in intensity (fig. 36(f)). Figures 36(g) and 36(h) show similar results for $\theta_l = 36.6^\circ$. The shadowgraph (fig. 36(g)) corresponds to the maximum mass flow and figure 36(h) to a reduced mass flow. The shadowgraphs in

figures 36(b), 36(f), 36(g), and 36(h) show the existence of the lambda shock at the surface of the cone.

Figure 37 shows the shadowgraphs at a Mach number of 2.75 for $\theta_c = 20^\circ$, the $7^\circ,10^\circ$ cowling and $\frac{D_B}{D_L} = 0.817$ for different values of θ_l at the condition of maximum pressure recovery. The tests were made at a 1° angle of attack. The corresponding values of pressure recovery as a function of the cowling-position parameter are given in figure 13(b). Figures 37(a) to 37(e) correspond to cowling-position parameters of 27.2°, 27.9°, 28.4°, 28.9°, and 29.4°, respectively. For all these conditions the flow at the entrance is supersonic. Figure 37(f) corresponds to a θ_l of 29.9° for which subsonic flow exists in front of the inlet. The strong compression in front of the inlet produces a separation at the surface of the central body and, therefore, the shock near the surface appears as a lambda shock. The separation is visible in the photograph.

Figure 38 shows the shadowgraphs at a Mach number of 2.45 for $\theta_c = 22^\circ$, the $7^\circ,10^\circ$ cowling, and $\frac{D_B}{D_L} = 0.752$ for different values of θ_l and at an angle of attack of 2°. The corresponding values of pressure recovery are given in figure 16(b) for zero angle of attack. For a 2° angle of attack the values do not change. Figure 38(b) corresponds to $\theta_l = 35.7^\circ$ and supersonic flow at the entrance, whereas figure 38(c) corresponds to the same θ_l but with a reduced mass flow. The photograph shows that when the flow into the inlet is subsonic, the flow phenomena is strongly dissymmetrical with respect to the axis of the inlet. This large dissymmetry of the flow phenomena always occurs for subsonic entrance flow when a small geometrical dissymmetry exists. This discontinuity produces a variation of external aerodynamical properties of the body and the variations occur discontinuously when the strong shock jumps in front of the inlet. In order to avoid discontinuities of the internal and external aerodynamic characteristics of the inlet, the inlet must be designed in such a manner that supersonic internal flow can be maintained over all the range of possible angles of attack. Figure 38(d) corresponds to a $\theta_l = 34.4^\circ$ and supersonic flow at the entrance, whereas figures 38(e) and 38(f) correspond to a θ_l of 35.1° with supersonic and subsonic flow at the entrance, respectively. The pressure recovery for the condition of subsonic flow at the entrance shown in figure 38(f) is larger than for the condition shown in figure 38(e); however, as can be seen by the shock configuration, the external drag is larger for the condition of subsonic flow. In figure 38(f) the lambda shock and the separation of the flow from the upper surface can be seen.

Figures 39(a) to 39(d) present some shadowgraphs for the inlet with large external compression at a Mach number of 3.30 and different values of θ_l and at a Mach number of 2.75 and $\theta_l = 30.5^\circ$. For comparison figures 39(e) and 39(h) show shock configurations for inlets designed

for low external compression and having supersonic or subsonic flow at the entrance. Figure 39(a) corresponds to a cowling-position parameter of 28.9° and a maximum pressure recovery of 0.49. Figure 39(b) corresponds to a cowling-position parameter of 30° and a maximum pressure recovery of 0.54. Figure 39(c) corresponds to a cowling-position parameter of 30.3° and a pressure recovery of 0.54. From an analysis of the three photographs it can be seen that the compression is more nearly isentropic in figure 39(a); however, the pressure recovery, because of the presence of the boundary layer, is less than the maximum value obtained when supersonic compression occurs all in front of the second deviation on the central body. All the results of these tests show that the phenomena in the boundary layer are of fundamental importance in the design of supersonic diffusers.

The formation of lambda shock seems to increase the value of the pressure recovery if the separation following the shock is small. When the lambda shock is followed by large separation and the wake fills a large part of the entrance region, the pressure recovery decreases.

The boundary-layer separation is also related to the fluctuation of the subsonic stream. These fluctuations are very important from the point of view of stability because a shock of some strength is required in order to have stability. This shock limits the value of the maximum pressure recovery that can be obtained for a given Mach number.

Figure 39(d) is the shadowgraph at a Mach number of 2.75 and $\theta_l = 30.5°$. Figure 39(e) is a shadowgraph for comparing the flow configuration for an inlet having a semicone angle of 22°, 7°,10° cowling, $\theta_l = 31.4°$, and $\frac{D_B}{D_L} = 0.85$, and a pressure recovery of 0.56, with the flow phenomena of figures 39(a) to 39(c). Figure 39(f) is a shadowgraph of an inlet with $\theta_c = 20°$, the 4°,7° cowling, and $\frac{D_B}{D_L} = 0.867$ for a Mach number of 3.30. The pressure recovery is 0.53. A shadowgraph for the same cowling and central body combination but $\theta_l = 30°$ is shown in figure 39(g). For this configuration the pressure recovery is 0.51 (fig. 12(c)). In figures 39(f) and 39(g) the lambda shock is clearly shown. Figure 39(h) shows a shadowgraph at $M = 2.75$ for the inlet having a semicone angle of 22°, the 4°,7° cowling, $\frac{D_B}{D_L} = 0.8000$ and $\theta_l = 32.9°$. The pressure recovery for this configuration is 0.67.

From the analysis of the shadowgraphs some indication for explaining the phenomena of vibration can be obtained. The vibrations occur only when the flow in the internal part of the diffuser is all subsonic. For this condition the disturbances from the subsonic part can be transmitted upstream. The vibrations occur when separation exists at the surface of the cone produced by the strong shock in front of the inlet. Any variation of the position of the point of separation

[redacted]

changes the position of the shock in front of the inlet and the dimension of the wake at the entrance of the diffuser, and, therefore, the mass flow entering the inlet. To a variation of mass flow there corresponds a variation of back pressure at the end of the diffuser which is transmitted upstream and thus produces a vibration. The intensity of the vibration seems to depend upon the intensity of the separation and does not exist if the separation is very small. The vibrations seem to be reduced if the position of the point at which the separation begins is fixed by the geometrical construction of the inlet.

CONCLUSIONS

From the analysis of the aerodynamic criteria of the design of supersonic inlets and from the analysis of the experimental results, the following conclusions can be obtained:

The inlets using external compression permit a larger pressure recovery than the inlets with all internal compression. For practical problems at low Mach numbers (of the order of 1.4 to 2.0) the supersonic compression can be obtained all outside the inlet without a large increase in external drag. For Mach numbers of the order of three in practical problems, the maximum cross section of the body which contains the inlet can be of the same order of magnitude as the cross section of the free-stream tube used for the internal flow. In this case the use of all external compression produces a very large increase of external drag and the increase in efficiency obtained is not justified when the external drag is considered.

A practical solution requires a good compromise between the increase of pressure recovery and the increase of external drag due to the external compression. When the external compression is reduced and the free-stream Mach number is large, to increase the pressure recovery it is convenient to use an internal supersonic diffuser. With a good combination of external and internal supersonic compression, pressure recoveries of the order of those obtained using very large external compression have been obtained. In this case, the corresponding external drag is reduced to a very small value. For practical applications it is possible to design inlets having the external drag required by the proportion between the cross section of the free-stream tube corresponding to the internal flow and the maximum cross section of the body and at the same time having high pressure recovery.

In order to avoid discontinuities of the aerodynamical properties, the inlets must be designed with the criteria of having supersonic flow for the range of angles of attack to be used.

The maximum possible contraction ratio in order to start the internal supersonic diffuser has been found to correspond practically to the value given by the one-dimensional theory.

The increase of the value of the internal contraction ratio using variable geometry does not increase the pressure recovery because of the disturbances from the subsonic diffuser. An increase in contraction ratio does not correspond to an increase in pressure recovery because the Mach number at which the flow in the divergent diffuser passes from supersonic to subsonic Mach numbers is not fixed by the Mach number at the minimum section, but is fixed by stability criteria. Also for constant geometry the shock occurs at somewhat higher Mach numbers than at the throat.

Experimental results show that the boundary layer along the surface of the central body has a large influence on the value of the pressure recovery which can be obtained. At high Mach numbers, if a strong compression occurs along the surface of the central body, a separation can be produced which reduces the gain expected by a large external compression.

When the internal mass flow is reduced somewhat from the maximum value possible for every configuration analyzed, instability phenomena have been found in the flow.

The tests have shown that supersonic flow can be established inside the inlet if the contraction ratio is fixed considering the starting conditions and if the shape of the channel permits reflection of the shock at the lip and from the surface of the central body.

For a Mach number of 3.30 a pressure recovery of 0.57 has been obtained with a configuration having very low external drag. This value is higher than any other value previously obtained.

At Mach numbers of 2.45 and 2.75 maximum pressure recoveries of 0.78 and 0.67 have been obtained with the configurations having low external drag as compared to 0.84 and 0.72 to configurations having external compression and high external drag.

A qualitative analysis of shadowgraph pictures taken during the tests shows that the drag of the inlets tested for supersonic entrance flow is small.

Langley Aeronautical Laboratory
National Advisory Committee for Aeronautics
Langley Field, Va.

REFERENCES

1. Ferri, Antonio, and Nucci, Louis M.: Preliminary Investigation of a New Type of Supersonic Inlet. NACA RM No. L6J31, 1946.

2. Kantrowitz, Arthur, and Donaldson, Coleman duP.: Preliminary Investigation of Supersonic Diffusers. NACA ACR No. L5D20, 1945.

3. Oswatitsch, Kl.: Der Druckrückgewinn bei Geschossen mit Rückstossantrieb bei hohen Überschallgeschwindigkeiten. Bericht Nr. 1005, Forsch. and Entwickl. des Heereswaffenamtes (Göttingen), 1944.

4. Oswatitsch, Kl., and Böhm, H.: Luftkräfte und Strömungsvorgänge bei angetriebenen Geschossen. Berichte Nr. 1010 and 1010/2, Forsch und Entwickl. des Heereswaffenamtes (Göttingen), 1944.

5. Ferri, Antonio: Application of the Method of Characteristics to Supersonic Rotational Flow. NACA TN No. 1135, 1946.

[redacted]

[redacted]

[redacted]

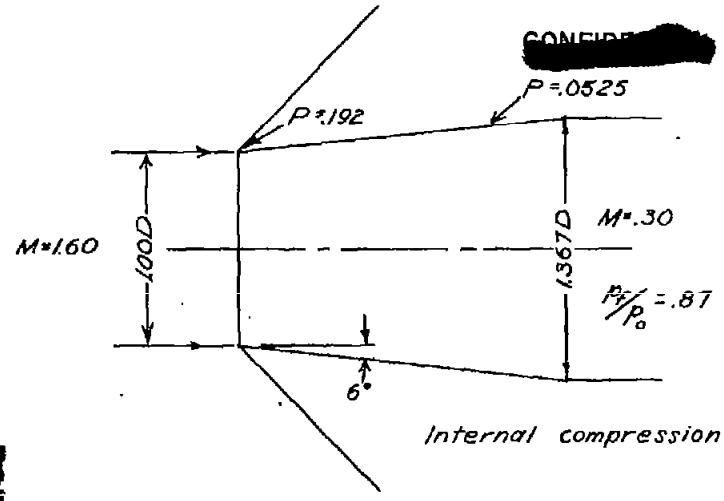

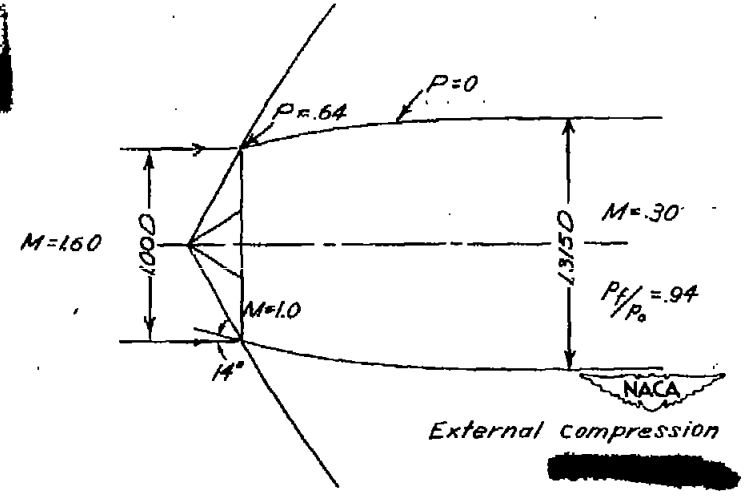

Figure 1.- Characteristics of inlets with all internal and all external compression for a Mach number of 1.6.

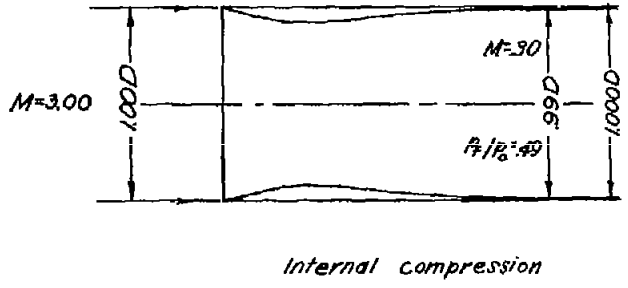

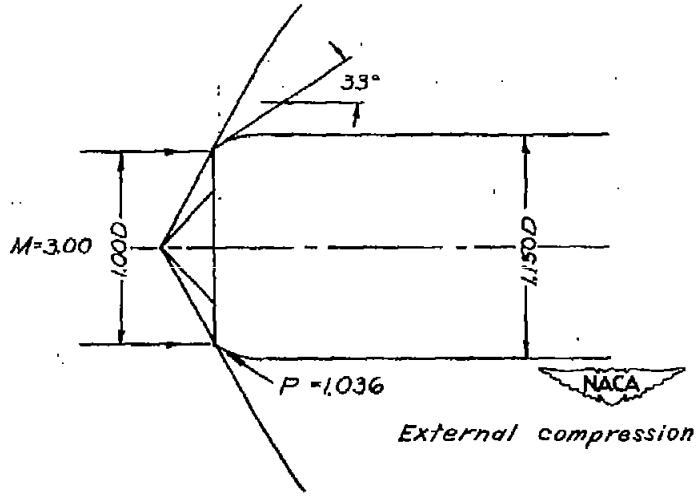

Figure 2.- Characteristics of inlets with all internal and all external compression for a Mach number of 3.0.

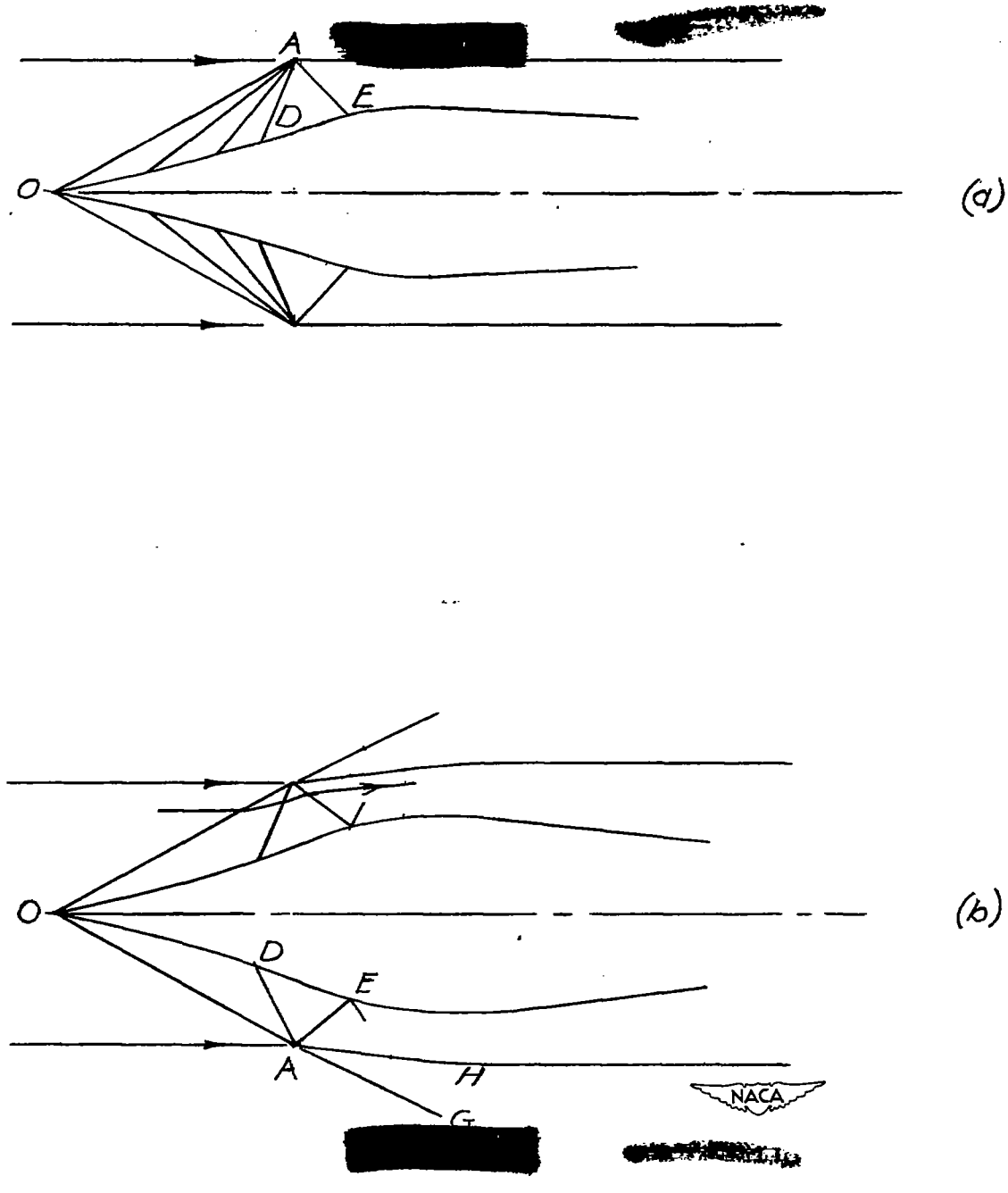

Figure 3.- Supersonic flow phenomena into inlets.

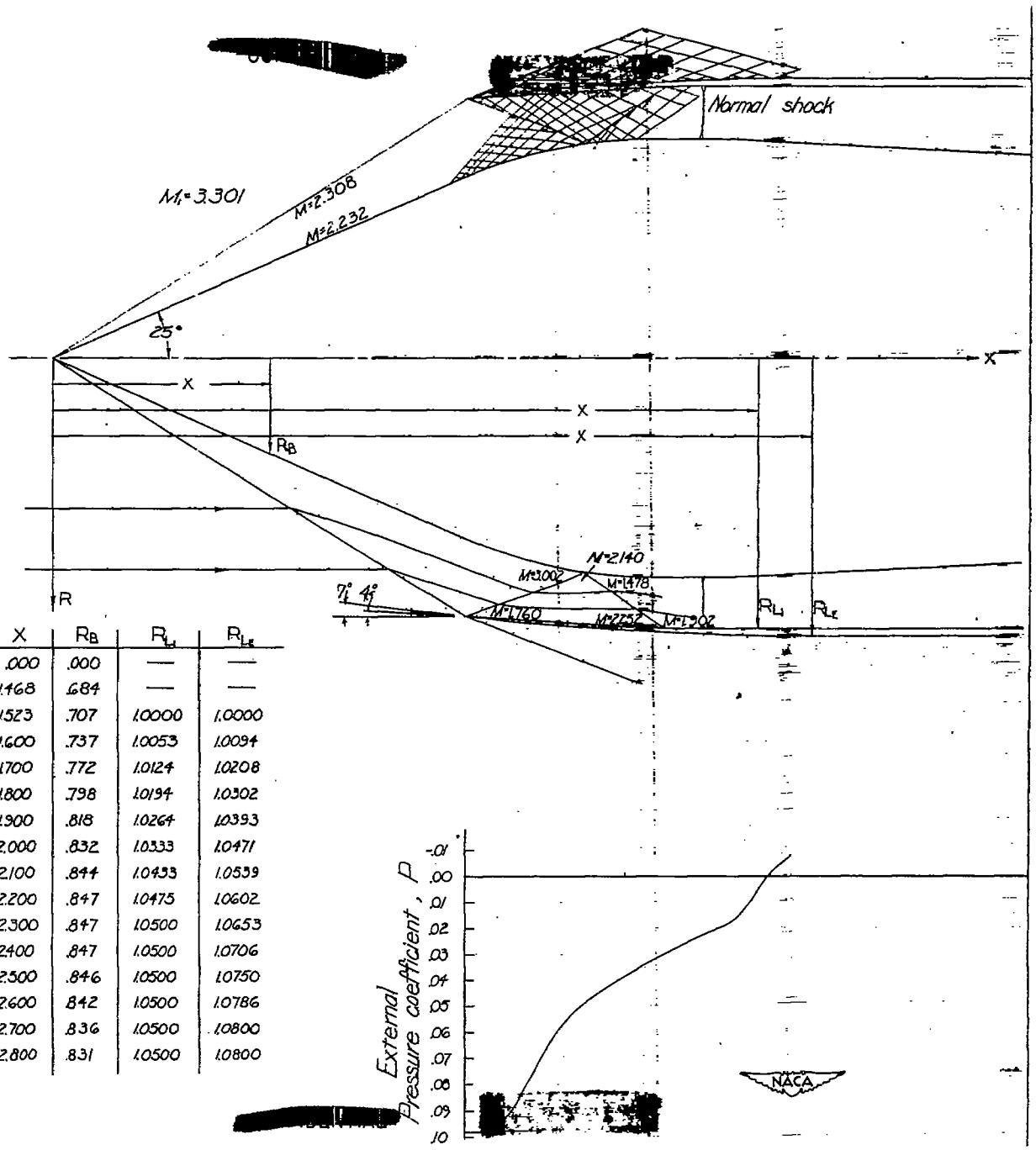

X	R_B	R_{L_1}	R_{L_2}
.000	.000	—	—
1.468	.684	—	—
1.523	.707	1.0000	1.0000
1.600	.737	1.0053	1.0094
1.700	.772	1.0124	1.0208
1.800	.798	1.0194	1.0302
1.900	.818	1.0264	1.0393
2.000	.832	1.0333	1.0471
2.100	.844	1.0433	1.0539
2.200	.847	1.0475	1.0602
2.300	.847	1.0500	1.0653
2.400	.847	1.0500	1.0706
2.500	.846	1.0500	1.0750
2.600	.842	1.0500	1.0786
2.700	.836	1.0500	1.0800
2.800	.831	1.0500	1.0800

Figure 4.- External and internal flow analysis of an inlet.

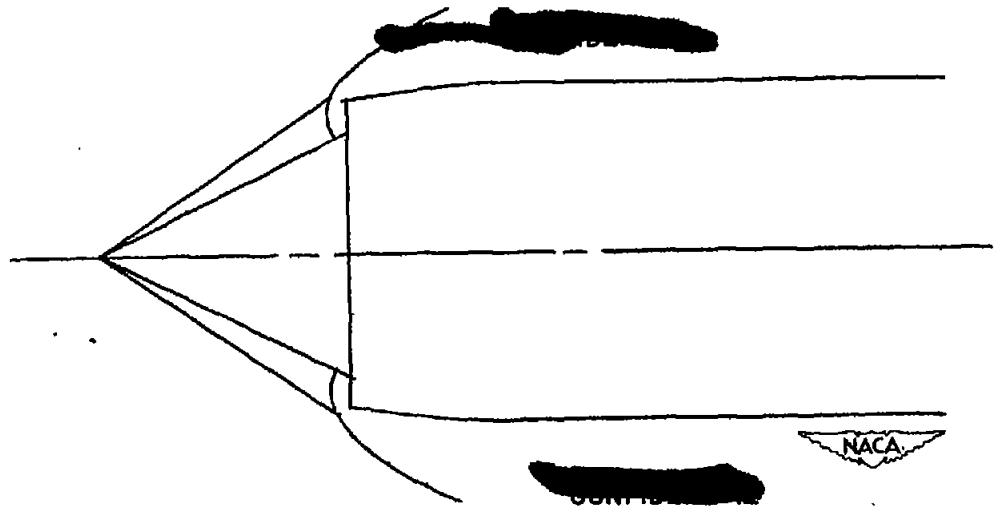

Figure 5.- Flow configuration of an inlet operating below the design Mach number.

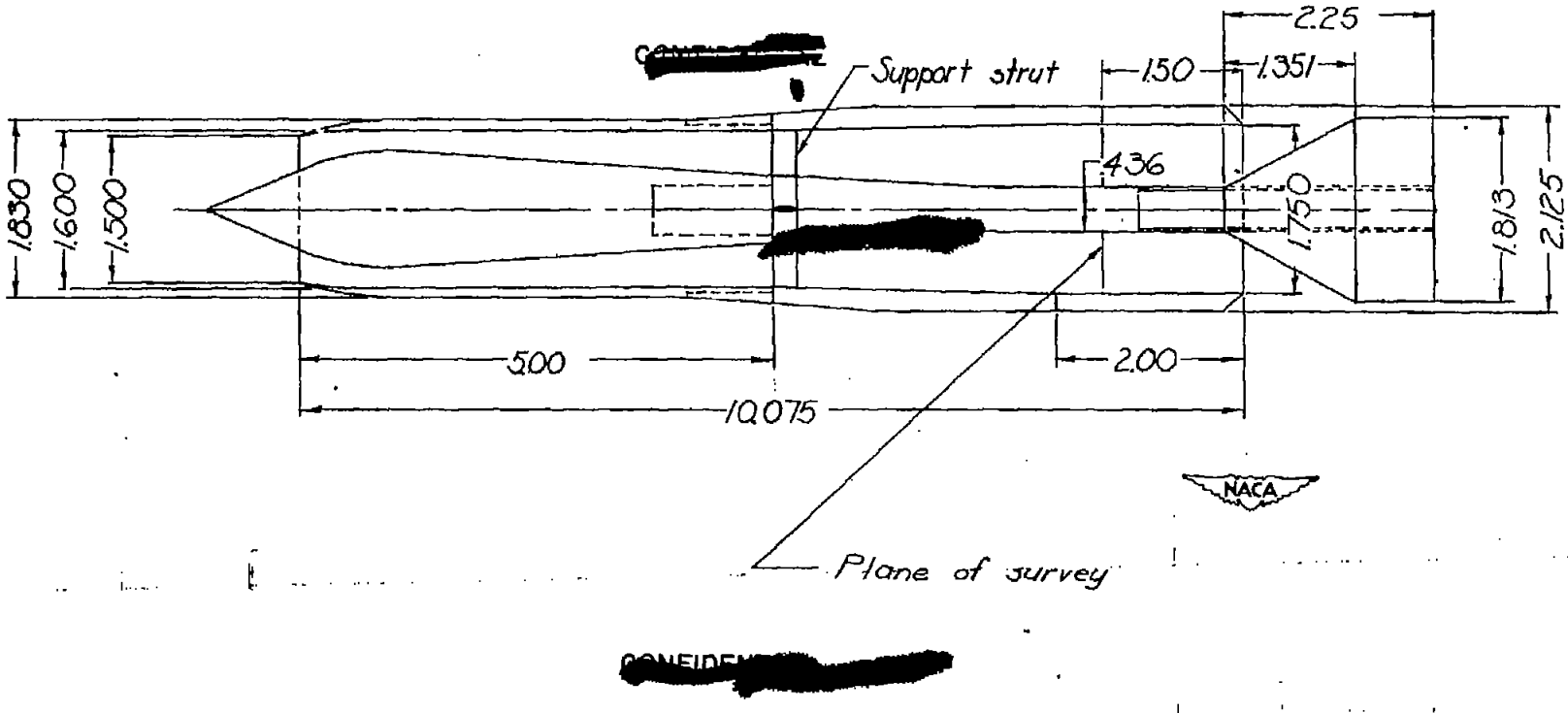

Figure 6.- General configuration of model tested.

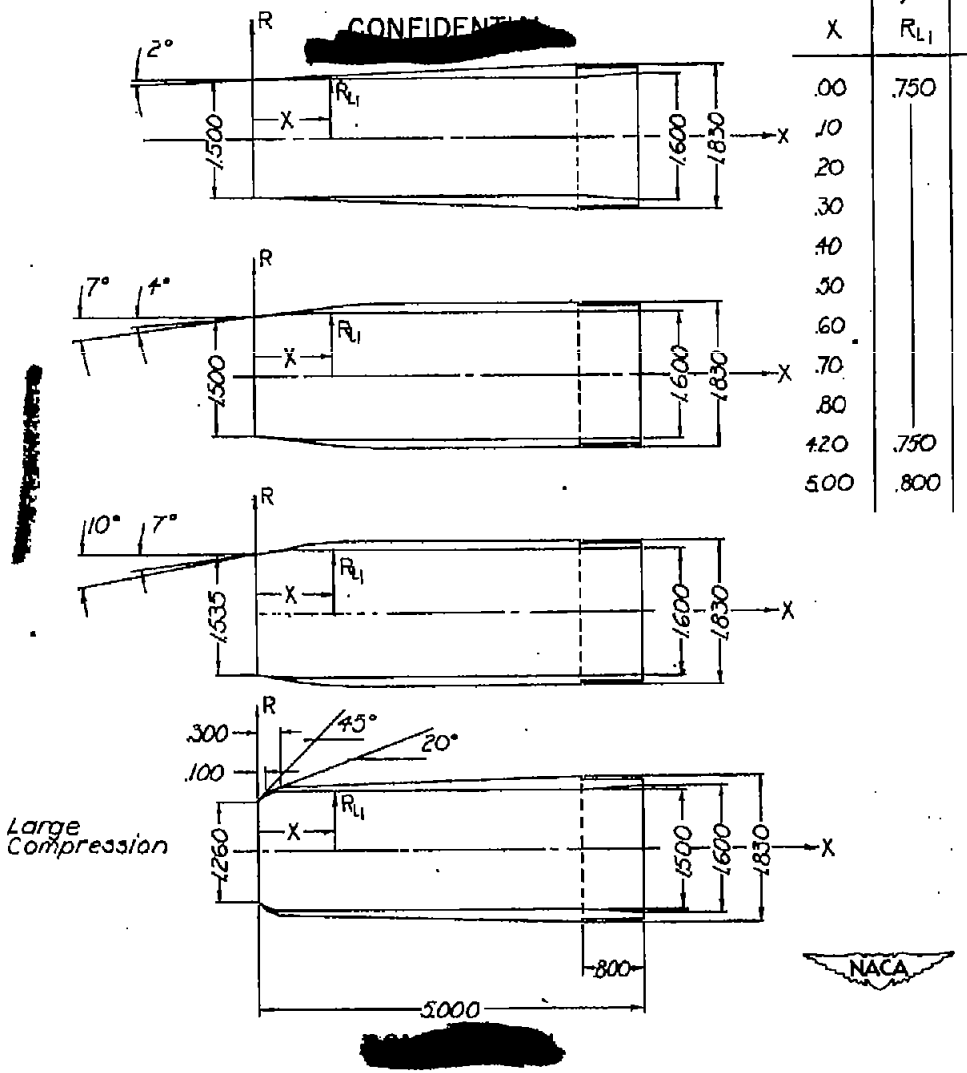

Internal cowling ordinates

X	0°, 2° R_{L_1}	4°, 7° R_{L_1}	7°, 10° R_{L_1}	Large Compression R_{L_1}
.00	.750	.750	.765	.63
.10		.757	.769	.70
.20		.764	.778	.732
.30		.770	.791	.750
.40		.778	.800	
.50		.785	.804	
.60		.791	.805	
.70		.797	.806	
.80		.800	.804	
4.20	.750	.800	.800	.750
5.00	.800	.800	.800	.800

Figure 7.- Cowlings tested.

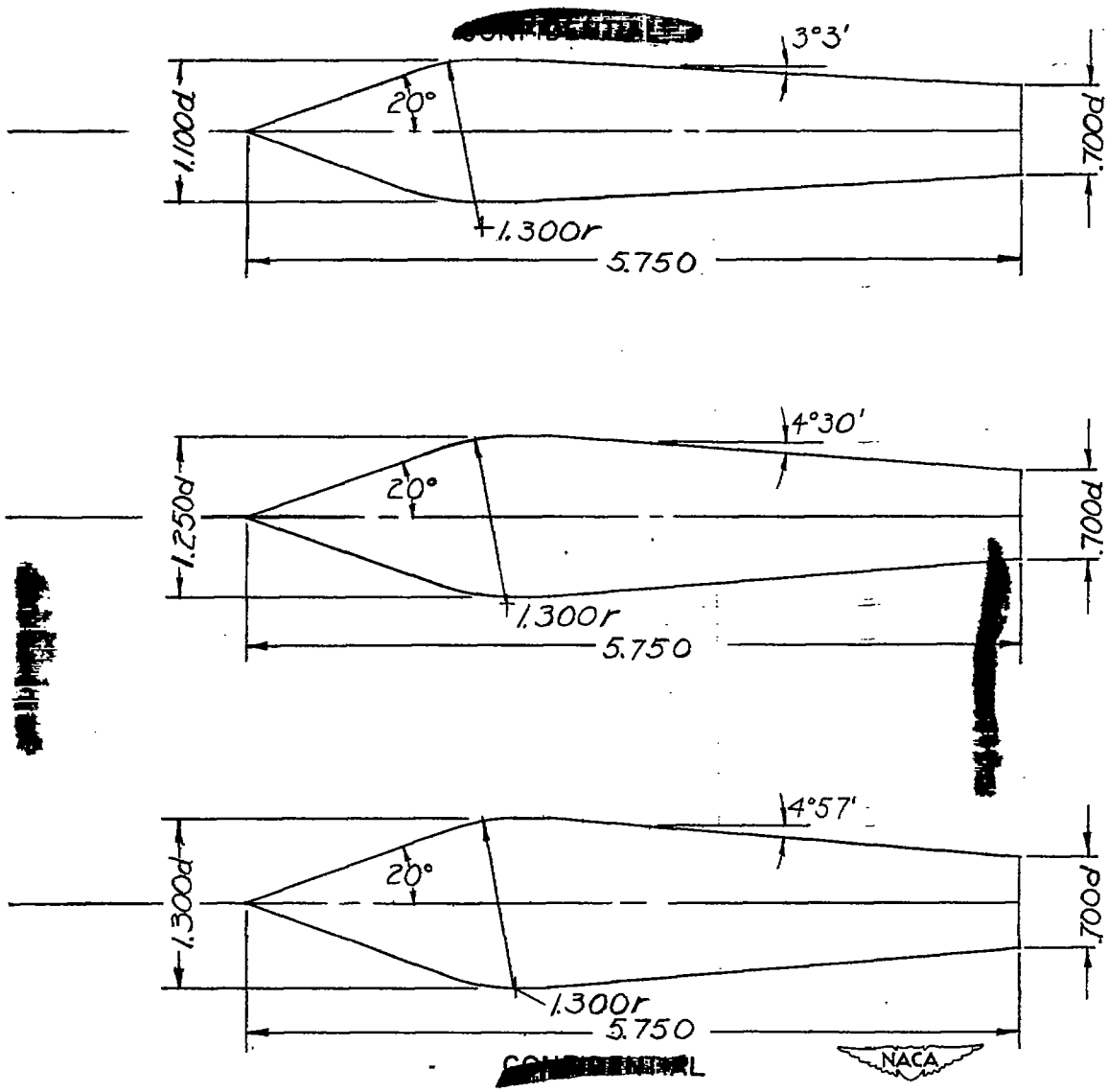

(a) 20° cones.

Figure 8.- Central bodies tested.

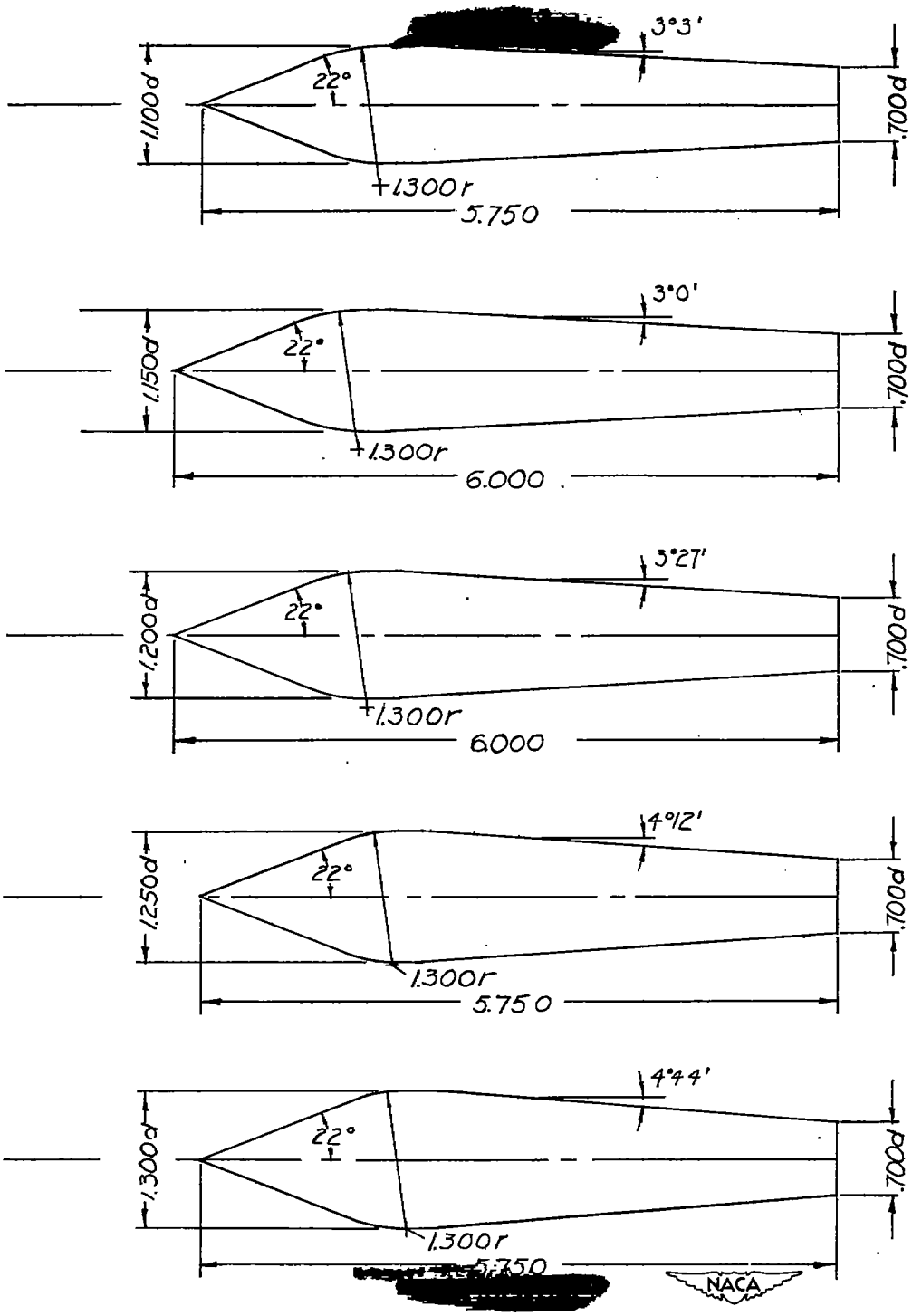

(b) 22° cones.

Figure 8.- Continued.

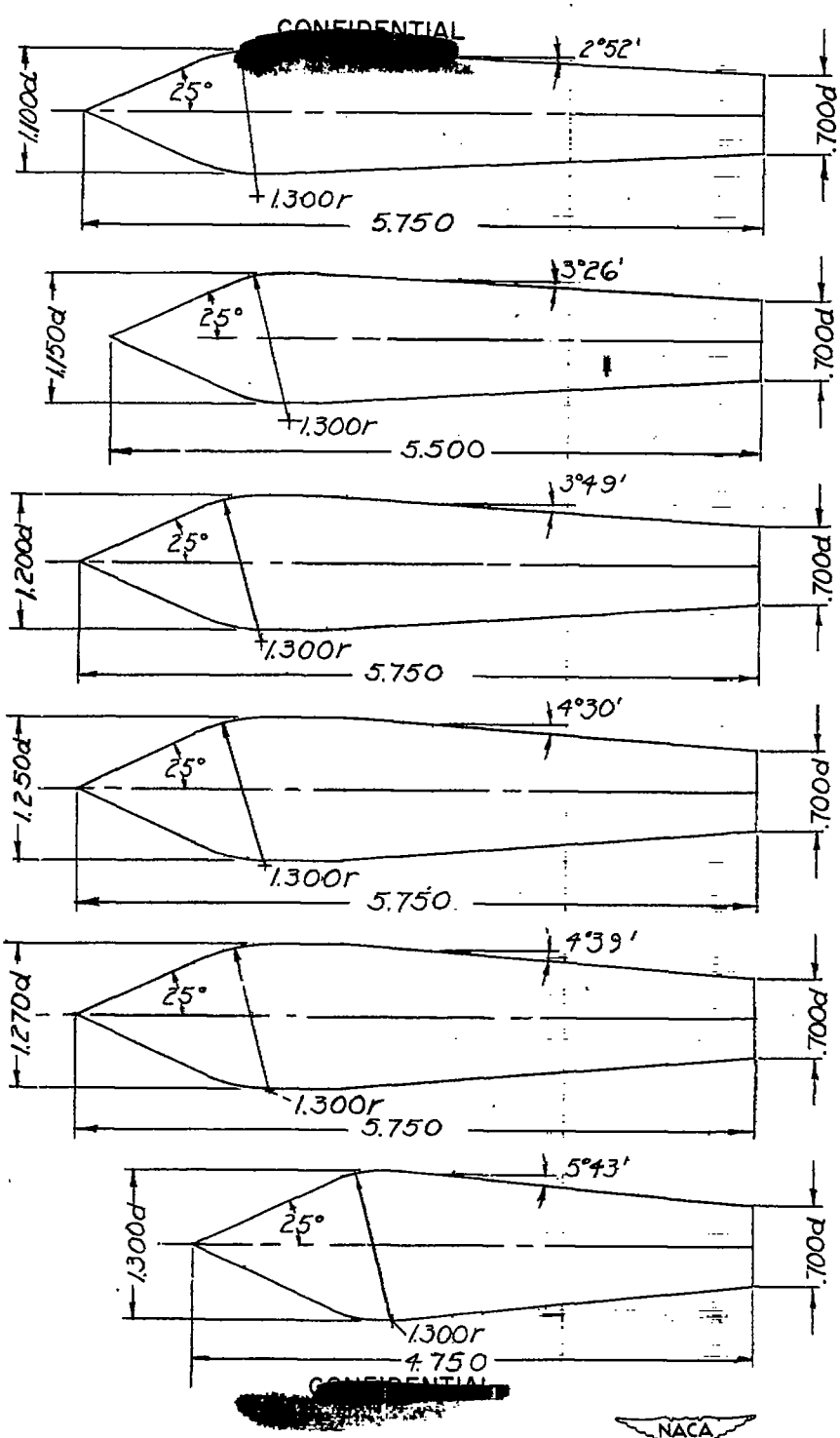

(c) 25° cones.

Figure 8.- Continued.

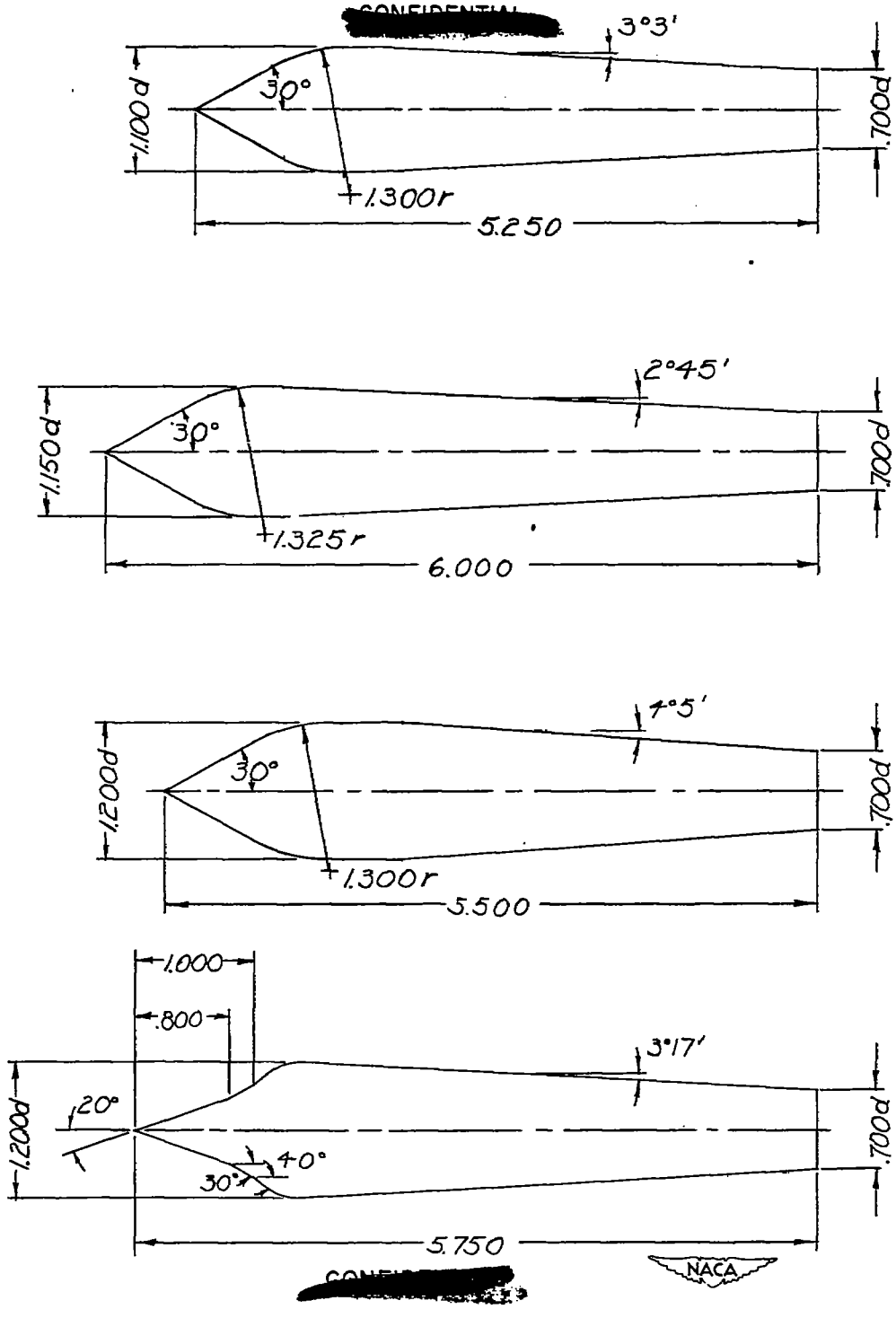

(d) 30° cones and central body derived from reference 3.

Figure 8.- Concluded.

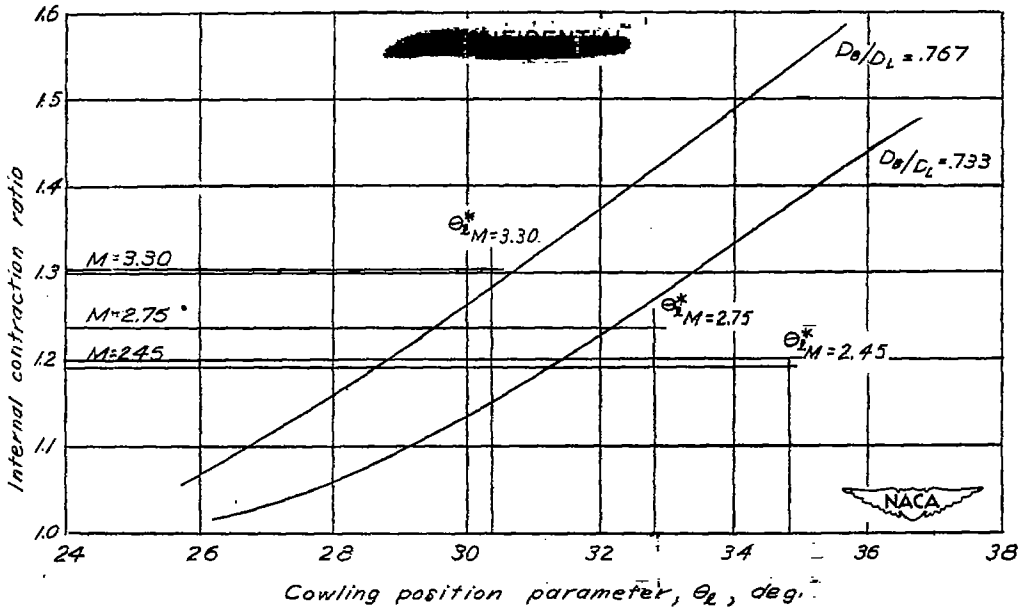

(a) $\theta_c = 22^\circ$.

Figure 9.- Internal contraction ratio as a function of the cowling position parameter for the 0°, 2° cowling.

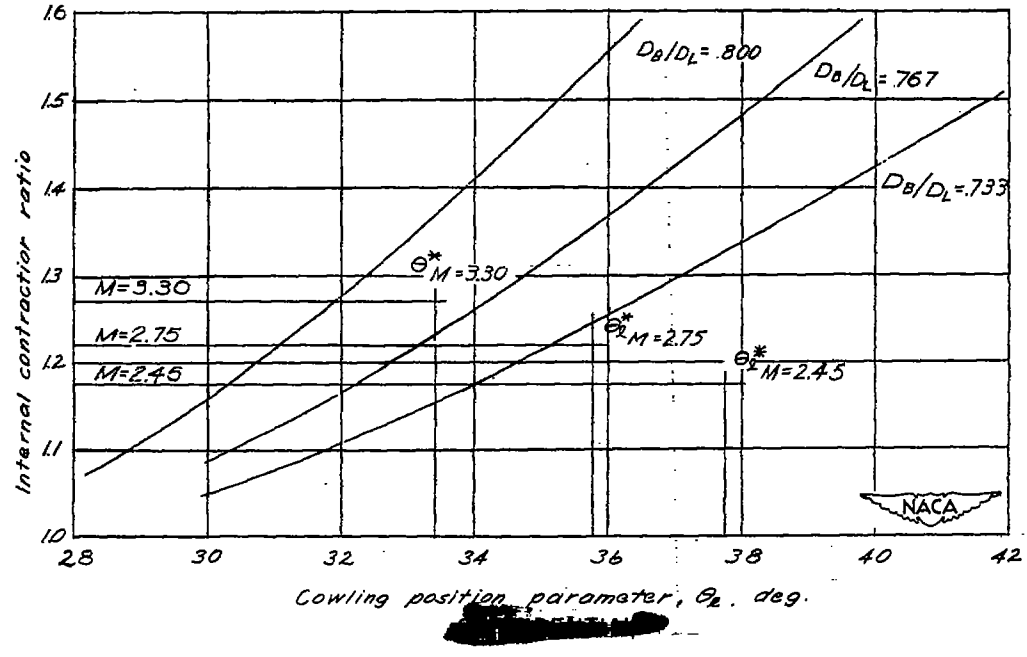

(b) $\theta_c = 25^\circ$.

Figure 9.- Continued.

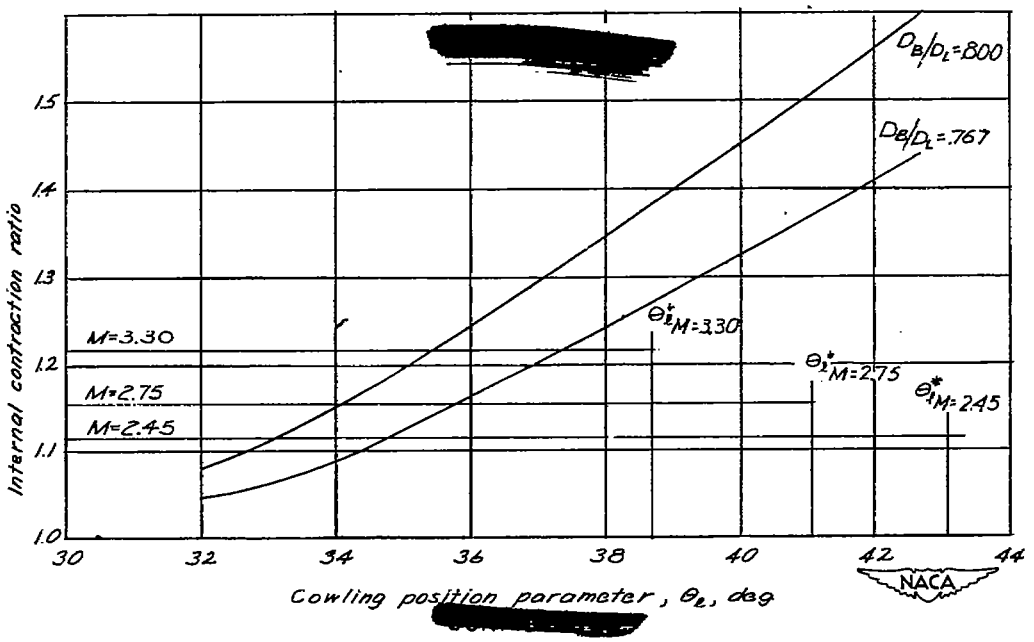

(c) $\theta_c = 30^\circ$.

Figure 9.- Concluded.

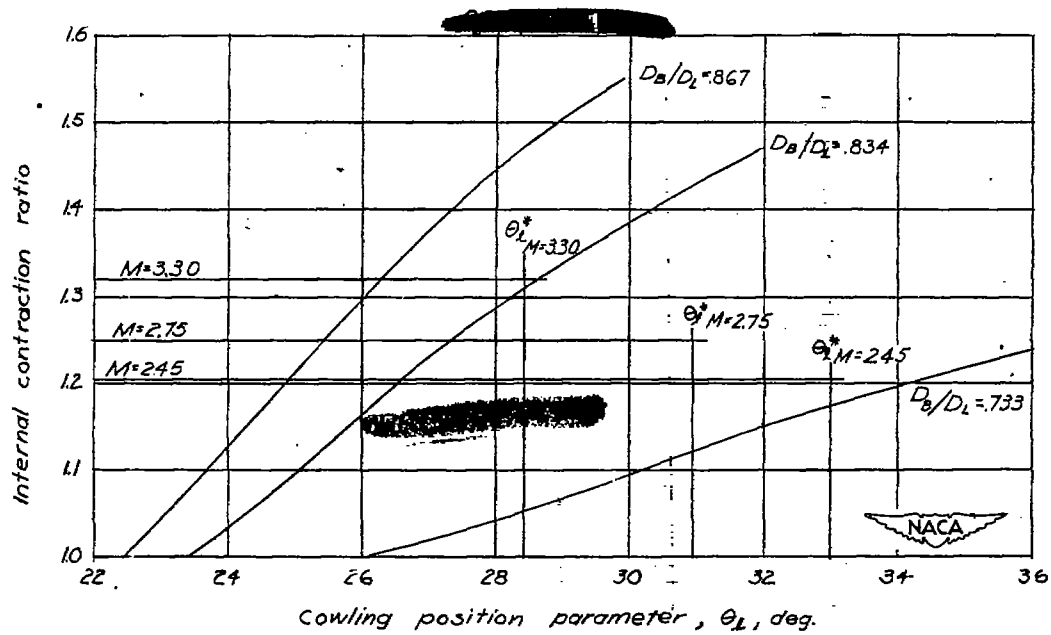

(a) $\theta_c = 20^\circ$.

Figure 10.- Internal contraction ratio as a function of the cowling position parameter for the 4°, 7° cowling.

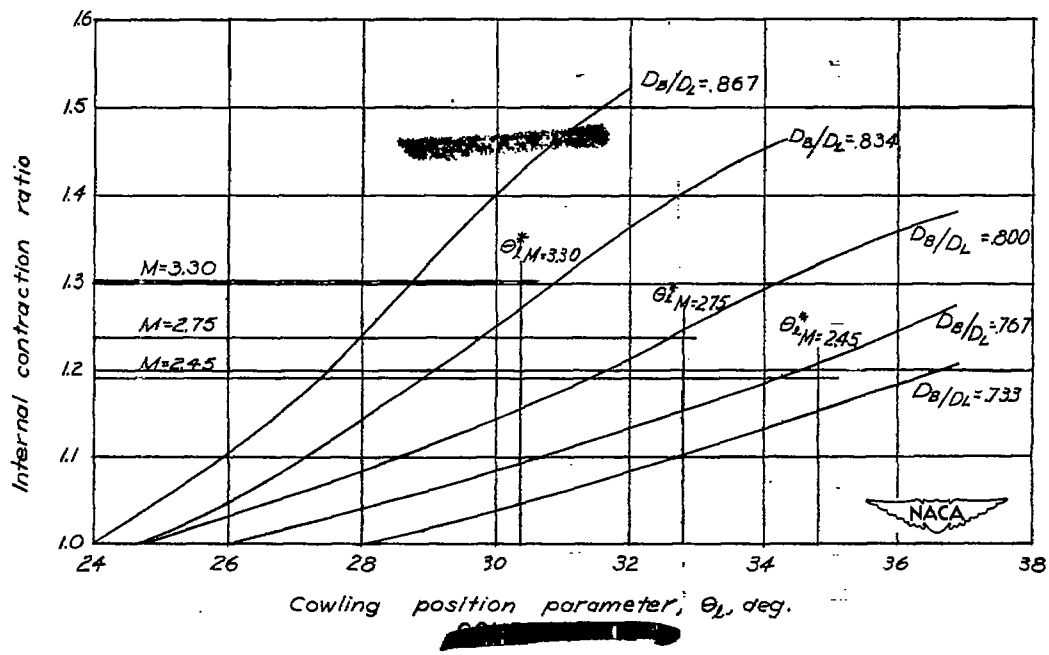

(b) $\theta_c = 22^\circ$.

Figure 10.- Continued.

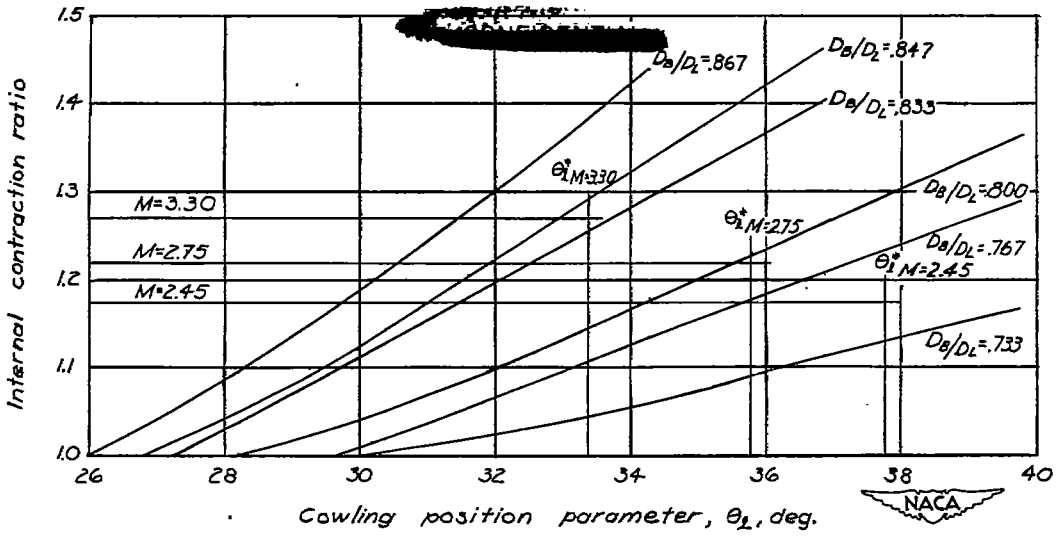

(c) $\theta_c = 25^\circ$.

Figure 10.- Continued.

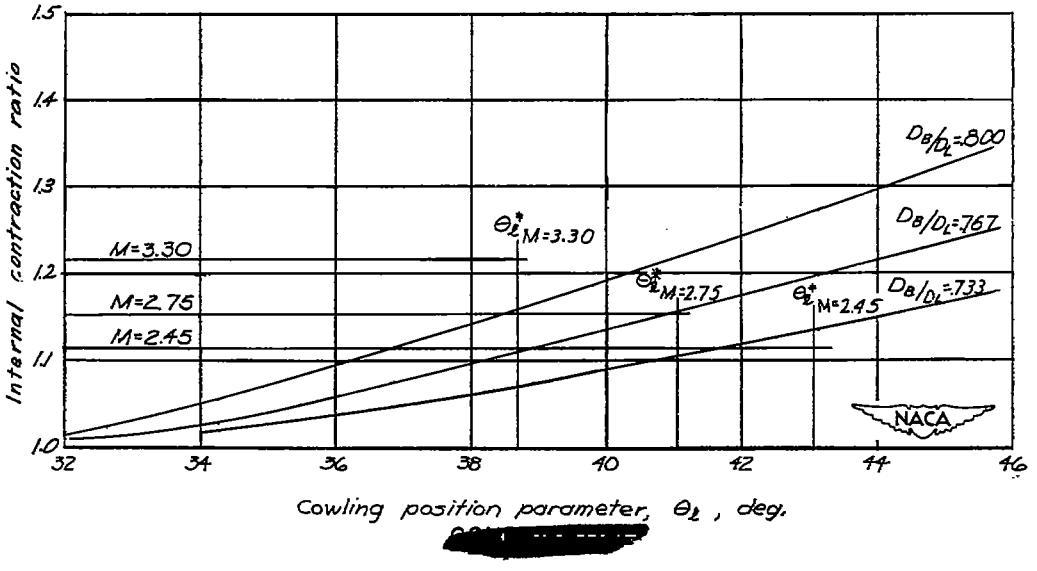

(d) $\theta_c = 30^\circ$.

Figure 10.- Concluded.

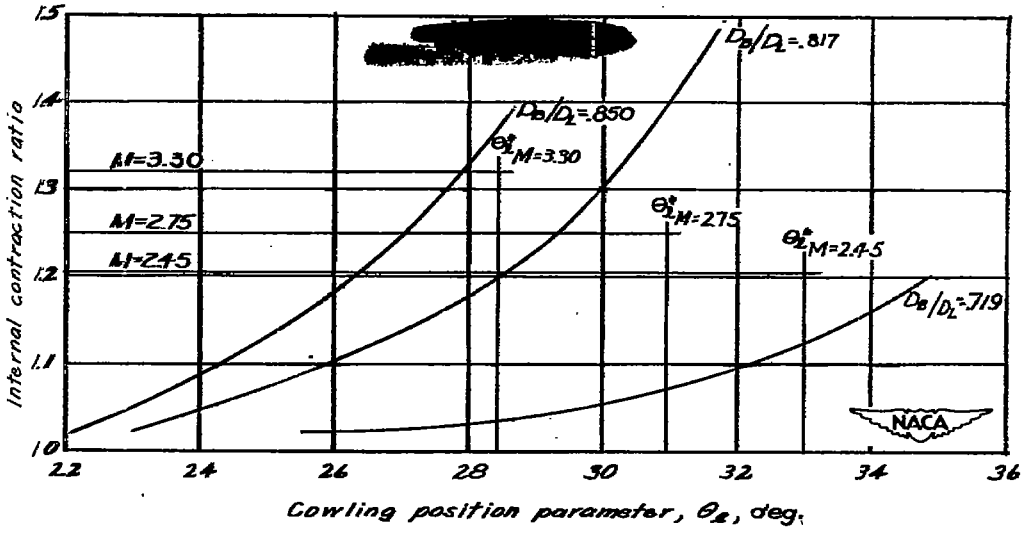

(a) $\theta_c = 20^\circ$.

Figure 11.- Internal contraction ratio as a function of the cowling position parameter for the 7°, 10° cowling.

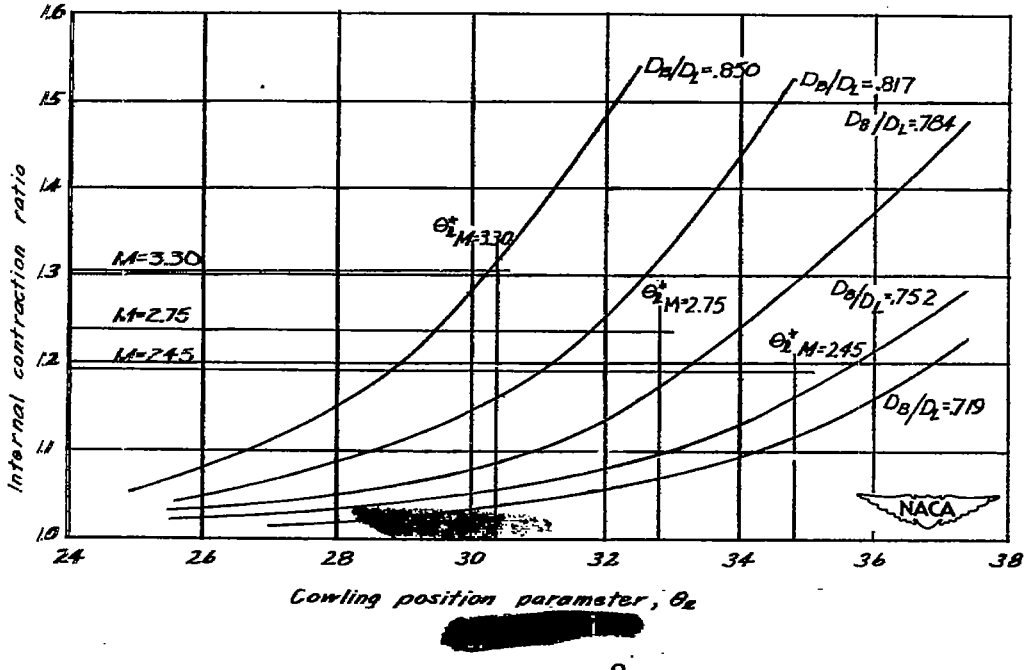

(b) $\theta_c = 22^\circ$.

Figure 11.- Continued.

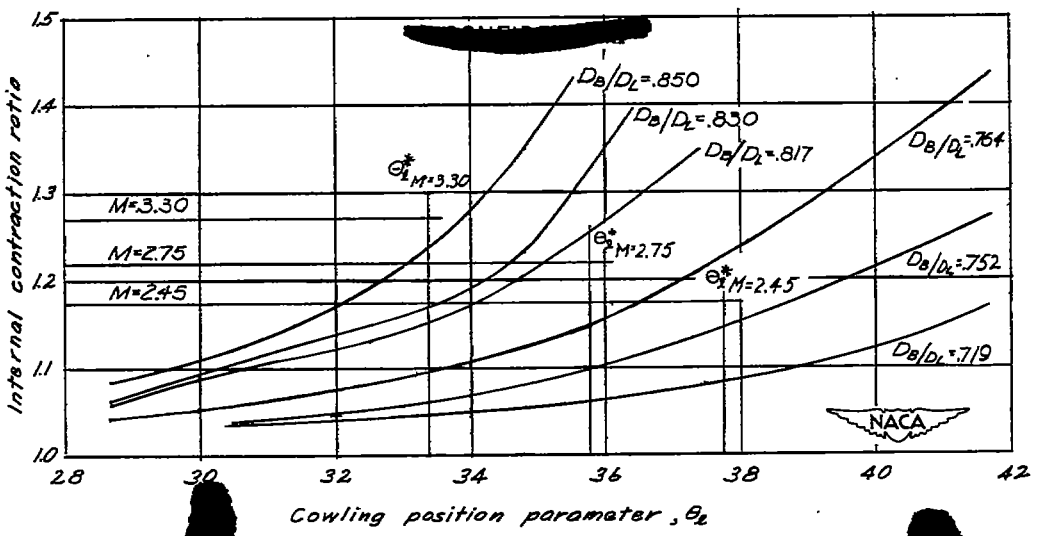

(c) $\theta_c = 25^\circ$.

Figure 11.- Continued.

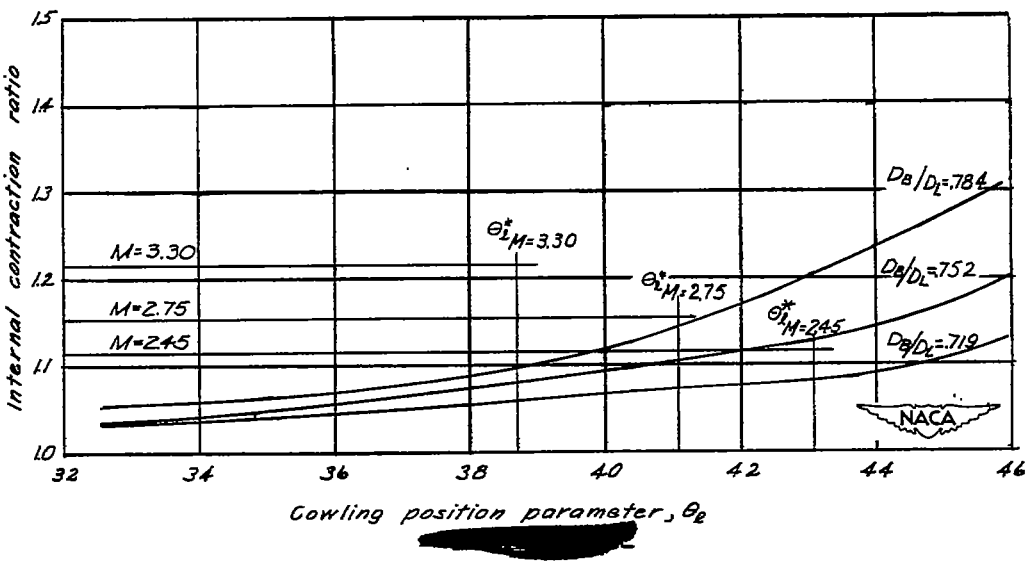

(d) $\theta_c = 30^\circ$.

Figure 11.- Concluded.

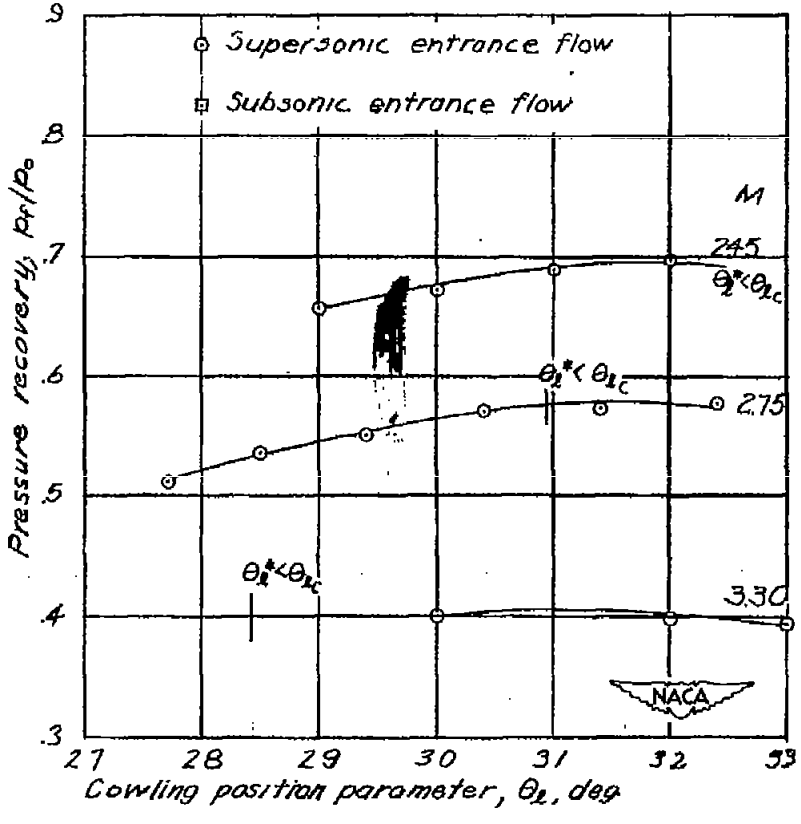

(a) 4°, 7° cowling; $D_B/D_L = 0.733$; $\theta_c = 20^\circ$.

Figure 12.- Pressure recovery as a function of the cowling position parameter for $\theta_c = 20^\circ$.

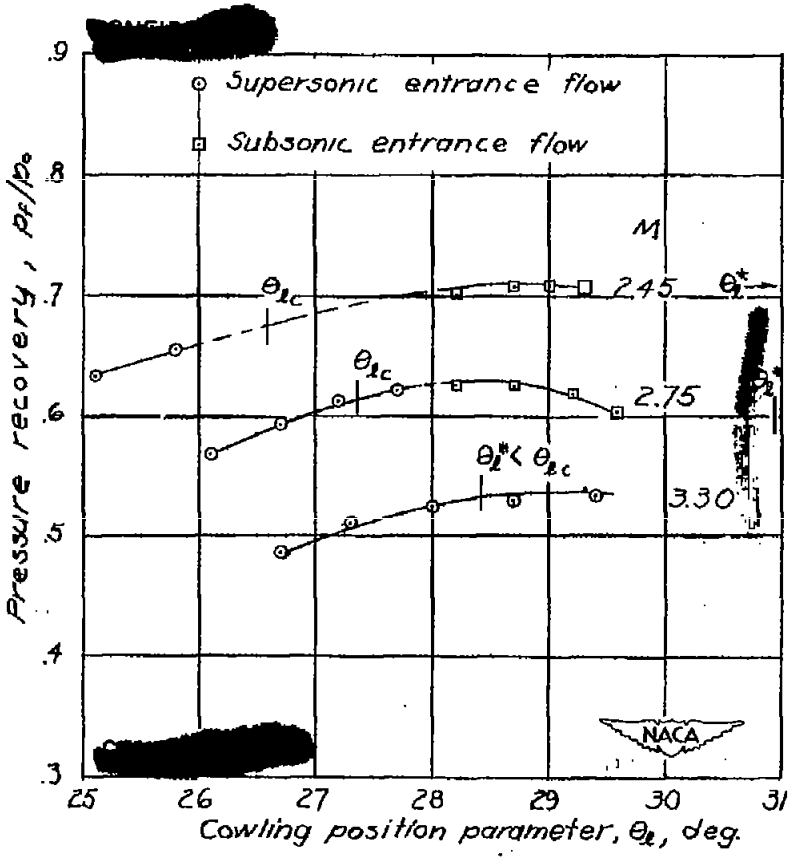

(b) 4°, 7° cowling; $D_B/D_L = 0.834$; $\theta_c = 20^\circ$.

Figure 12.- Continued.

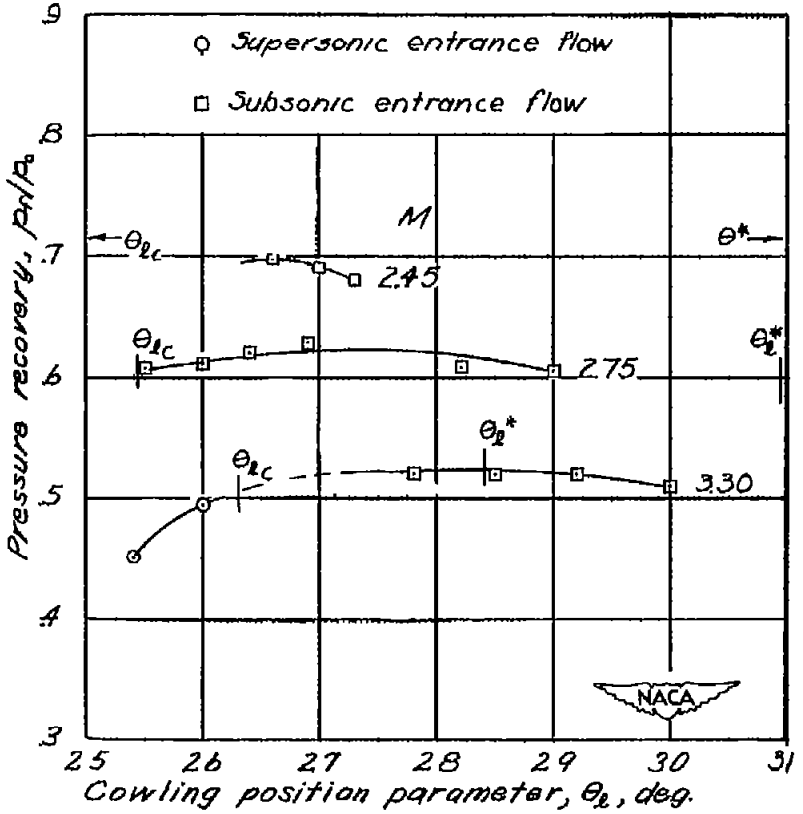

(c) $4^\circ, 7^\circ$ cowling; $D_B/D_L = 0.867$; $\theta_c = 20^\circ$.

Figure 12.- Concluded.

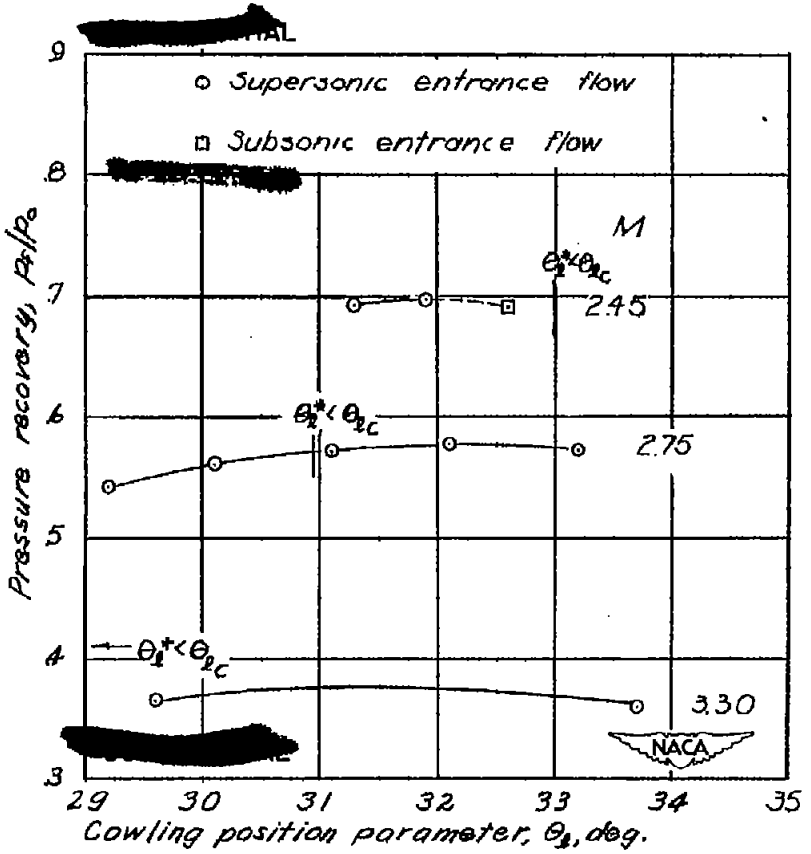

(a) [redacted] cowling; $D_B/D_L = 0.719$; $\theta_c = 20^\circ$.

Figure 13.- Pressure recovery as a function of the cowling position parameter for $\theta_c = 20^\circ$ at different Mach numbers.

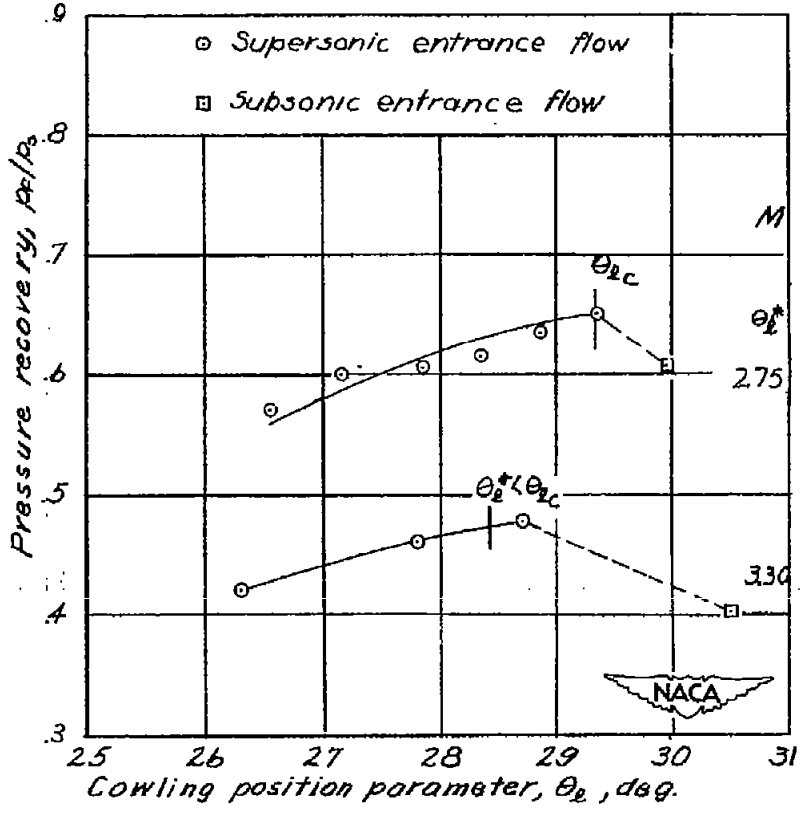

(b) 7°, 10° cowling; $D_B/D_L = 0.817$; $\theta_c = 20^\circ$.

Figure 13.- Continued.

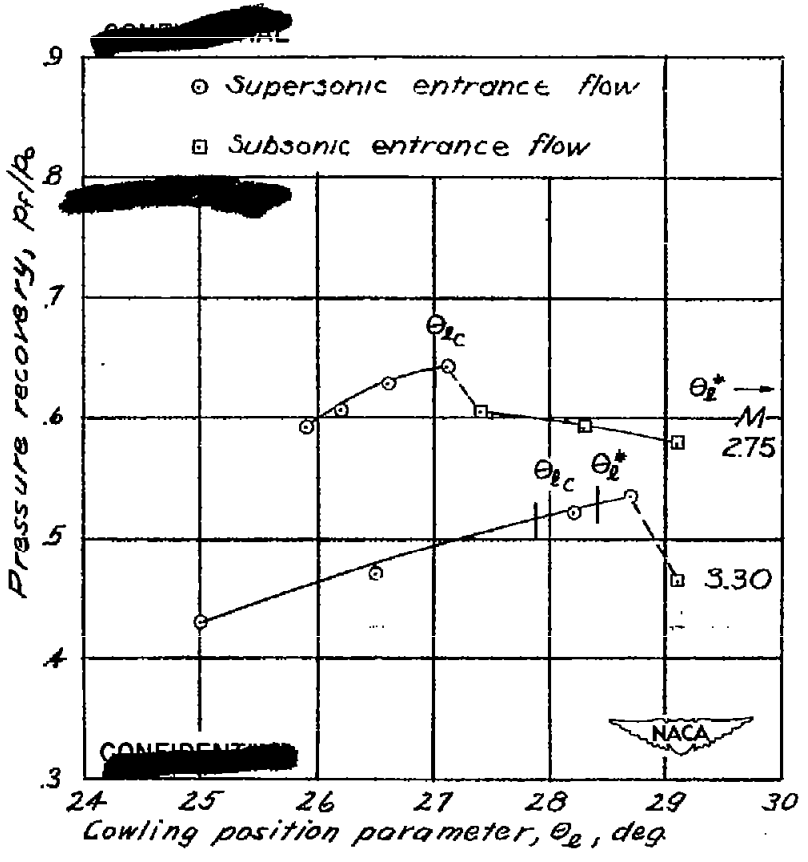

(c) [redacted] cowling; $D_B/D_L = 0.850$; $\theta_c = 20^\circ$.

Figure 13.- Concluded.

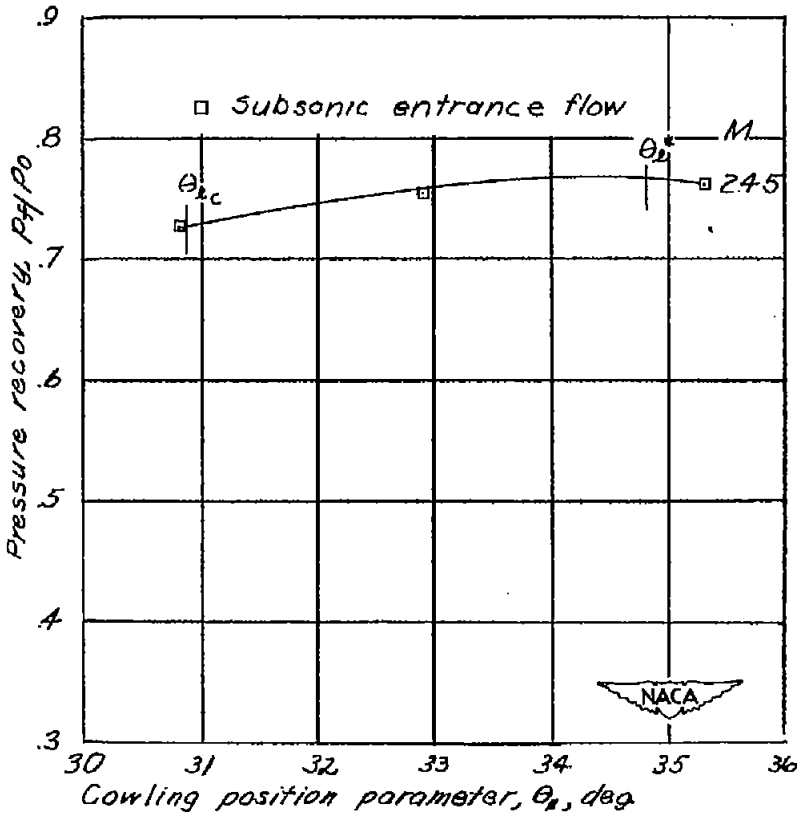

(a) 0°, 2° cowling; $D_B/D_L = 0.733$; $\theta_c = 22^\circ$.

Figure 14.- Pressure recovery as a function of the cowling position parameter for $\theta_c = 22^\circ$ at $M = 2.45$.

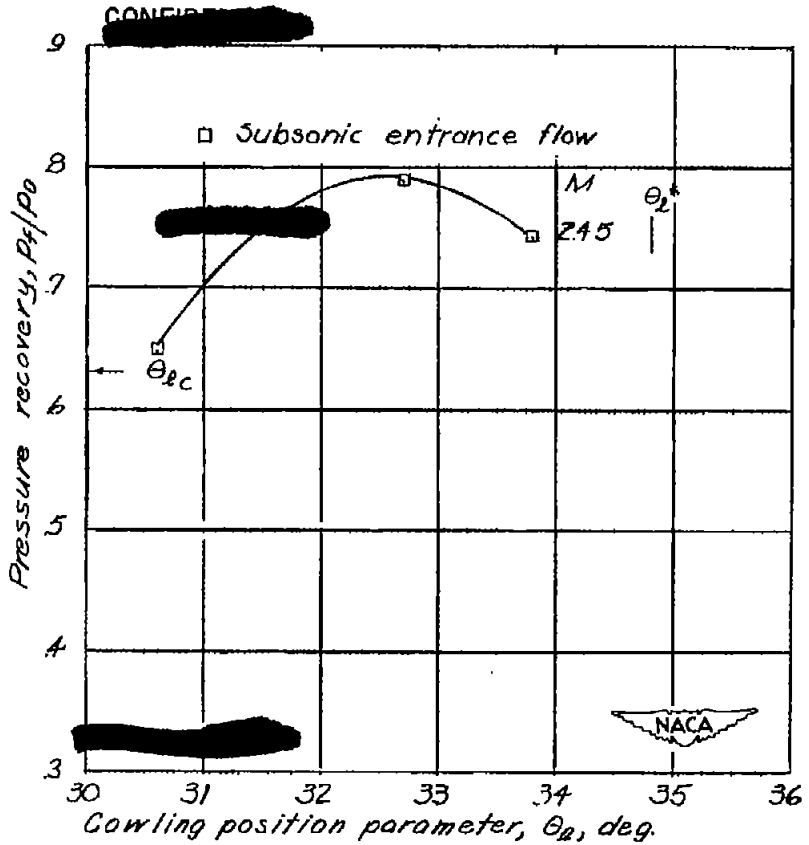

(b) 0°, 2° cowling; $D_B/D_L = 0.767$; $\theta_c = 22^\circ$.

Figure 14.- Concluded.

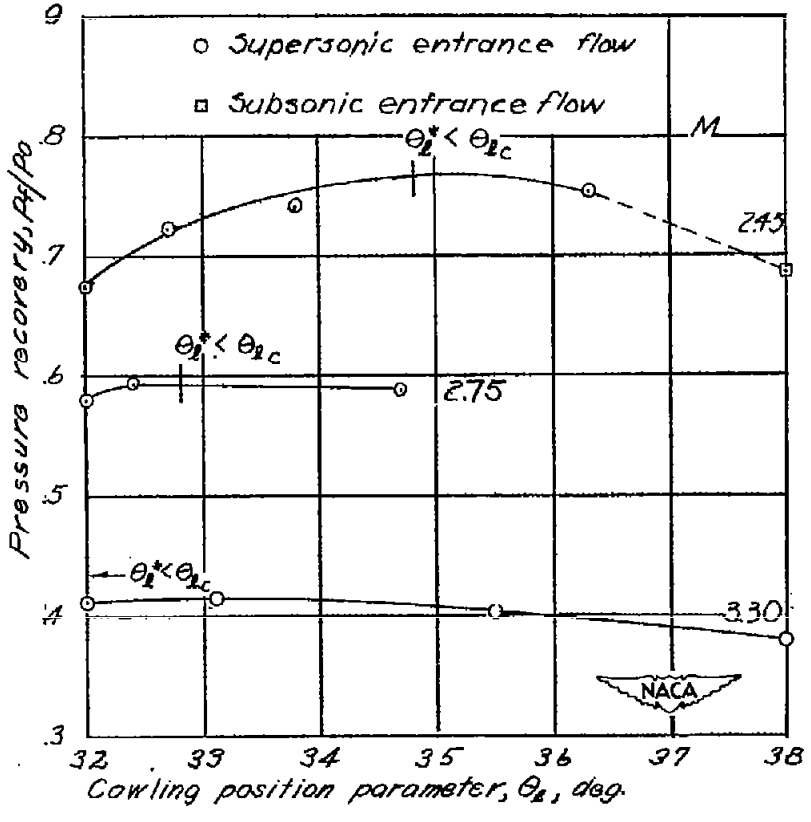

(a) 4°, 7° cowling; $D_B/D_L = 0.733$; $\theta_c = 22^\circ$.

Figure 15.- Pressure recovery as a function of the cowling position parameter for $\theta_c = 22^\circ$ at different Mach numbers.

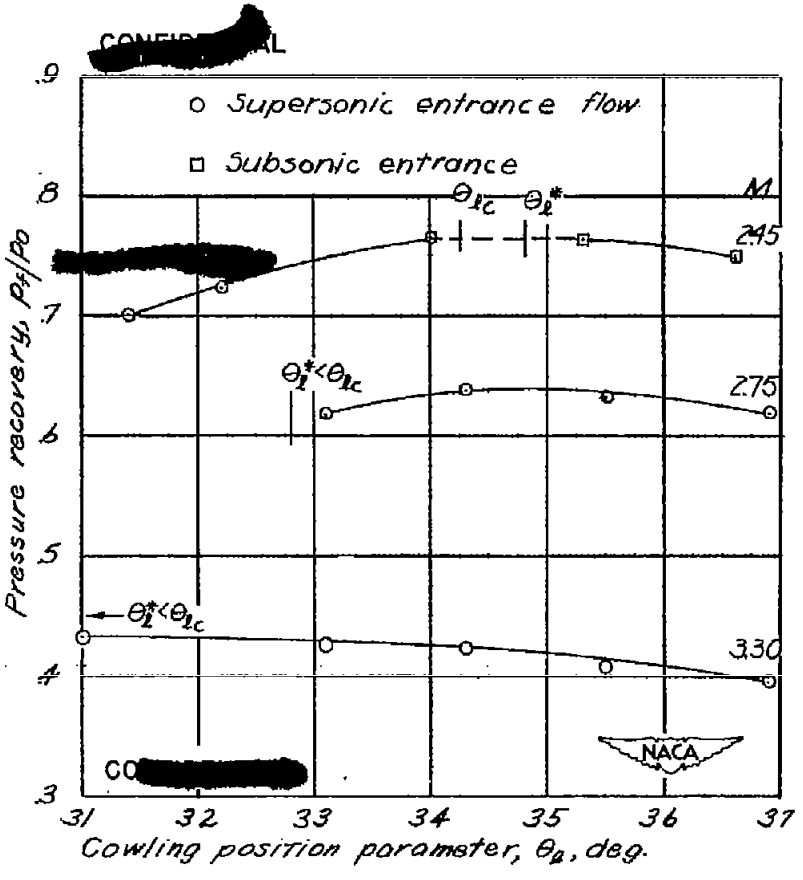

(b) 4°, 7° cowling; $D_B/D_L = 0.767$; $\theta_c = 22^\circ$.

Figure 15.- Continued.

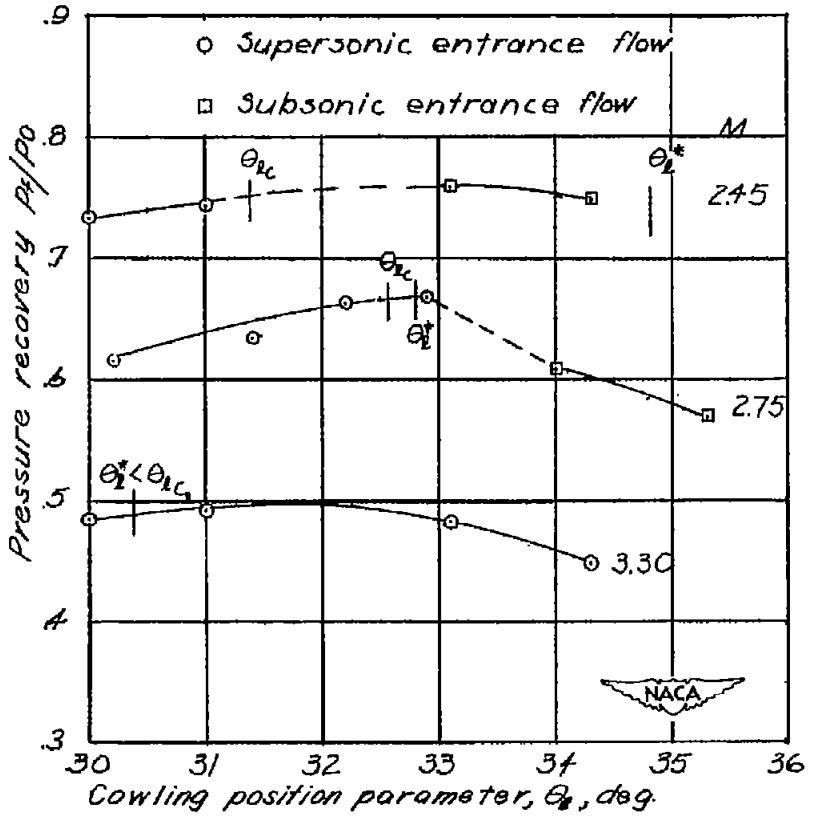

(c) 4°, 7° cowling; $D_B/D_L = 0.800$; $\theta_c = 22^\circ$.

Figure 15.- Continued.

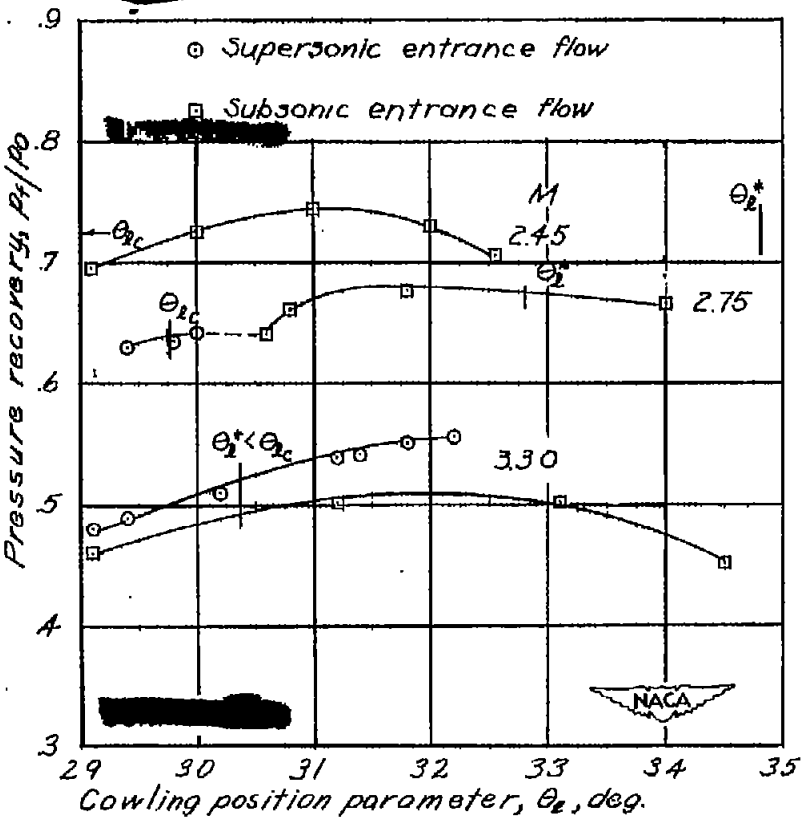

(d) 4°, 7° cowling; $D_B/D_L = 0.834$; $\theta_c = 22^\circ$.

Figure 15.- Continued.

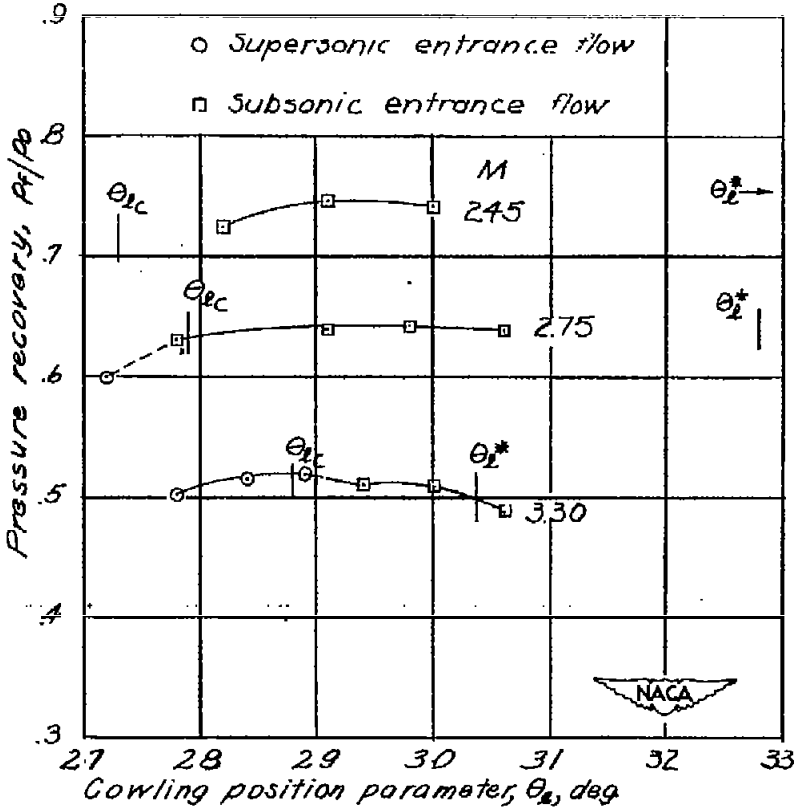

(e) 4°, 7° cowling; $D_B/D_L = 0.867$; $\theta_c = 22^\circ$.

Figure 15.- Concluded.

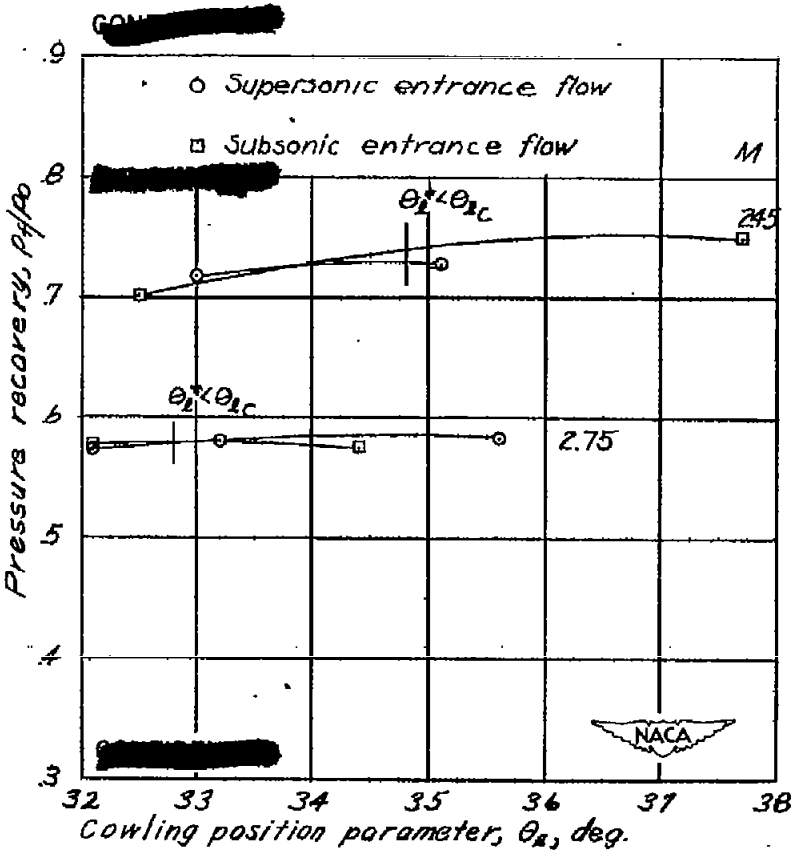

(a) [redacted]ing; $D_B/D_L = 0.719$; $\theta_c = 22^\circ$.

Figure 16.- Pressure recovery as a function of the cowling position parameter for $\theta_c = 22^\circ$ at different Mach numbers.

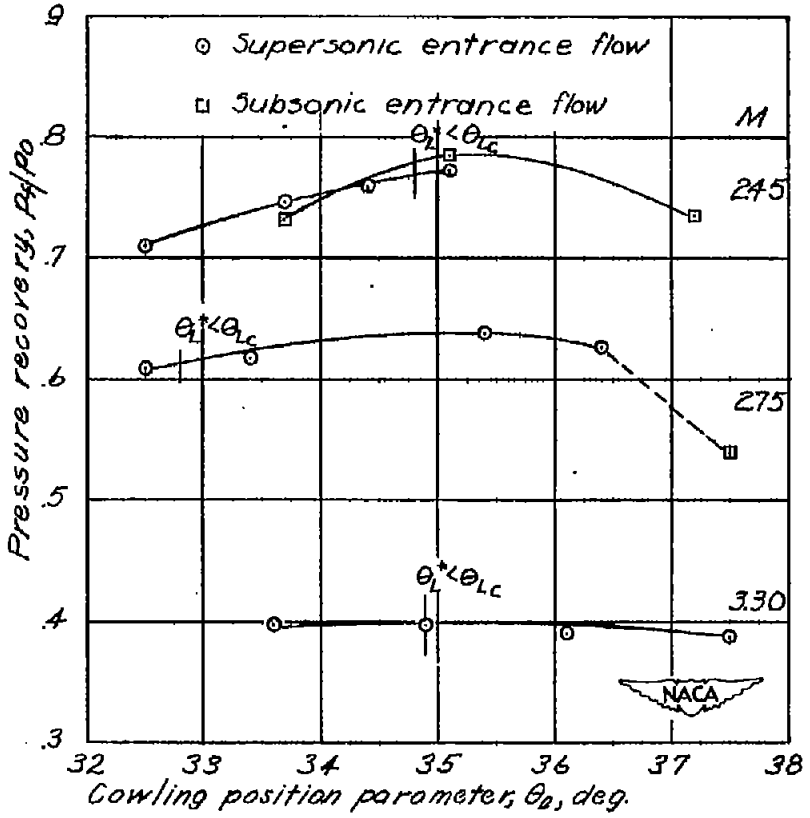

(b) 7°, 10° cowling; $D_B/D_L = 0.752$; $\theta_c = 22°$.

Figure 16.- Continued.

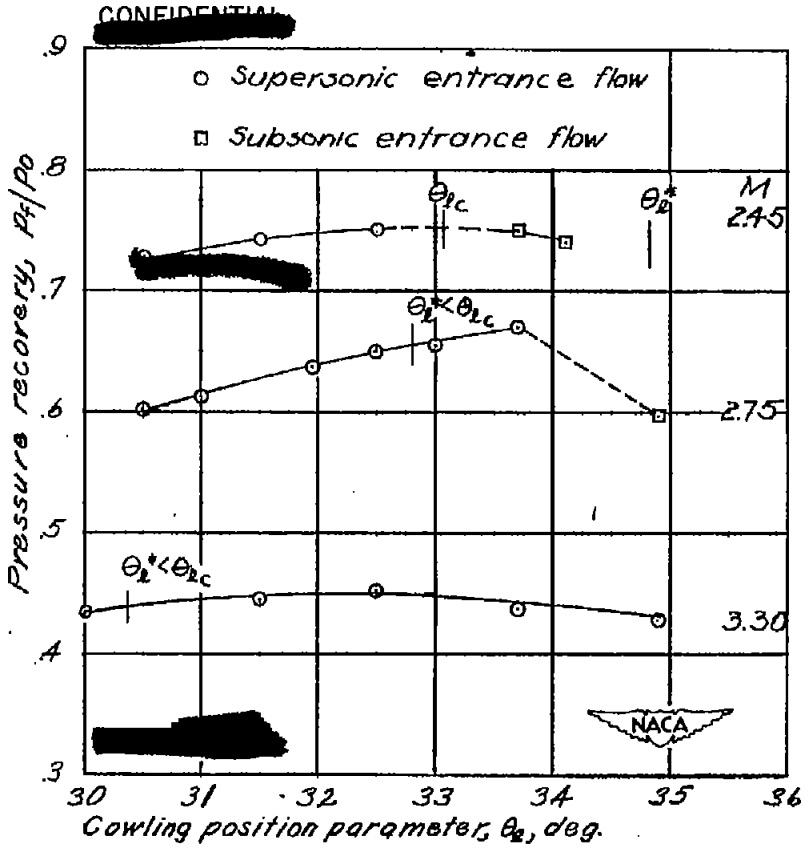

(c) 7°, 10° cowling; $D_B/D_L = 0.784$; $\theta_c = 22°$.

Figure 16.- Continued.

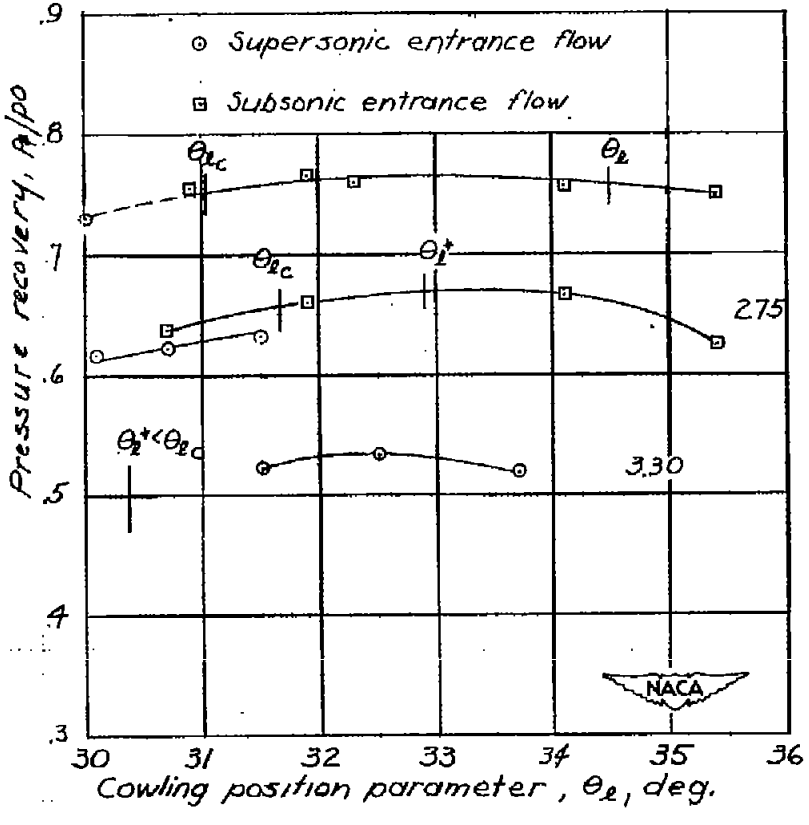

(d) 7°, 10° cowling; $D_B/D_L = 0.817$; $\theta_c = 22^\circ$.

Figure 16.- Continued.

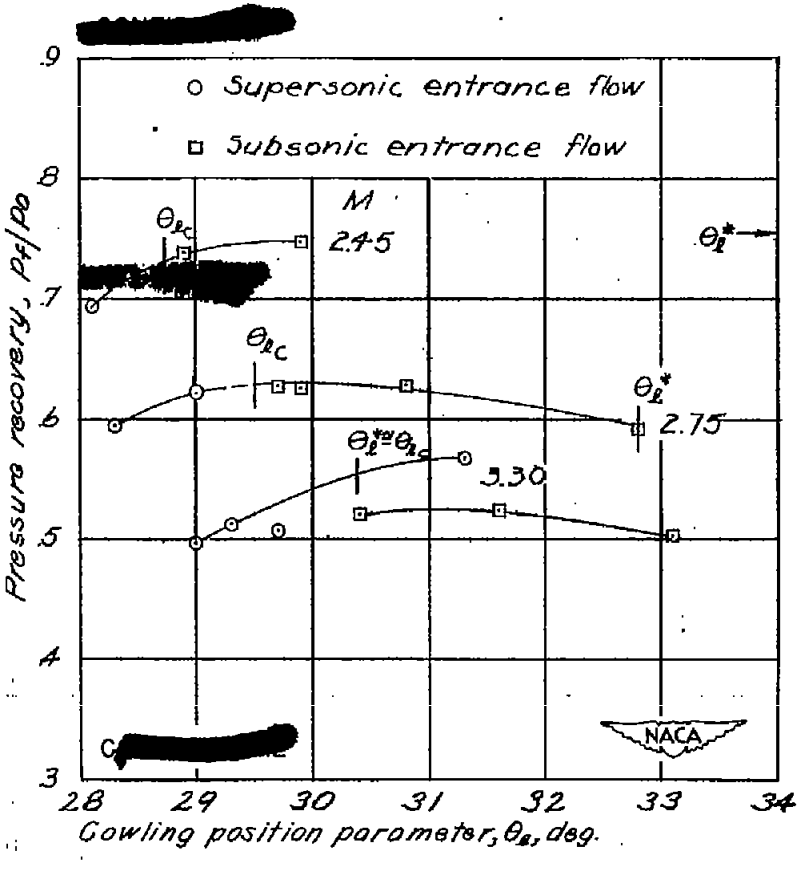

(e) 7°, 10° cowling; $D_B/D_L = 0.850$; $\theta_c = 22^\circ$.

Figure 16.- Concluded.

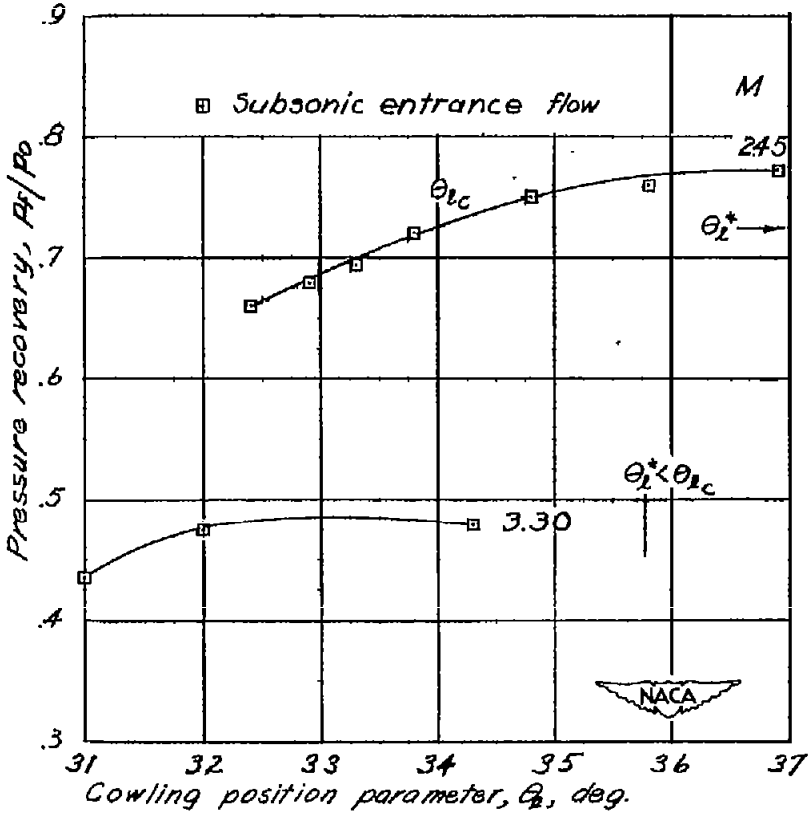

(a) 0°, 2° cowling; $D_B/D_L = 0.733$; $\theta_c = 25^\circ$.

Figure 17.- Pressure recovery as a function of the cowling position parameter for $\theta_c = 25^\circ$.

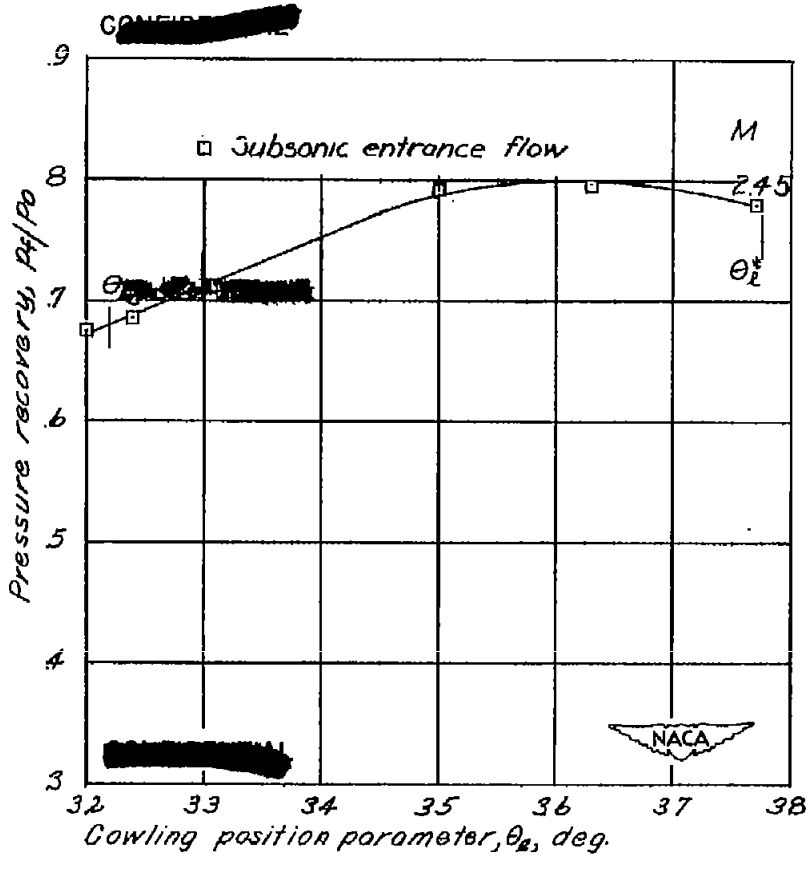

(b) 0°, 2° cowling; $D_B/D_L = 0.767$; $\theta_c = 25^\circ$.

Figure 17.- Continued.

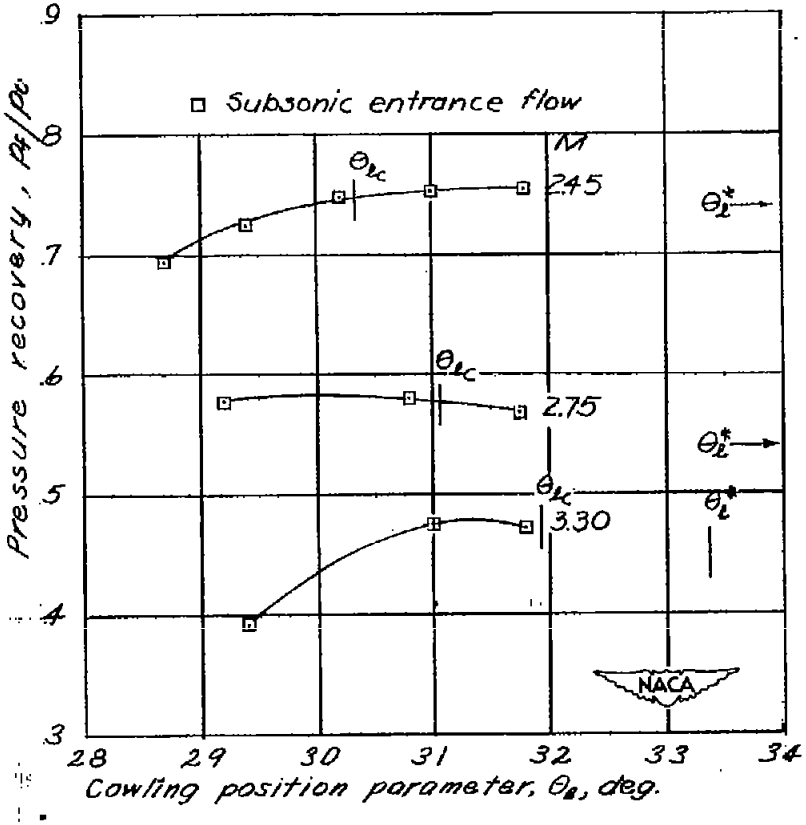

(c) 0°, 2° cowling; $D_B/D_L = 0.800$; $\theta_c = 25^\circ$.

Figure 17.- Concluded.

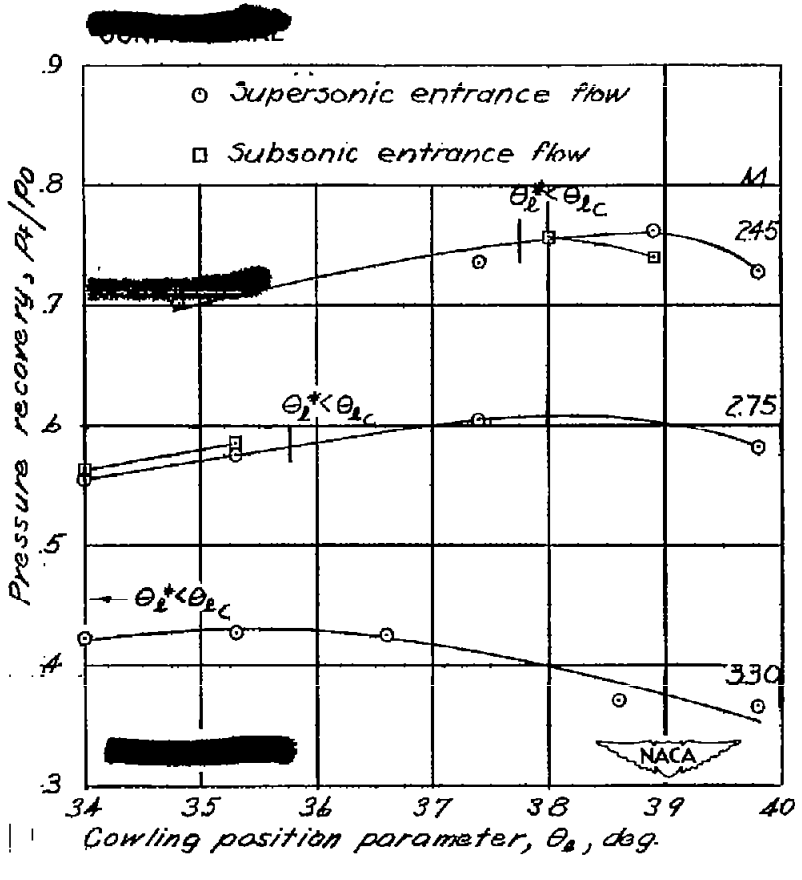

(a) 4°, 7° cowling; $D_B/D_L = 0.733$; $\theta_c = 25^\circ$.

Figure 18.- Pressure recovery as a function of the cowling position parameter for $\theta_c = 25^\circ$.

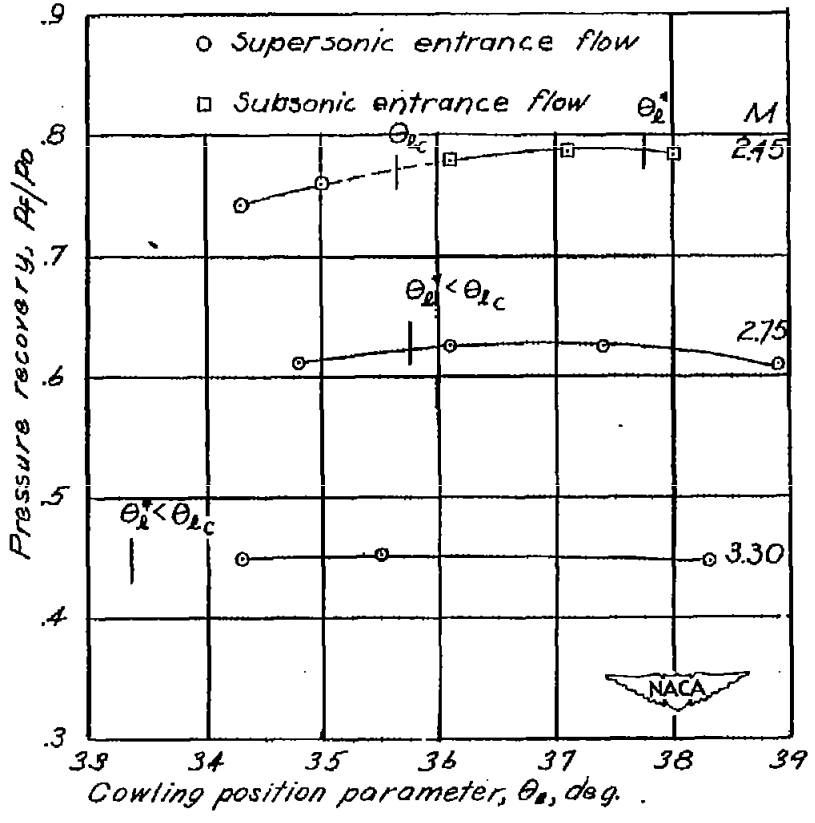

(b) 4°, 7° cowling; $D_B/D_L = 0.767$; $\theta_c = 25°$.

Figure 18.- Continued.

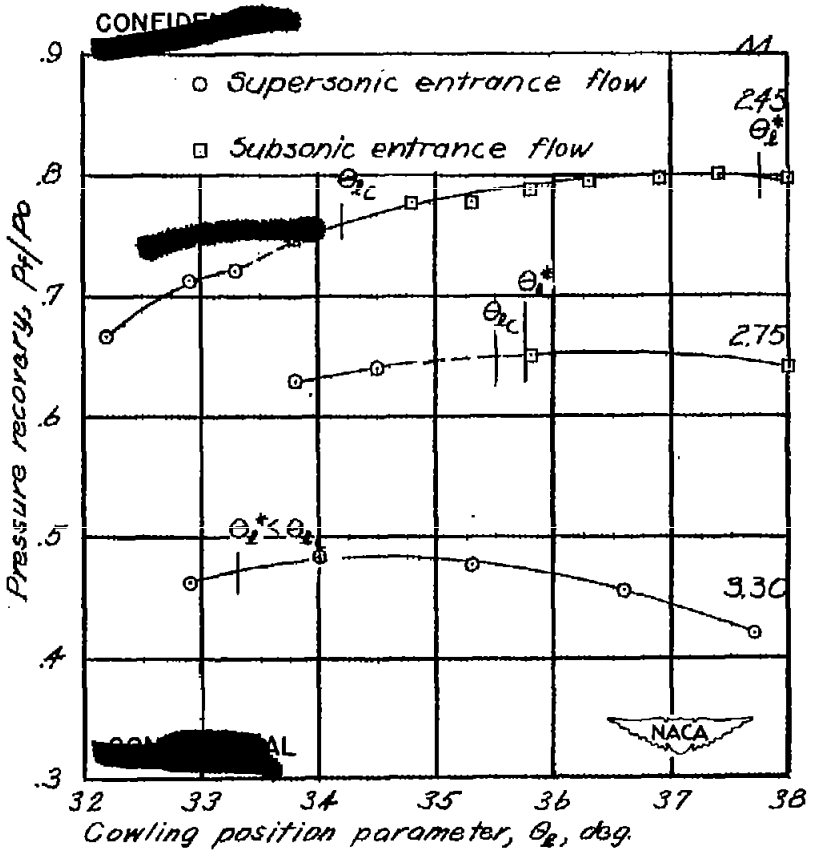

(c) 4°, 7° cowling; $D_B/D_L = 0.800$; $\theta_c = 25°$.

Figure 18.- Continued.

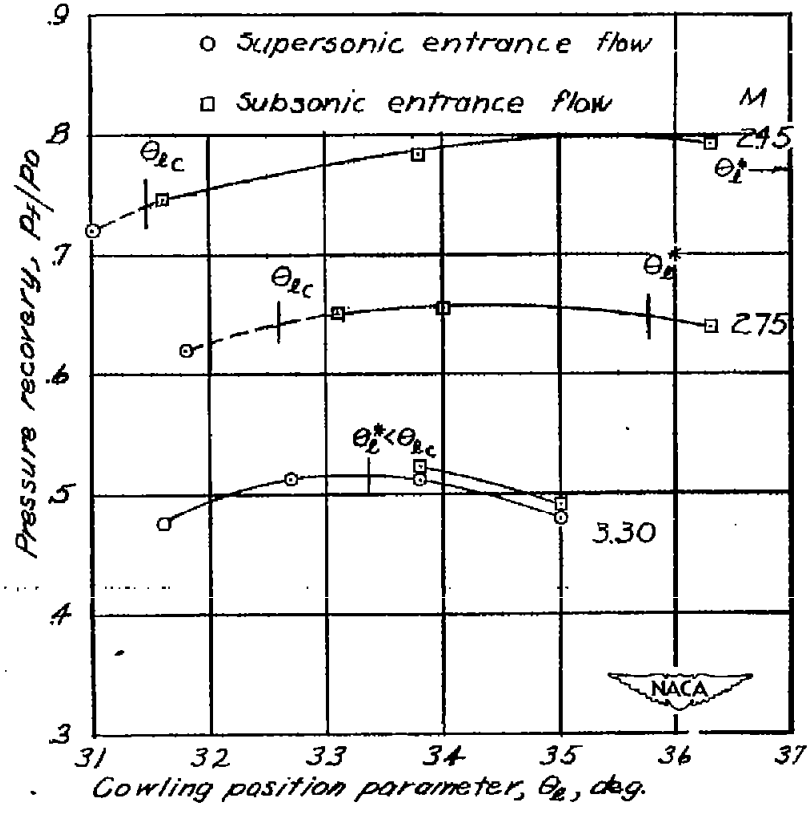

(d) 4°, 7° cowling; $D_B/D_L = 0.834$; $\theta_c = 25^\circ$.

Figure 18.- Continued.

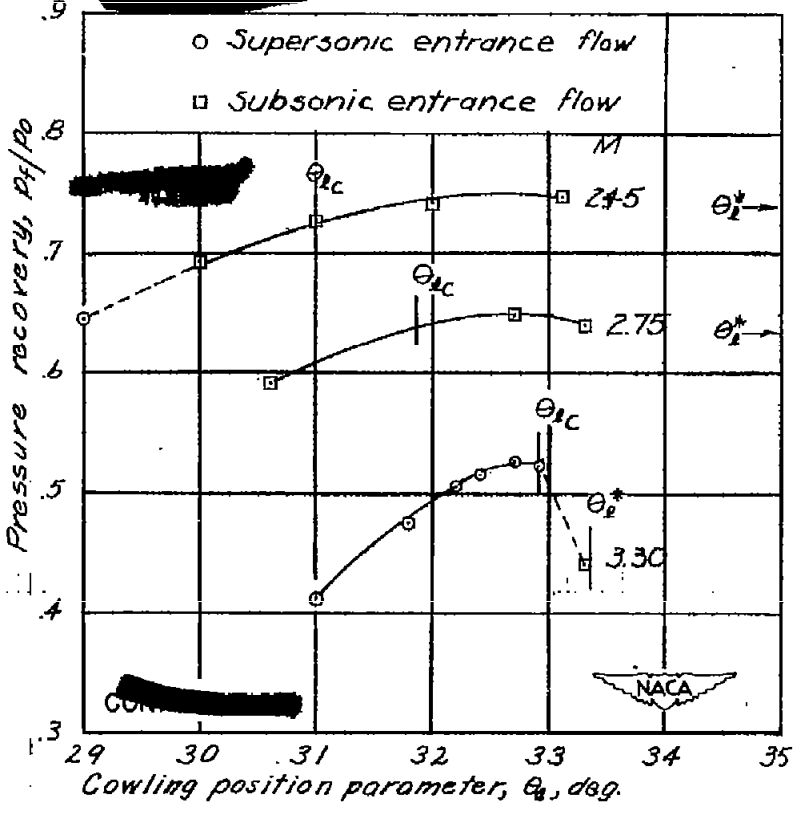

(e) 4°, 7° cowling; $D_B/D_L = 0.847$; $\theta_c = 25^\circ$.

Figure 18.- Continued.

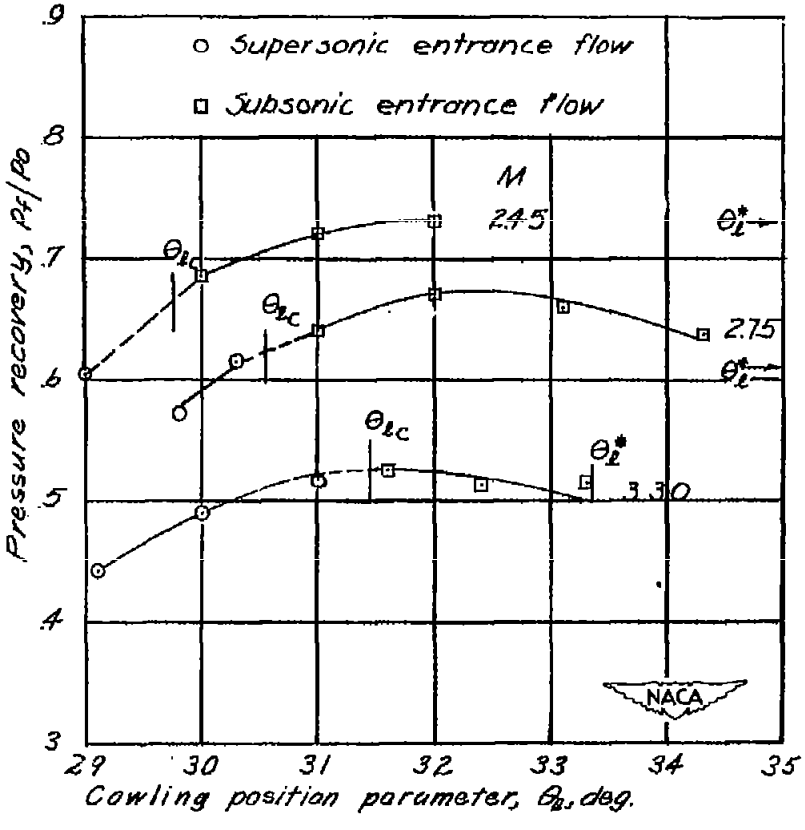

(f) 4°, 7° cowling; $D_B/D_L = 0.867$; $\theta_c = 25^\circ$.

Figure 18.- Concluded.

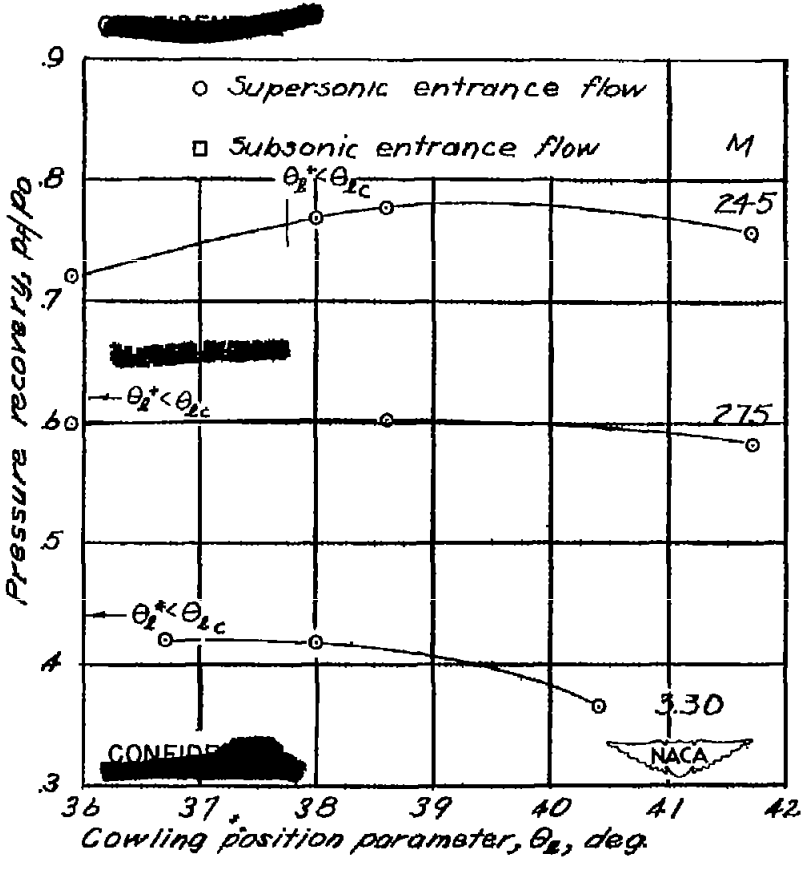

(a) 7°, 10° cowling; $D_B/D_L = 0.719$; $\theta_c = 25^\circ$.

Figure 19.- Pressure recovery as a function of the cowling position parameter for $\theta_c = 25^\circ$ at different Mach numbers.

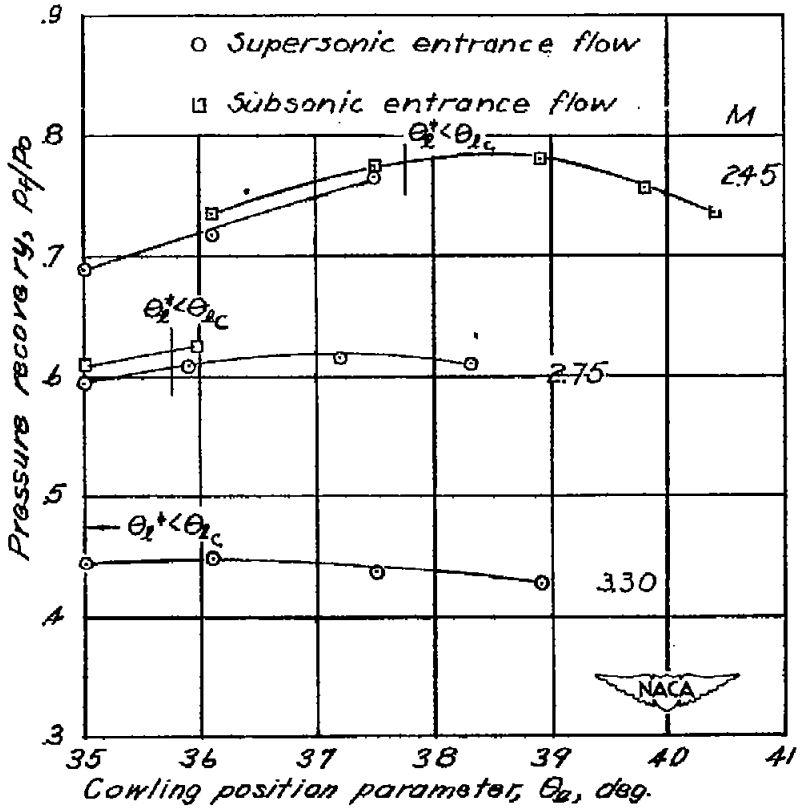

(b) 7°, 10° cowling; $D_B/D_L = 0.752$; $\theta_c = 25^\circ$.

Figure 19.- Continued.

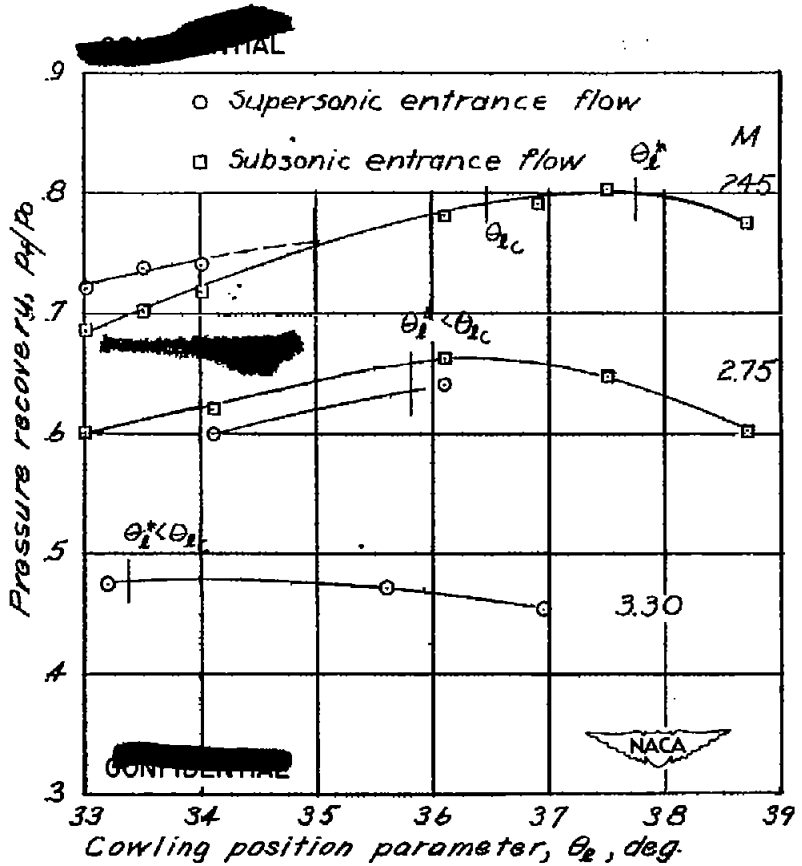

(c) 7°, 10° cowling; $D_B/D_L = 0.784$; $\theta_c = 25^\circ$.

Figure 19.- Continued.

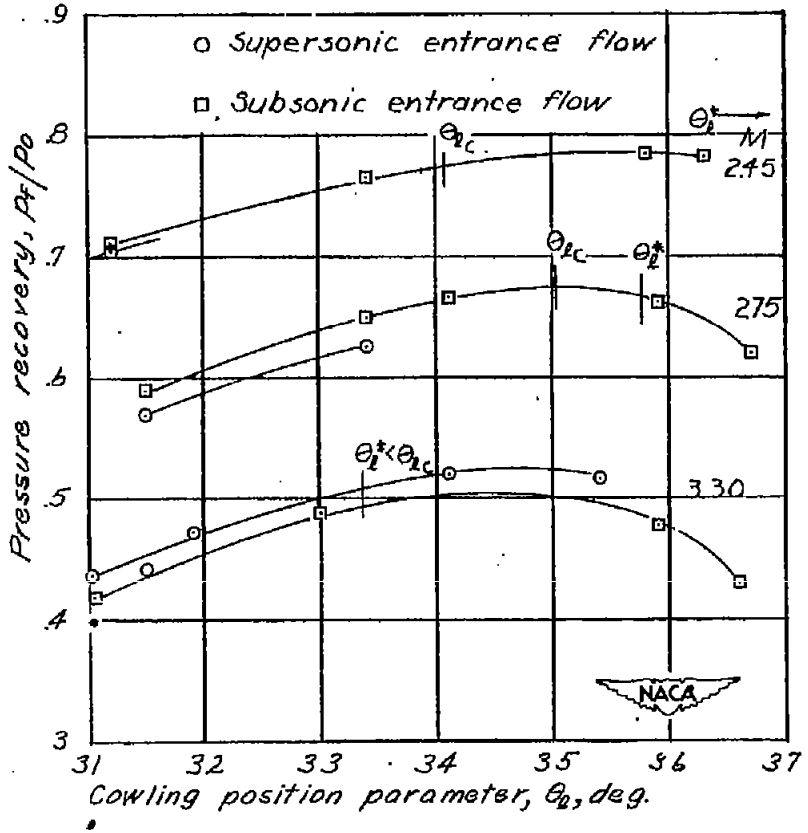

(d) 7°, 10° cowling; $D_B/D_L = 0.817$; $\theta_c = 25^\circ$.

Figure 19.- Continued.

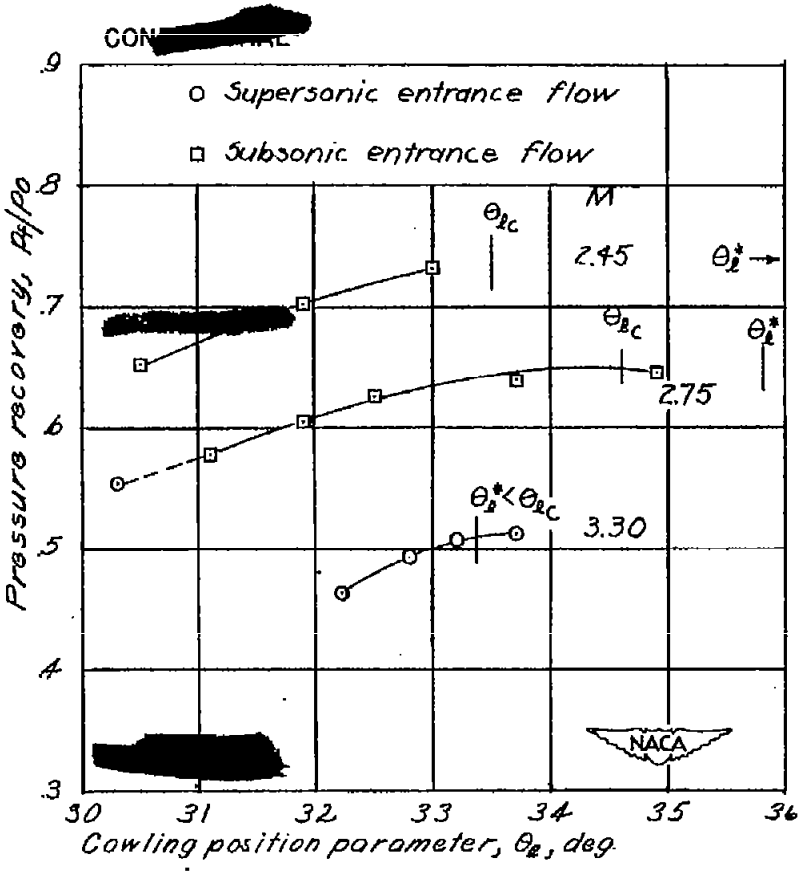

(e) 7°, 10° cowling; $D_B/D_L = 0.830$; $\theta_c = 25^\circ$.

Figure 19.- Continued.

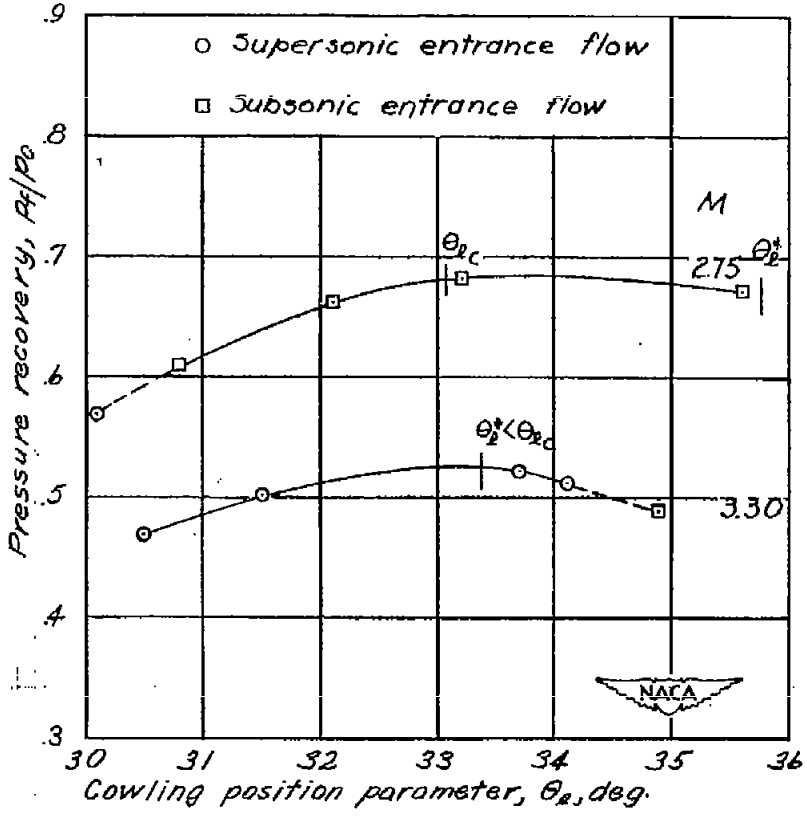

(f) 7°, 10° cowling; $D_B/D_L = 0.850$; $\theta_c = 25^\circ$.

Figure 19.- Concluded.

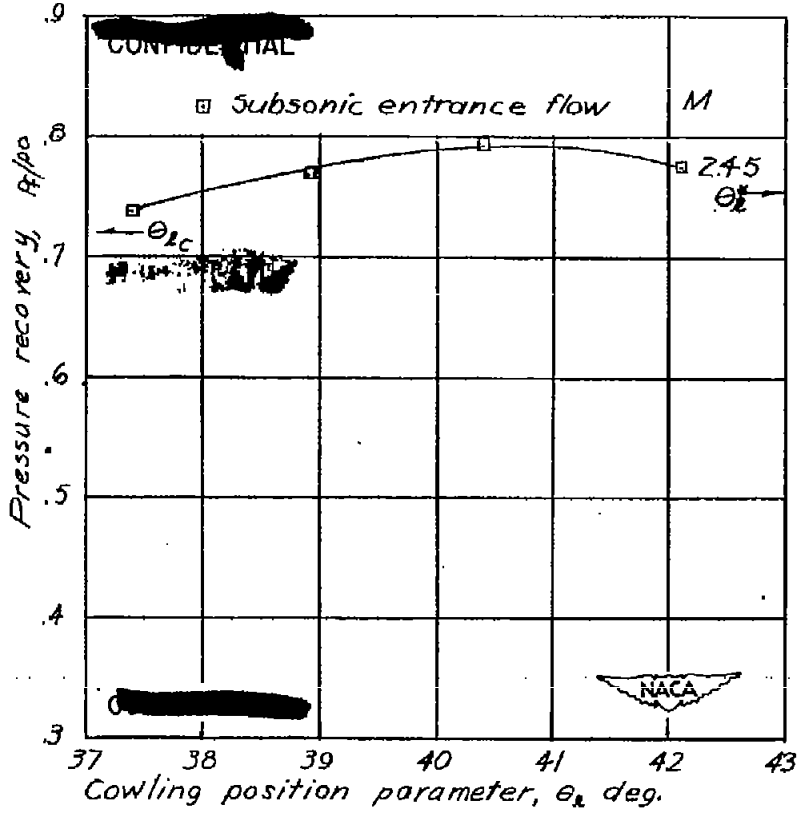

(a) 0°, 2° cowling; $D_B/D_L = 0.767$; $\theta_c = 30^\circ$.

Figure 20.- Pressure recovery as a function of the cowling position parameter for $\theta_c = 30^\circ$ at M = 2.45.

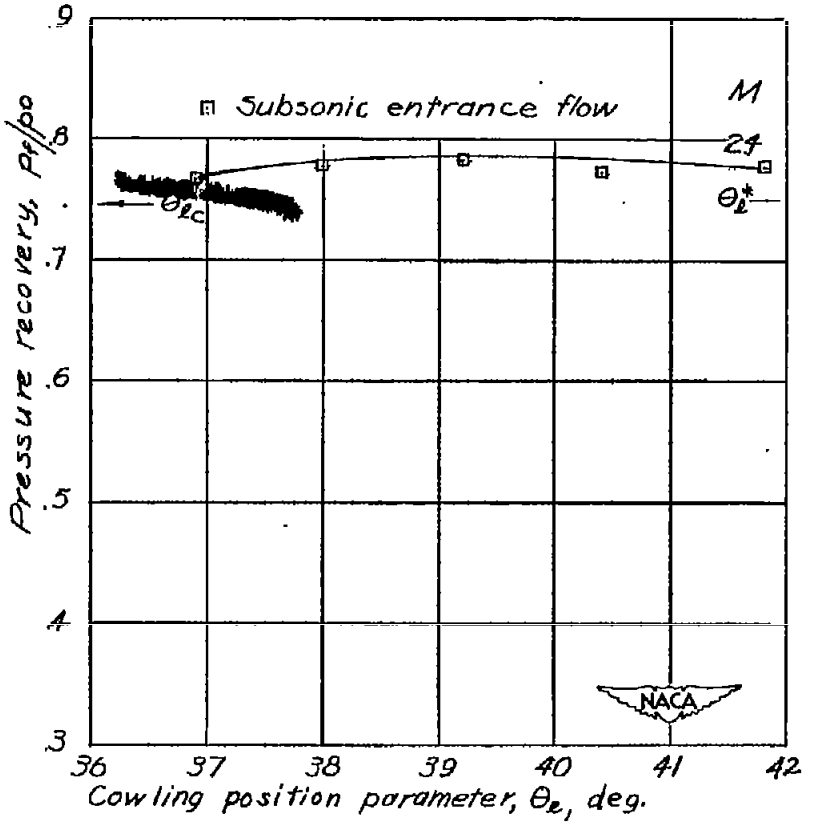

(b) 0°, 2° cowling; $D_B/D_L = 0.800$; $\theta_c = 30^\circ$.

Figure 20.- Concluded.

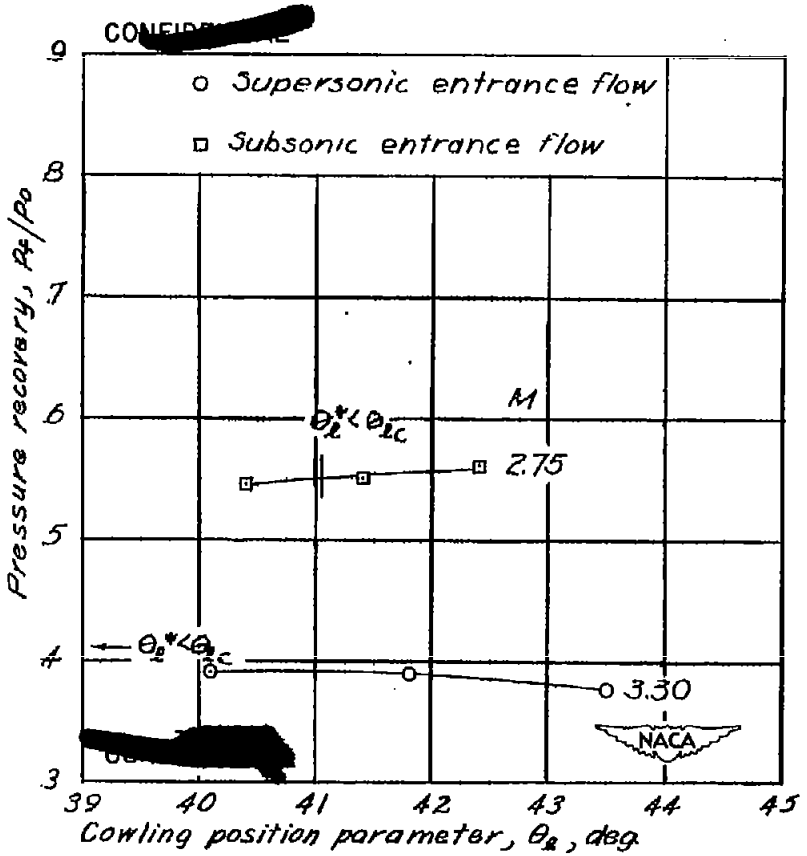

(a) 4°, 7° cowling; $D_B/D_L = 0.733$; $\theta_c = 30^\circ$.

Figure 21.- Pressure recovery as a function of the cowling position parameter for $\theta_c = 30^\circ$ at different Mach numbers.

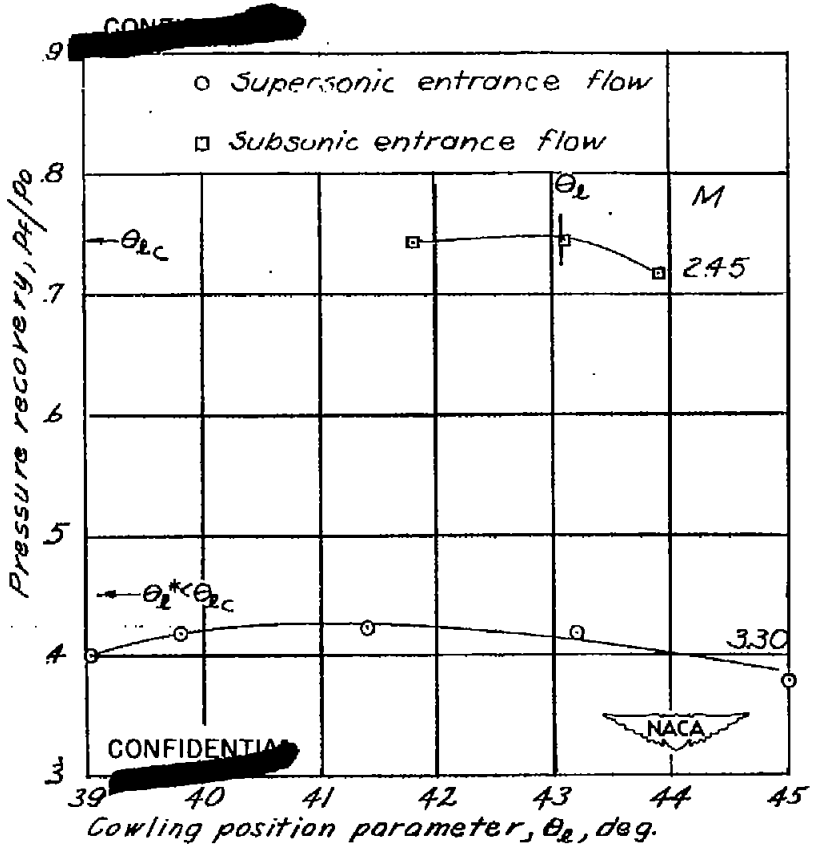

(b) 4°, 7° cowling; $D_B/D_L = 0.767$; $\theta_c = 30^\circ$.

Figure 21.- Continued.

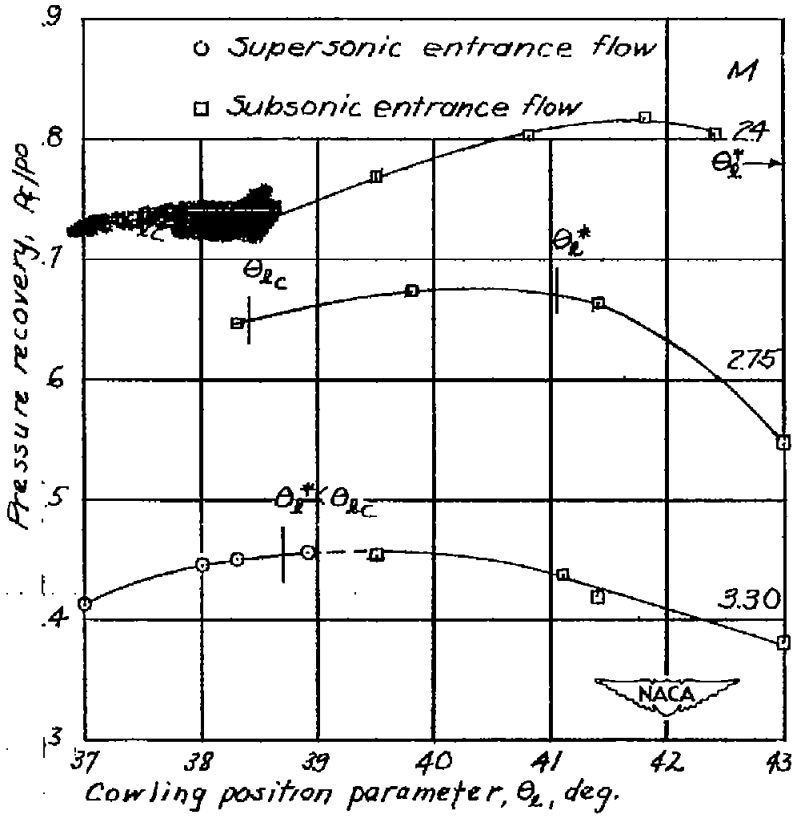

(c) 4°, 7° cowling; $D_B/D_L = 0.800$.

ure 21.- Concluded.

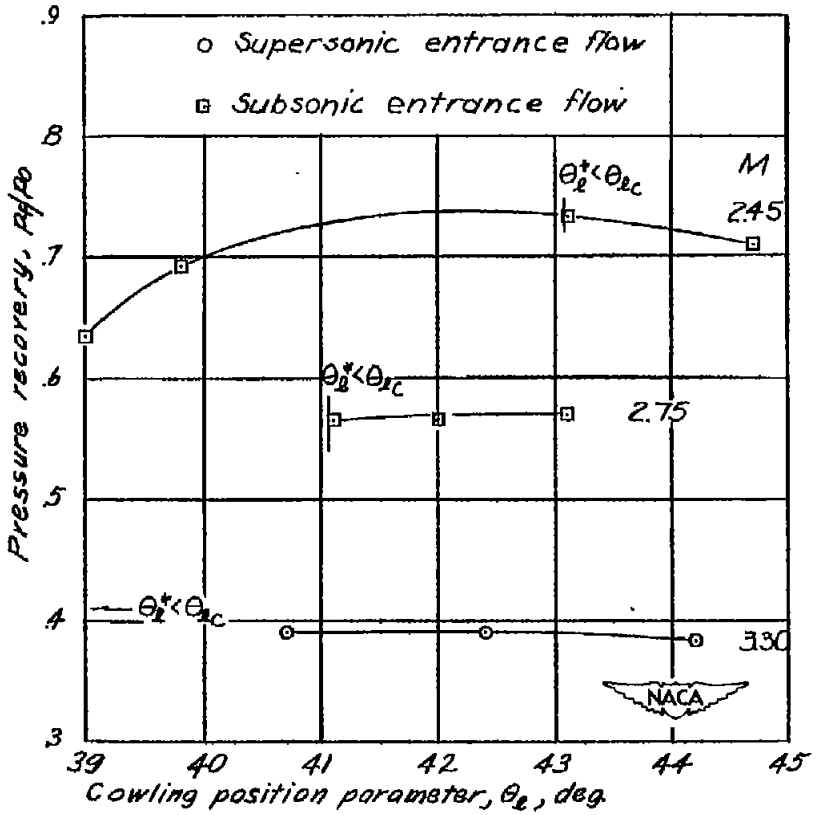

(a) 7°, 10° cowling; $D_B/D_L = 0.719$; $\theta_c = 30^\circ$.

Figure 22.- Pressure recovery as a function of the cowling position parameter for $\theta_c = 30^\circ$ at different Mach numbers.

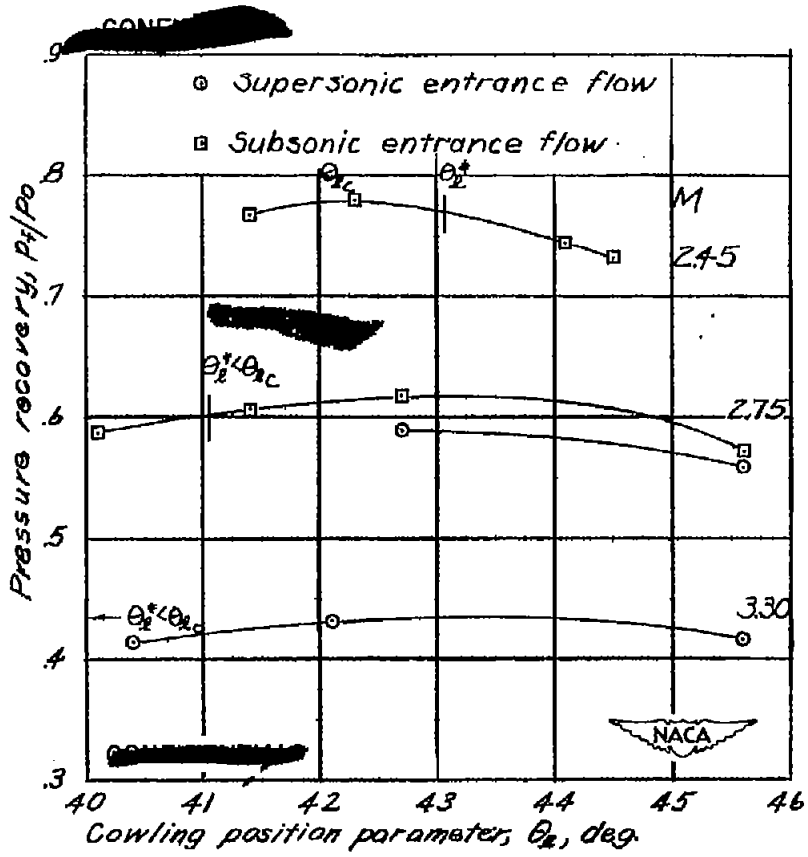

(b) 7°, 10° cowling; $D_B/D_L = 0.752$; $\theta_c = 30^\circ$.

Figure 22.- Continued.

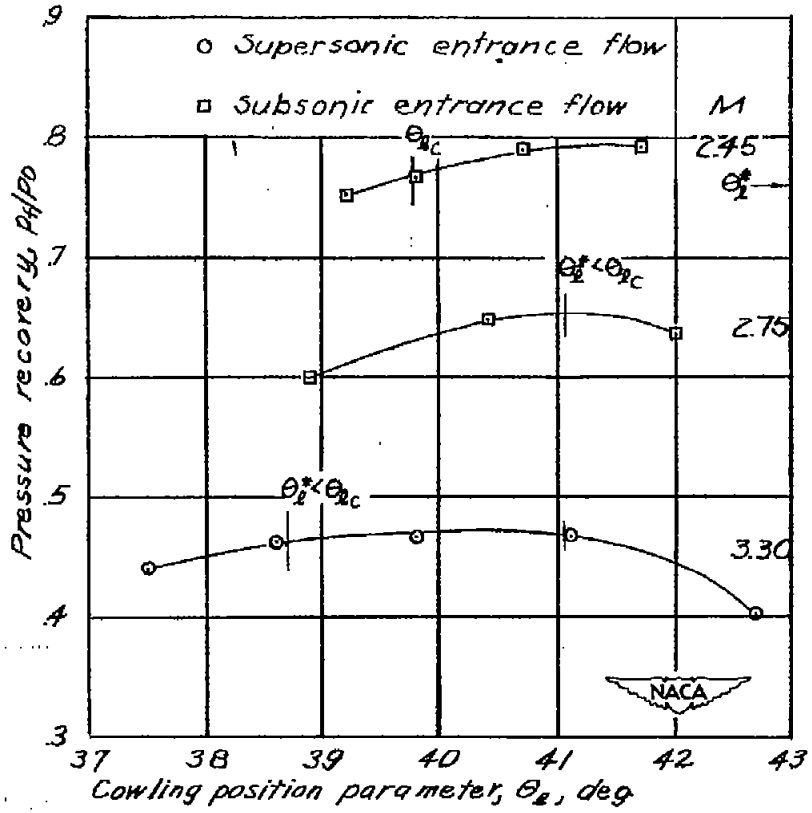

(c) 7°, 10° cowling; $D_B/D_L = 0.784$; $\theta_c = 30^\circ$.

Figure 22.- Concluded.

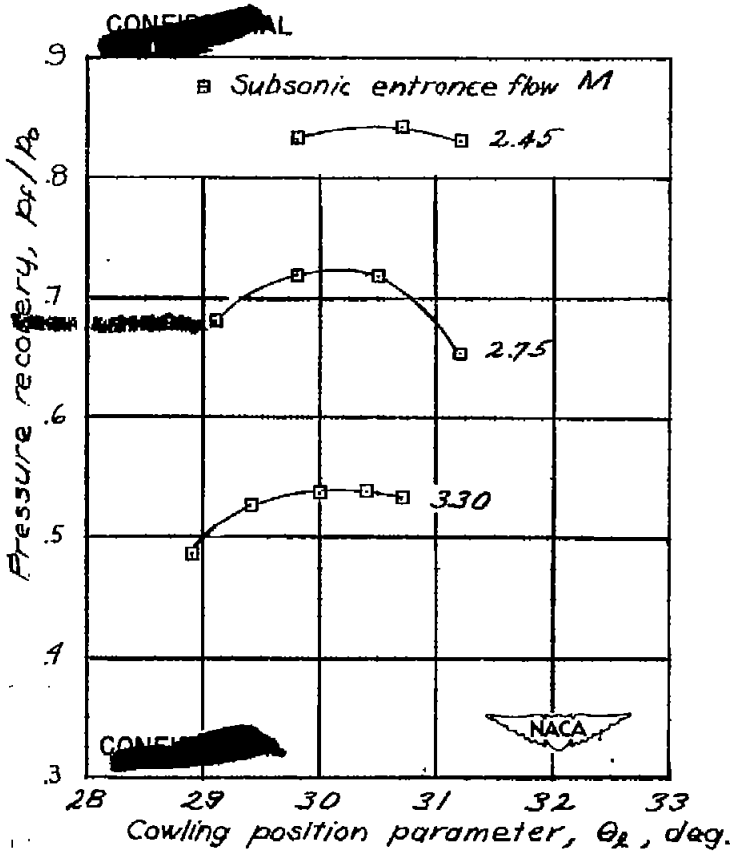

Figure 23.- Pressure recovery as a function of the cowling position parameter for the inlet with large external compression at different Mach numbers.

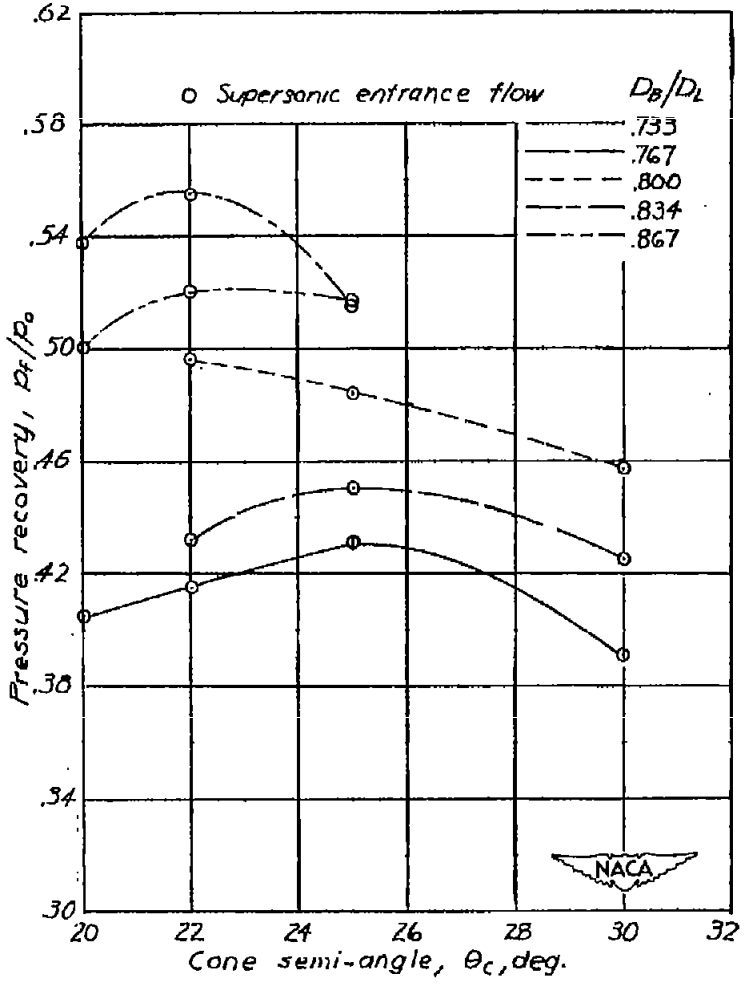

(a) 4°, 7° cowling.

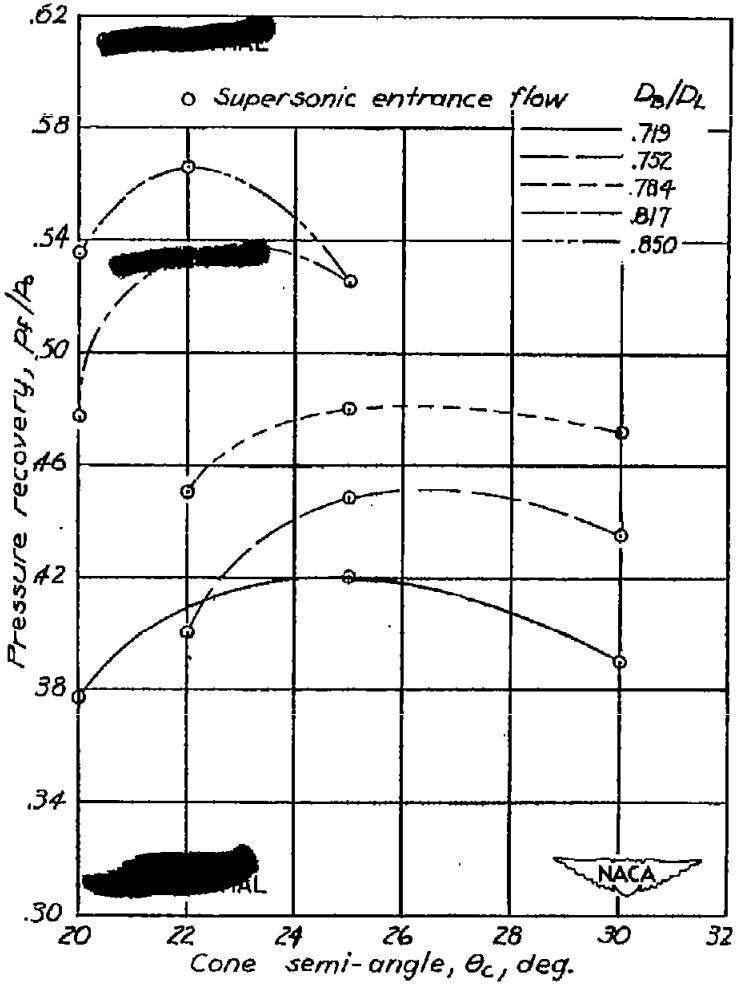

(b) 7°, 10° cowling.

Figure 24.- Highest pressure recovery obtained as a function of the cone semi-angle for various central body diameter parameters for M = 3.30.

Figure 24.- Concluded.

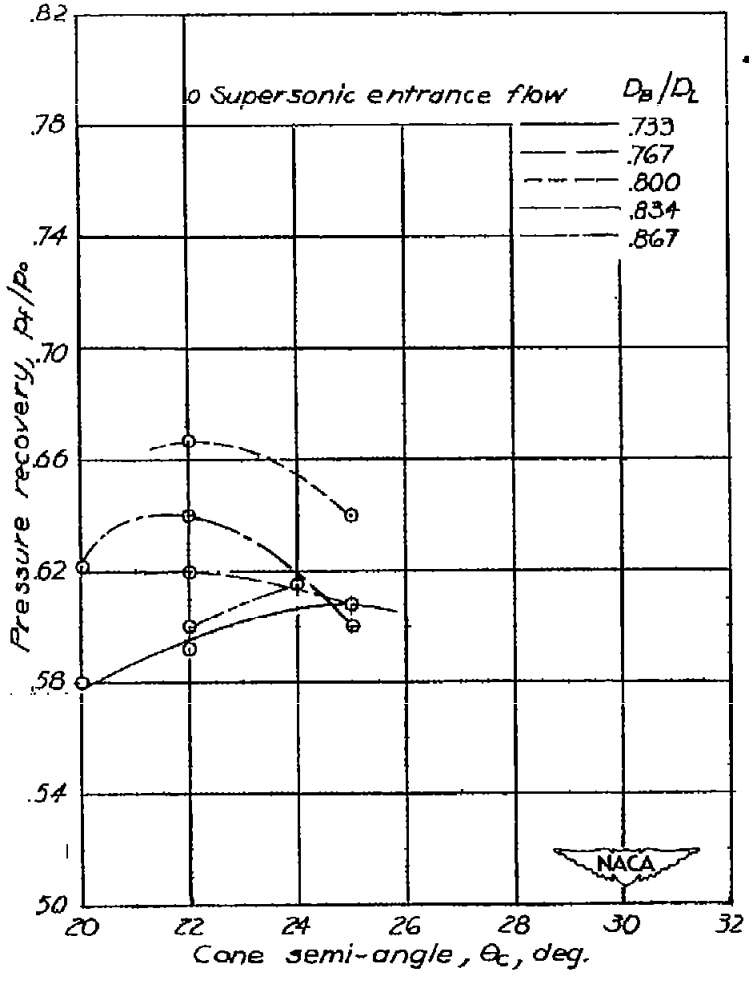

(a) 4°, 7° cowling.

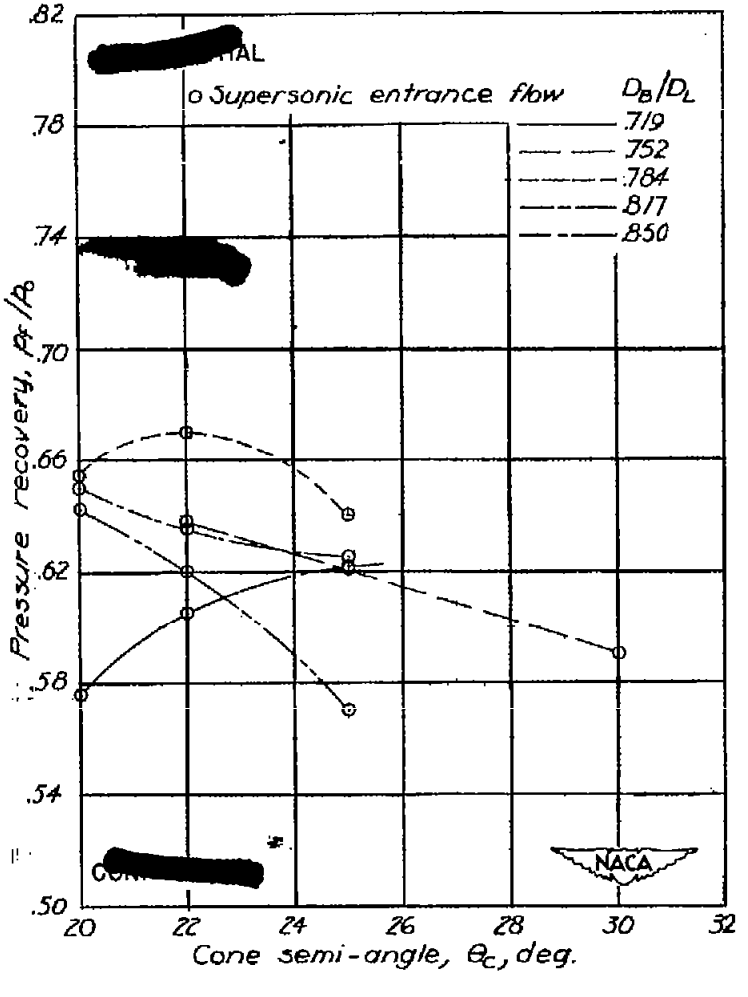

(b) 7°, 10° cowling.

Figure 25.- Highest pressure recovery obtained as a function of the cone semi-angle for various central body diameter parameters for M = 2.75.

[redacted]gure 25.- Continued.

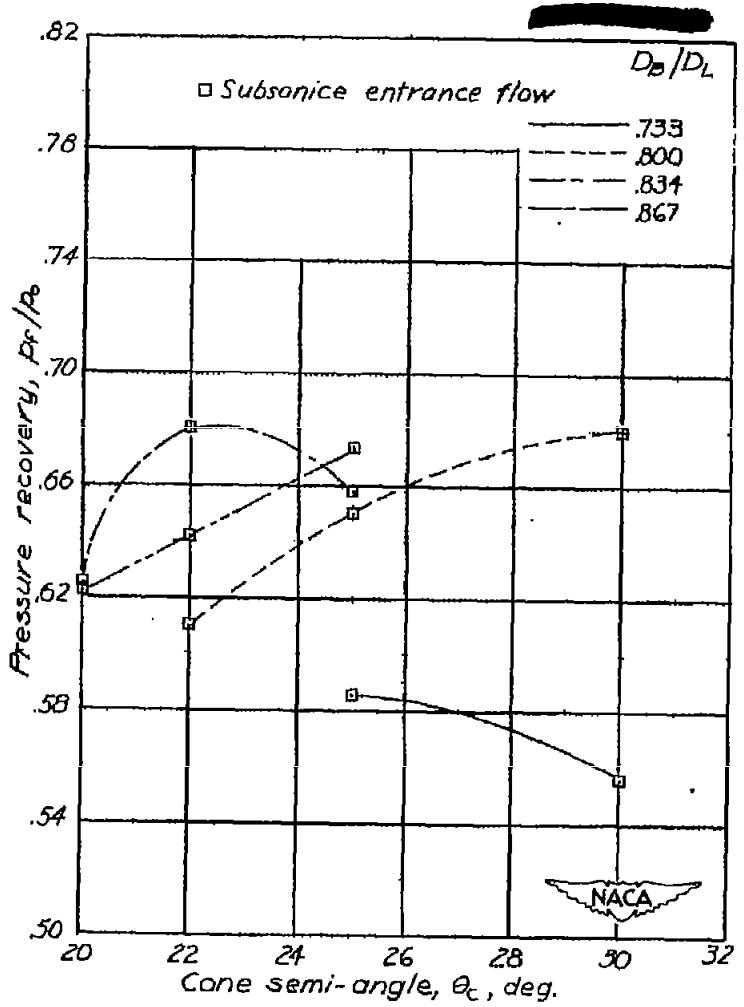

(c) 4°, 7° cowling.

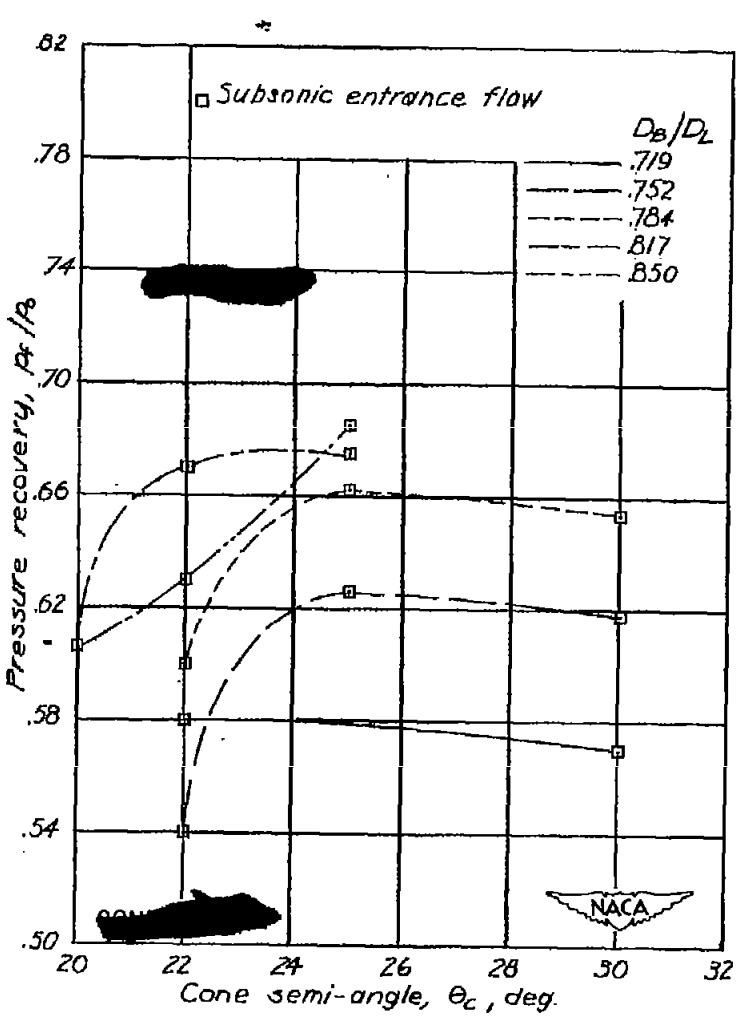

(d) 7°, 10° cowling.

Figure 25.- Continued.

Figure 25.- Concluded.

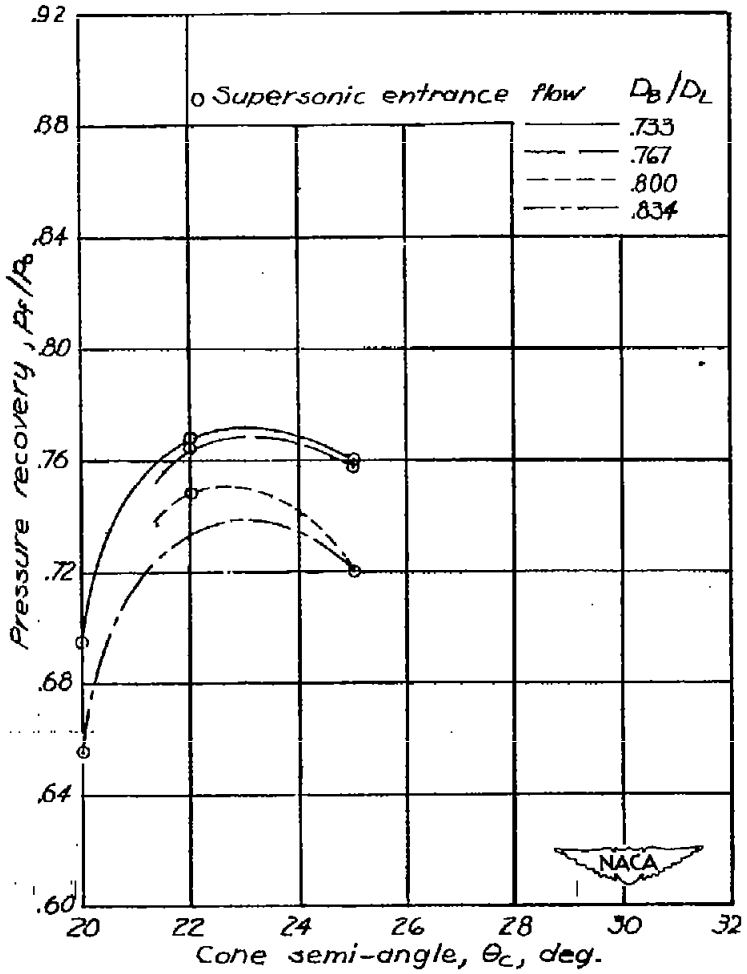

(a) 4°, 7° cowling.

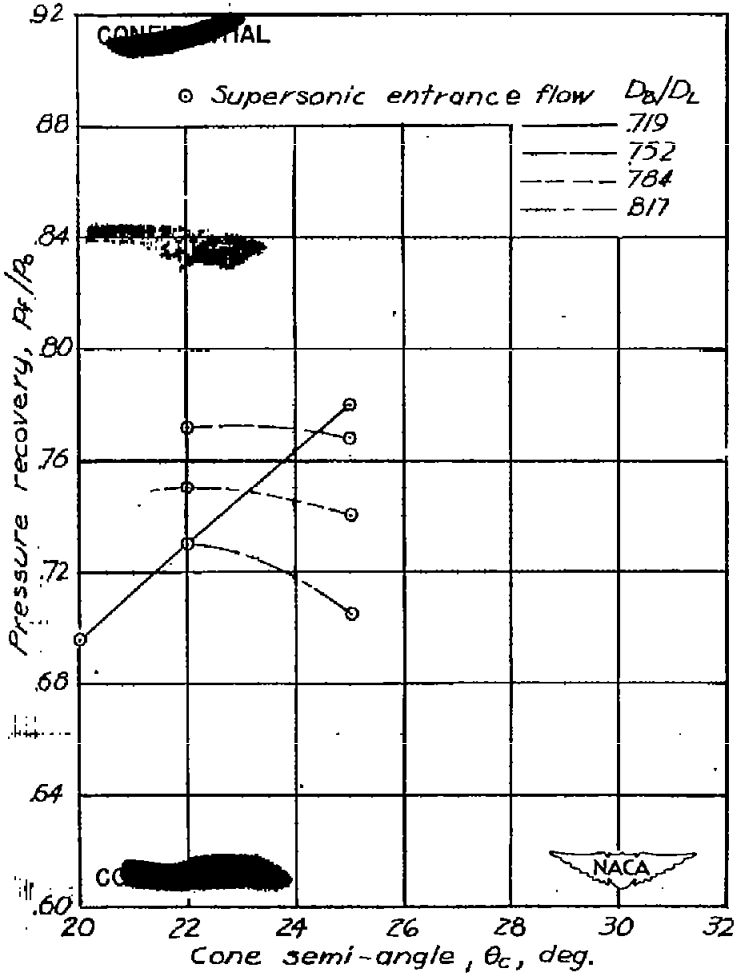

(b) 7°, 10° cowling.

Figure 26.- Highest pressure recovery obtained as a function of the cone semi-angle and central body diameter parameters for M = 2.45.

Figure 26.- Continued.

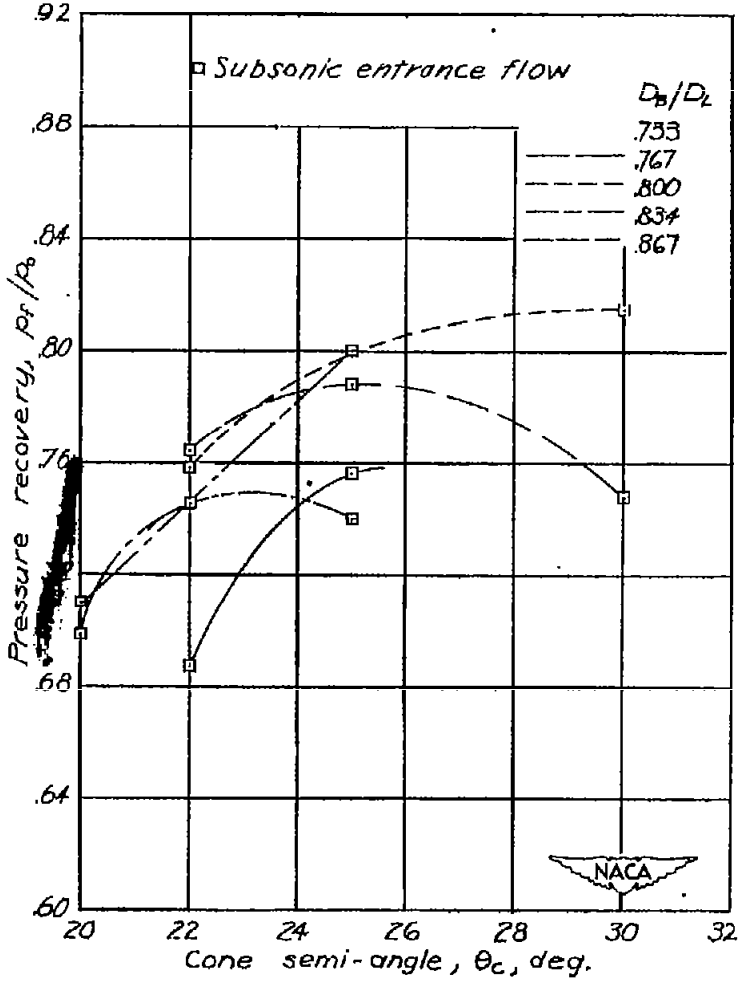

(c) 4°, 7° cowling.

Figure 26.- Continued.

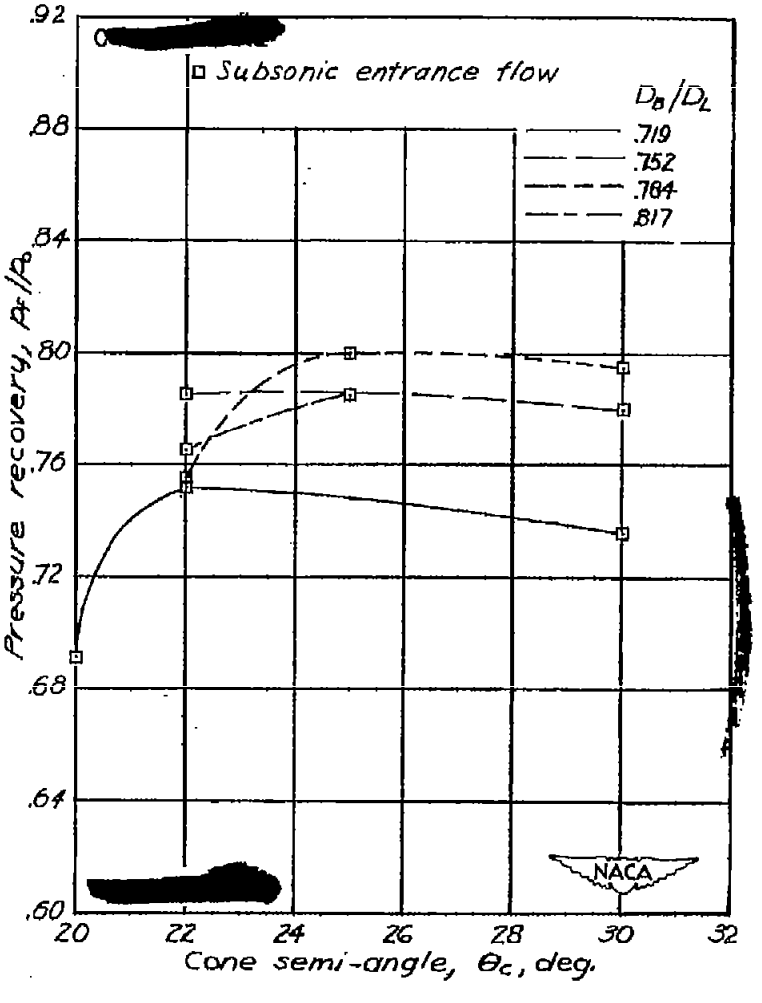

(d) 7°, 10° cowling.

Figure 26.- Concluded.

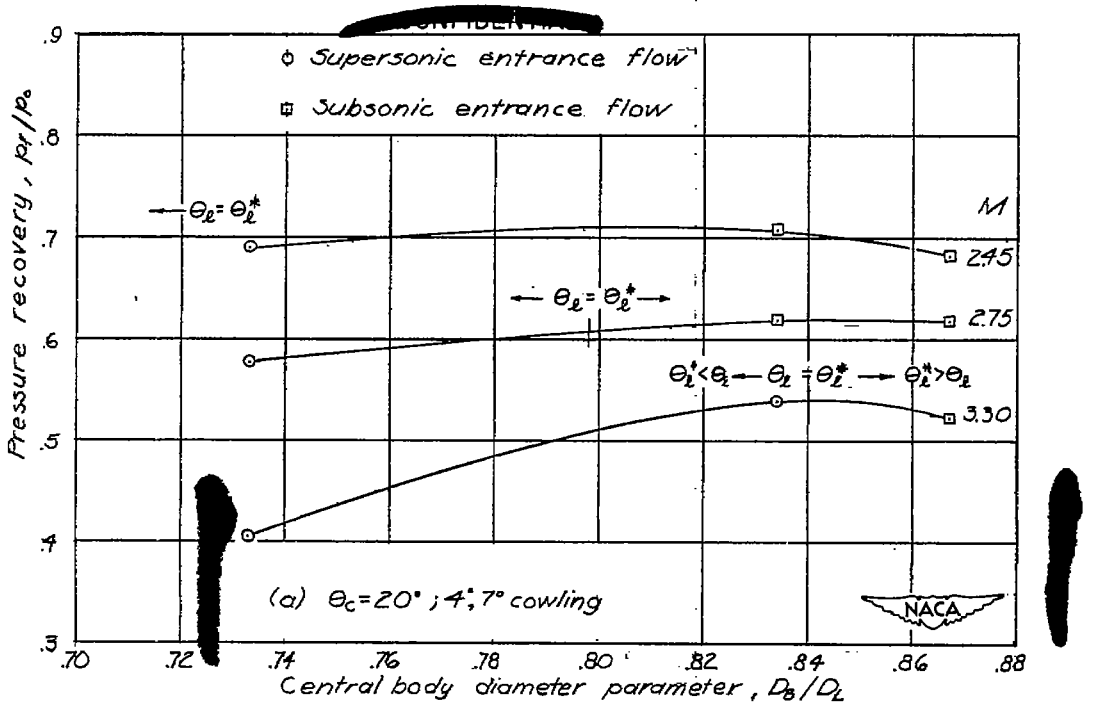

Figure 27.- Highest pressure recovery obtained as a function of the central-body diameter ratio for M = 3.30. (The maximum pressure recovery obtained at M = 2.75 and M = 2.45 for the same cowling position parameter are also shown.)

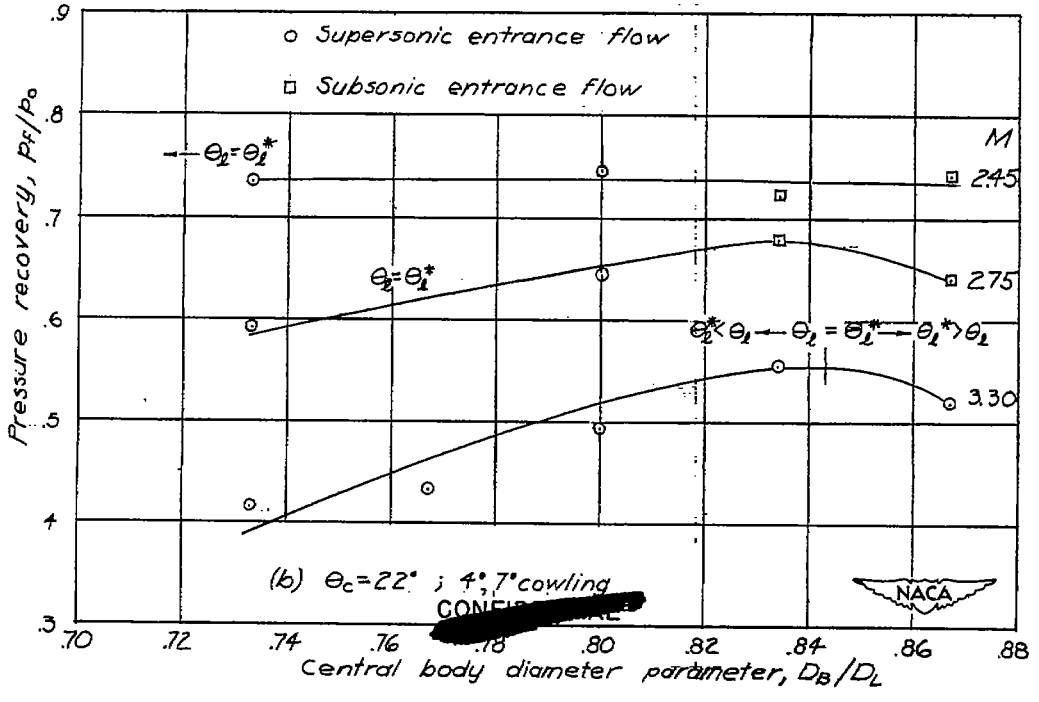

Figure 27.- Continued.

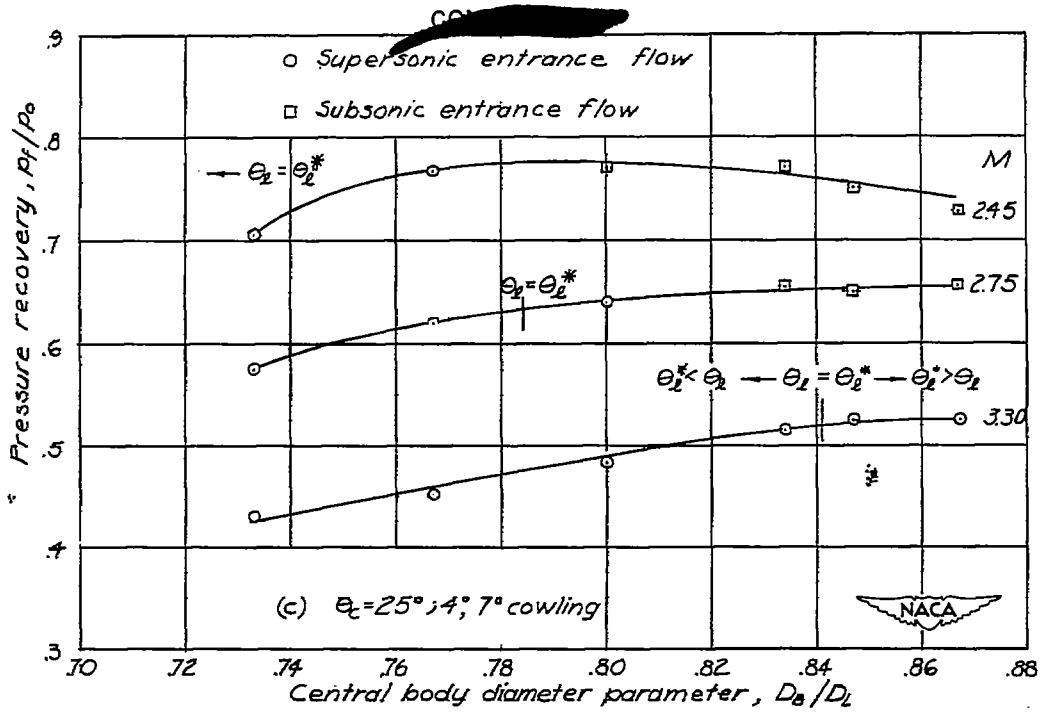

Figure 27.- Continued.

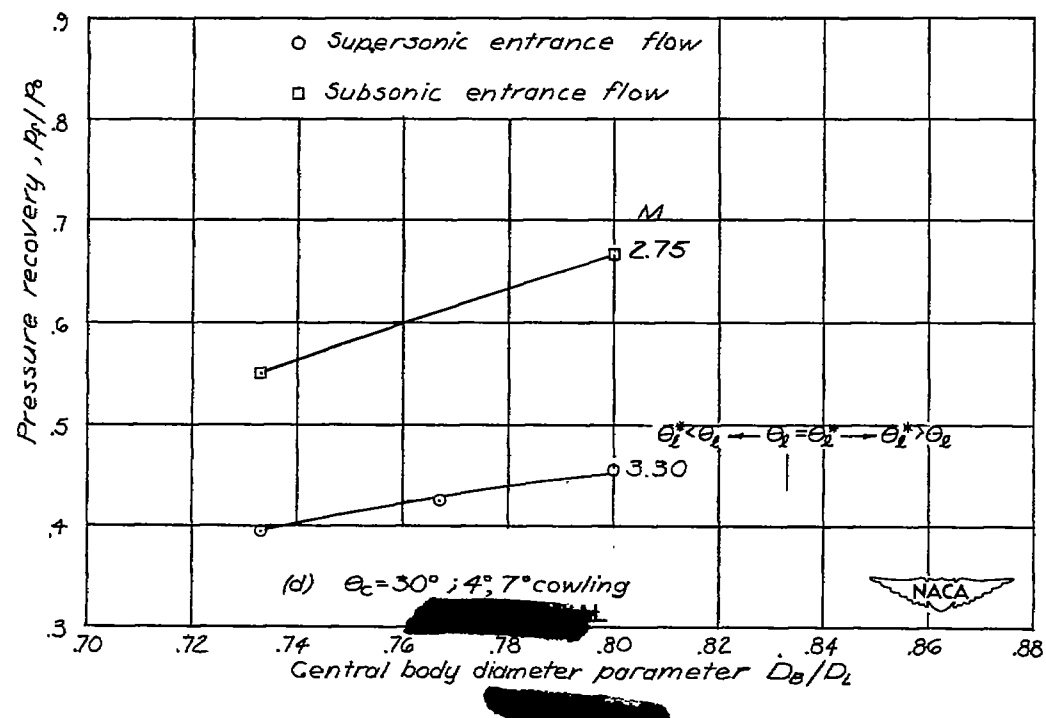

Figure 27.- Concluded.

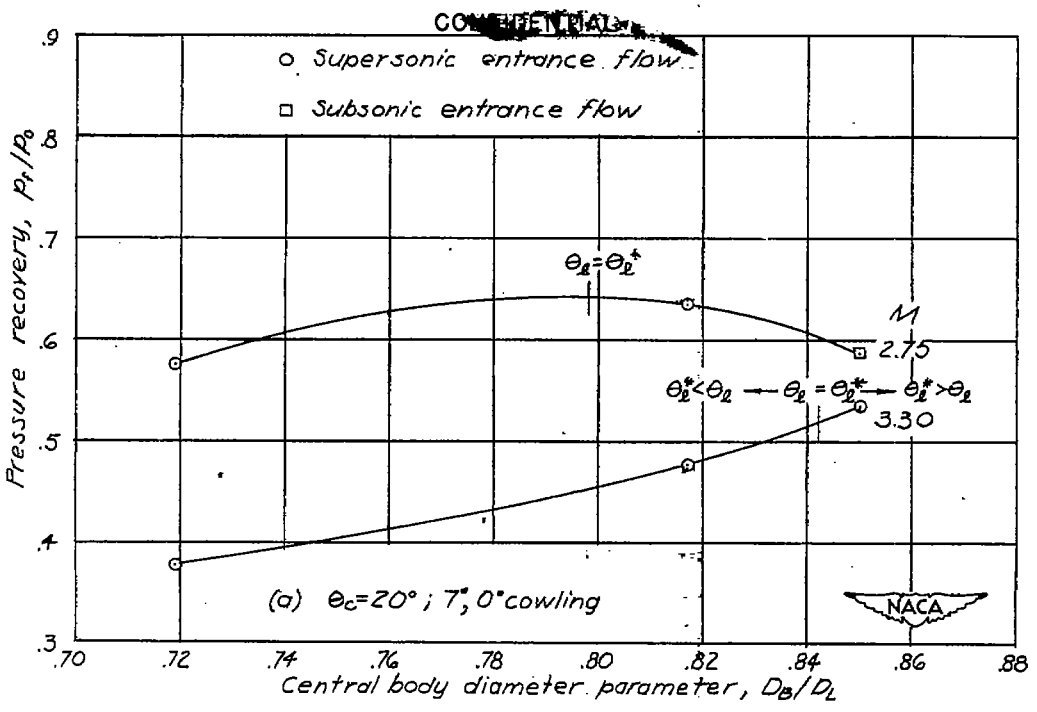

Figure 28.- Highest pressure recovery obtained as a function of the central-body diameter ratio for M = 3.30. (The maximum pressure recovery obtained at M = 2.75 and M = 2.45 for the same cowling position parameter are also shown.)

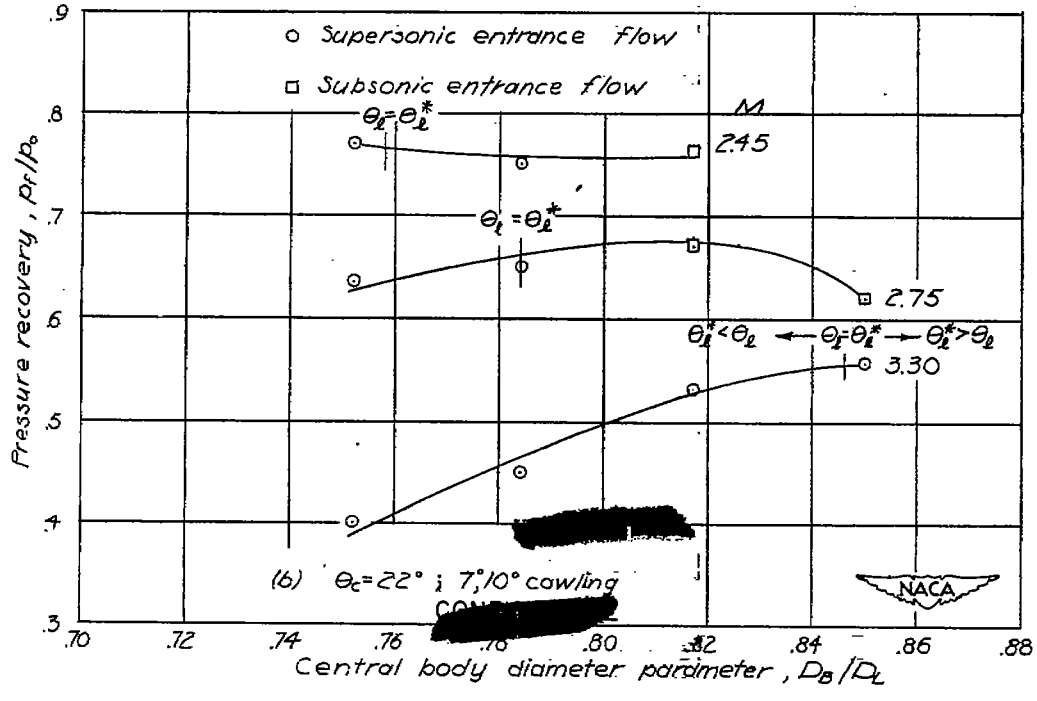

Figure 28.- Continued.

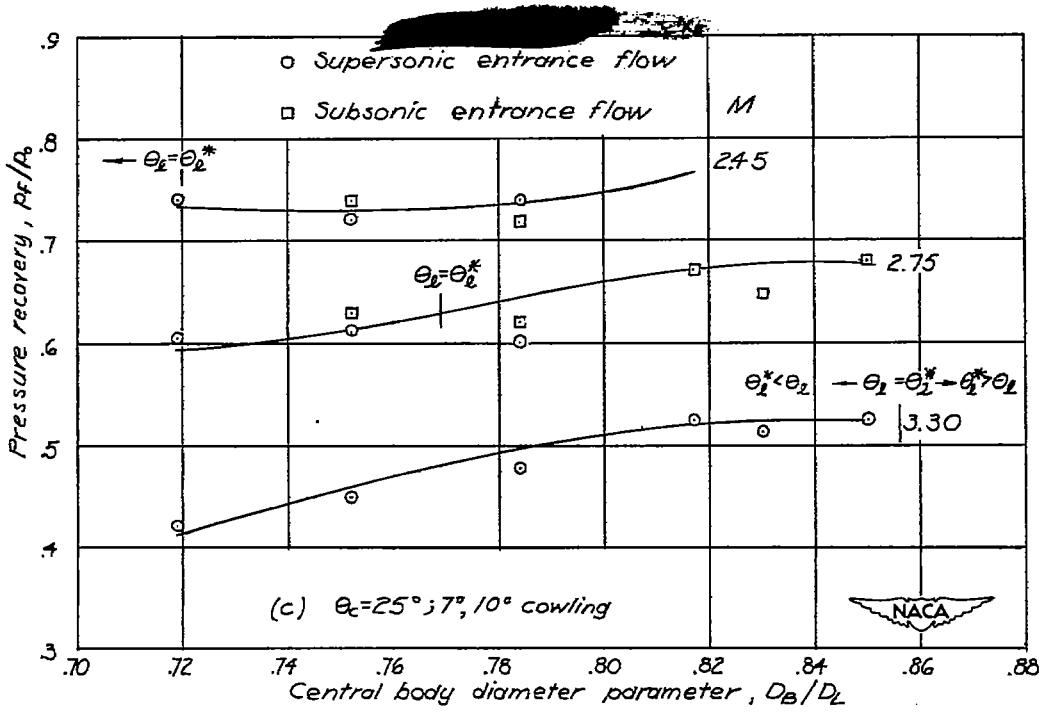

Figure 28.- Continued.

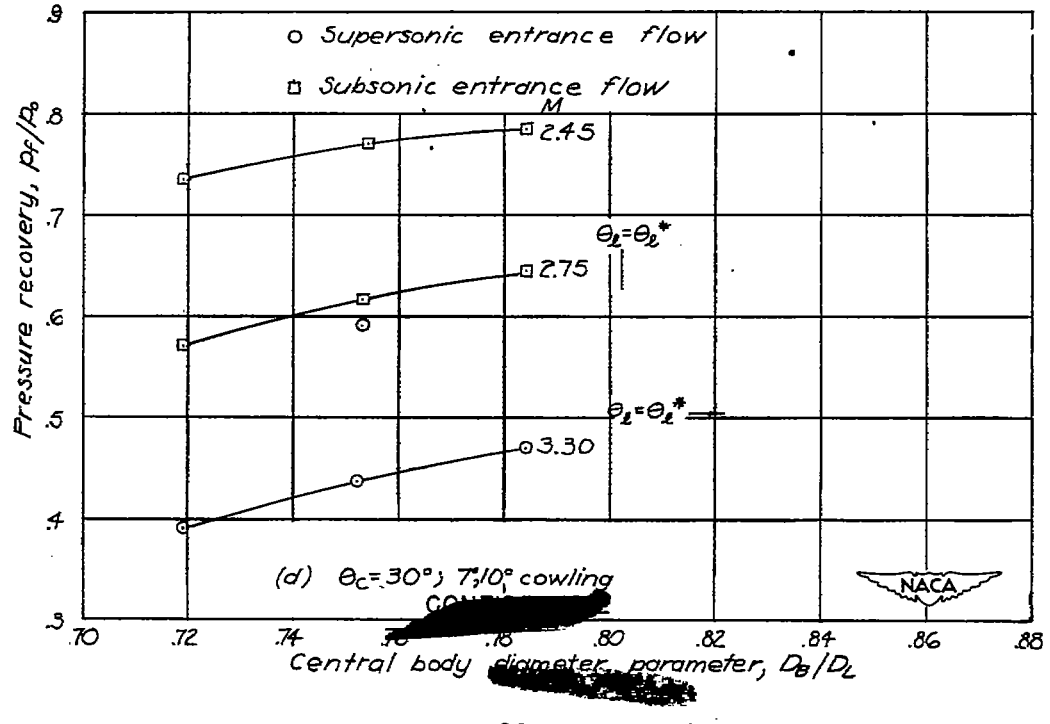

Figure 28.- Concluded.

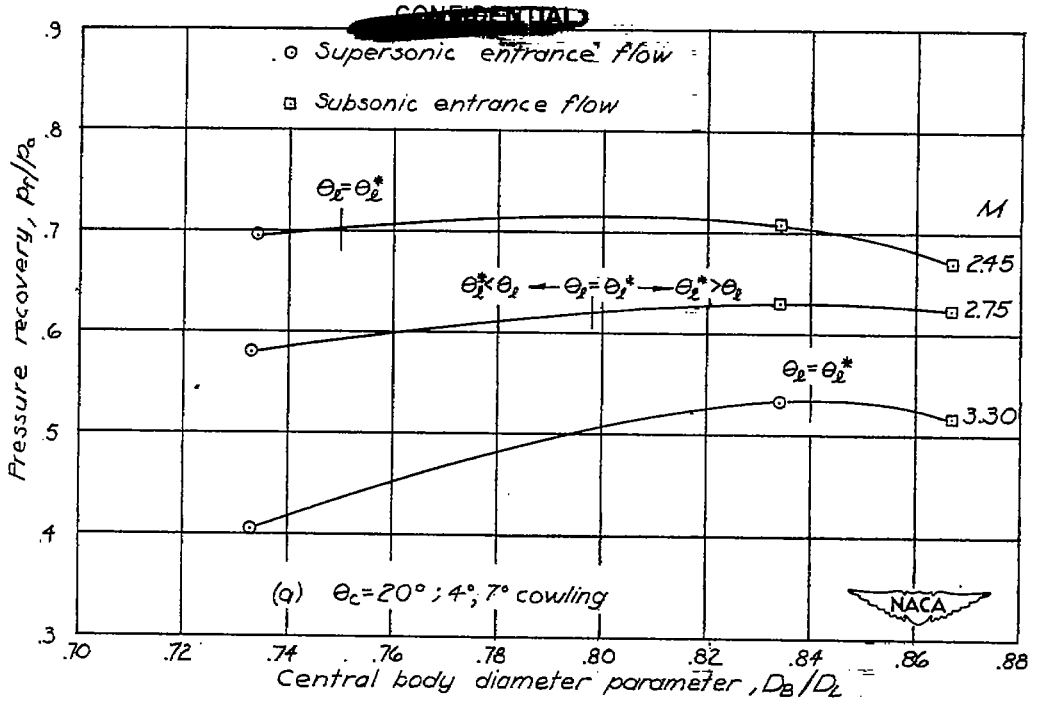

Figure 29.- Highest pressure recovery obtained as a function of the central-body diameter ratio for M = 2.75. (The maximum pressure recovery obtained at M = 3.30 and 2.45 for the same cowling position parameter are also shown.)

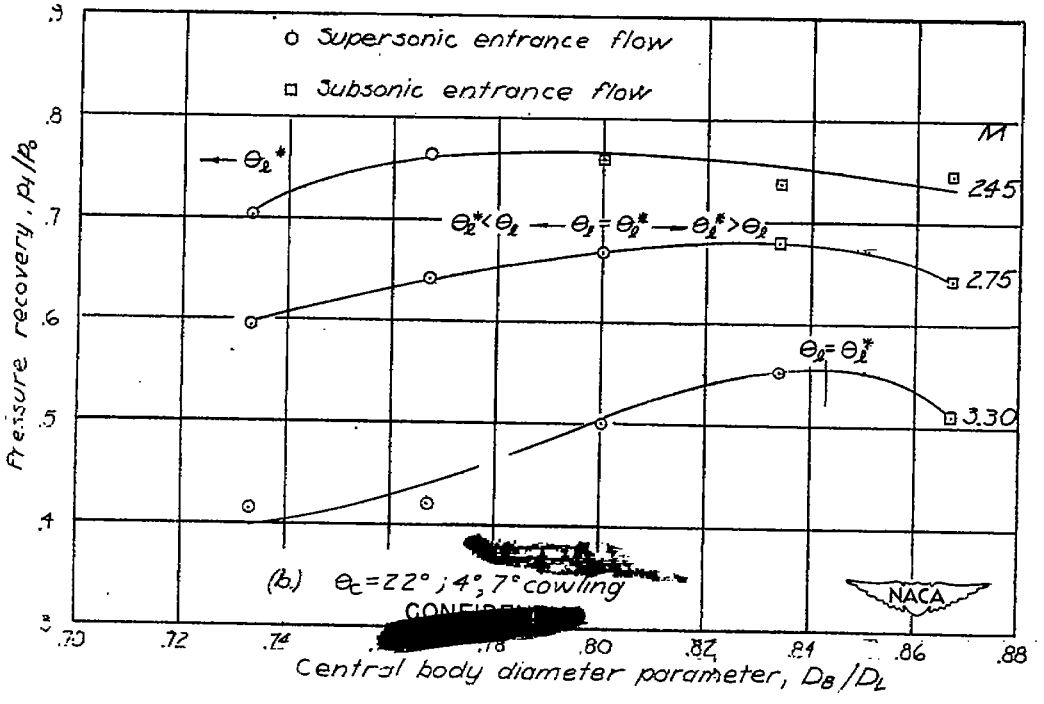

Figure 29.- Continued.

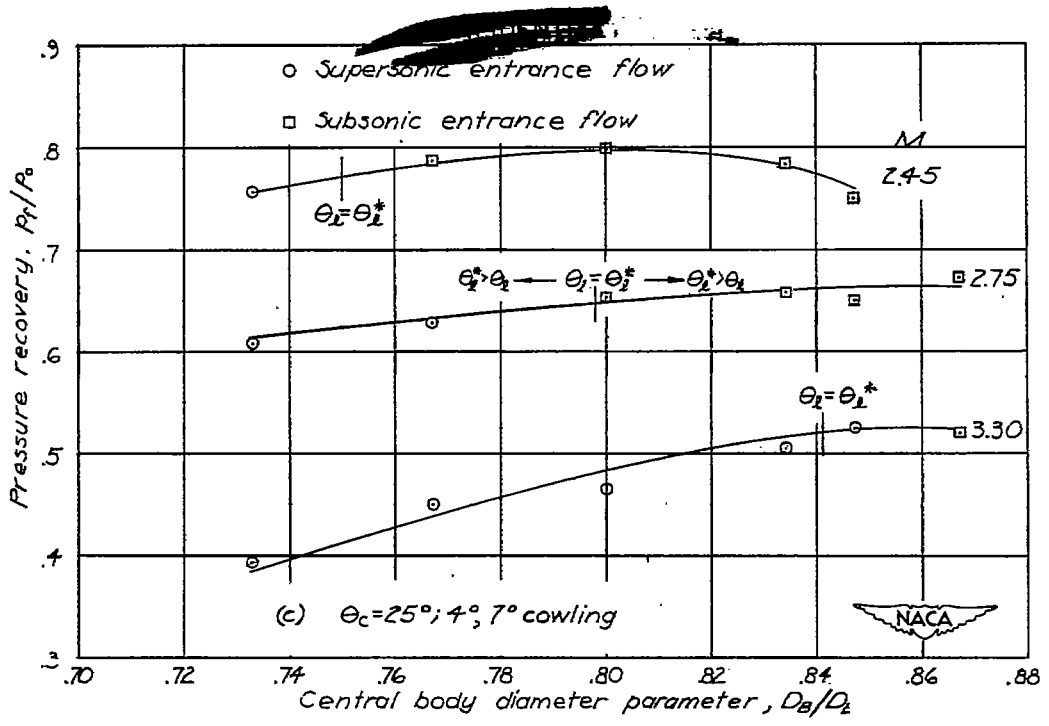

Figure 29.- Concluded.

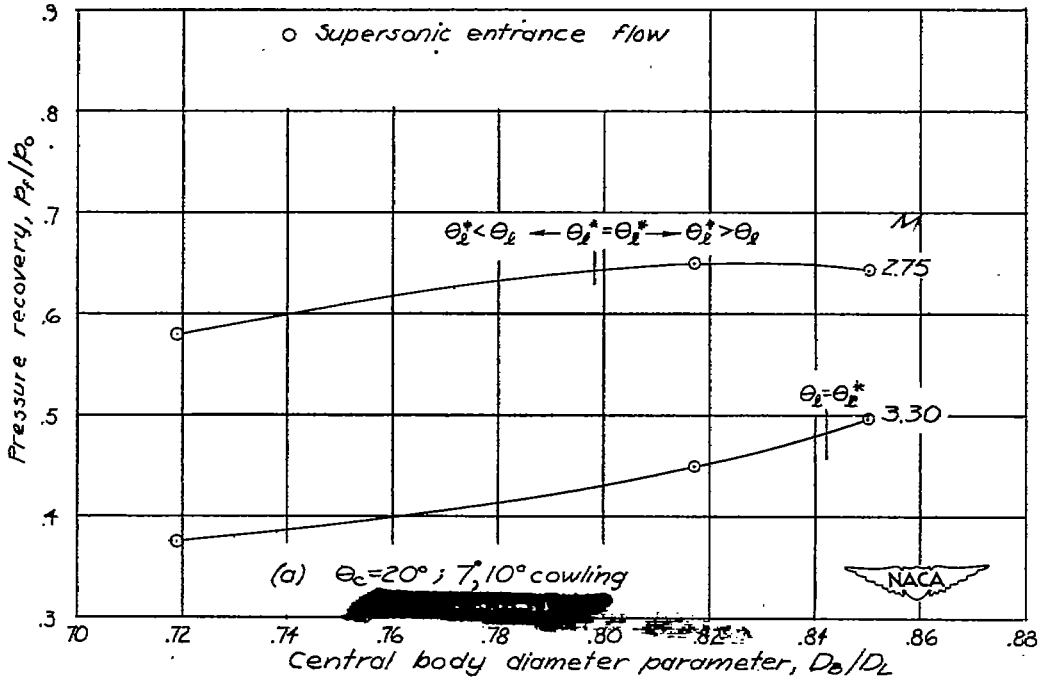

Figure 30.- Highest pressure recovery obtained as a function of the central-body diameter ratio for M = 2.75. (The maximum pressure recovery obtained at M = 3.30 and 2.45 for the same cowling position parameter are also shown.)

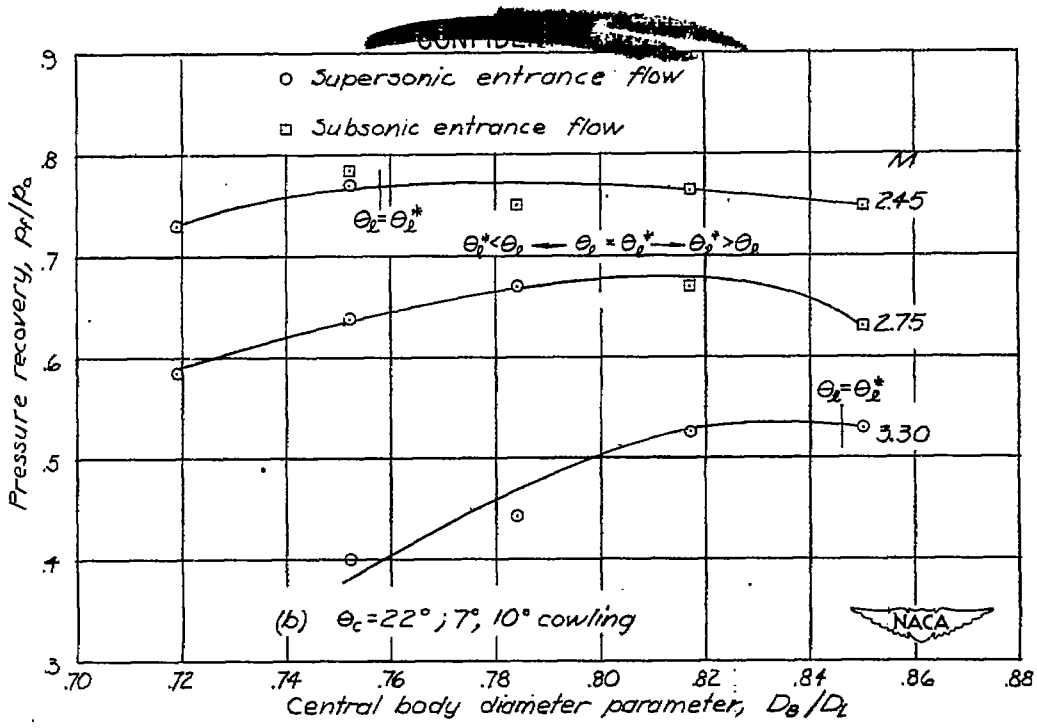

Figure 30.- Continued.

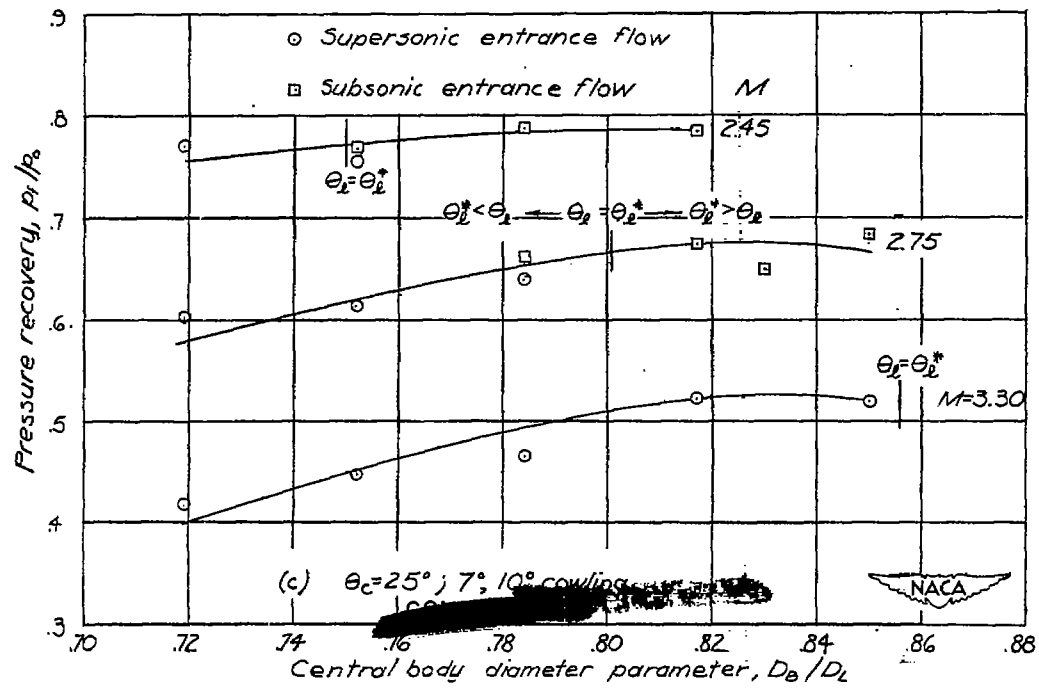

Figure 30.- Continued.

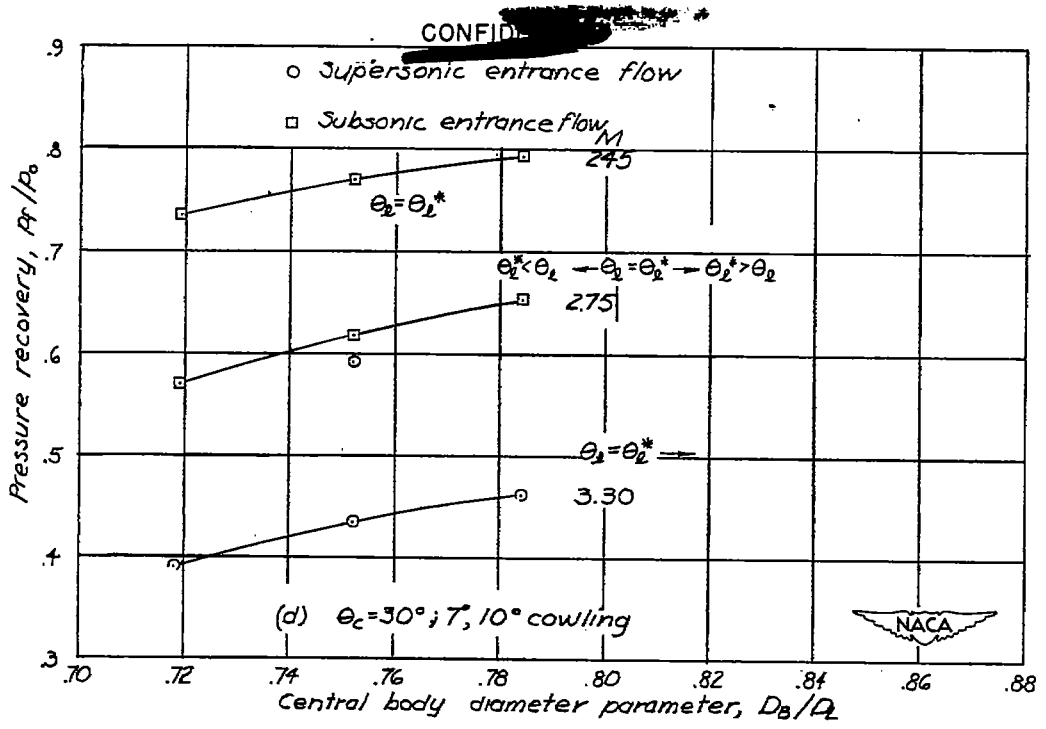

Figure 30.- Concluded.

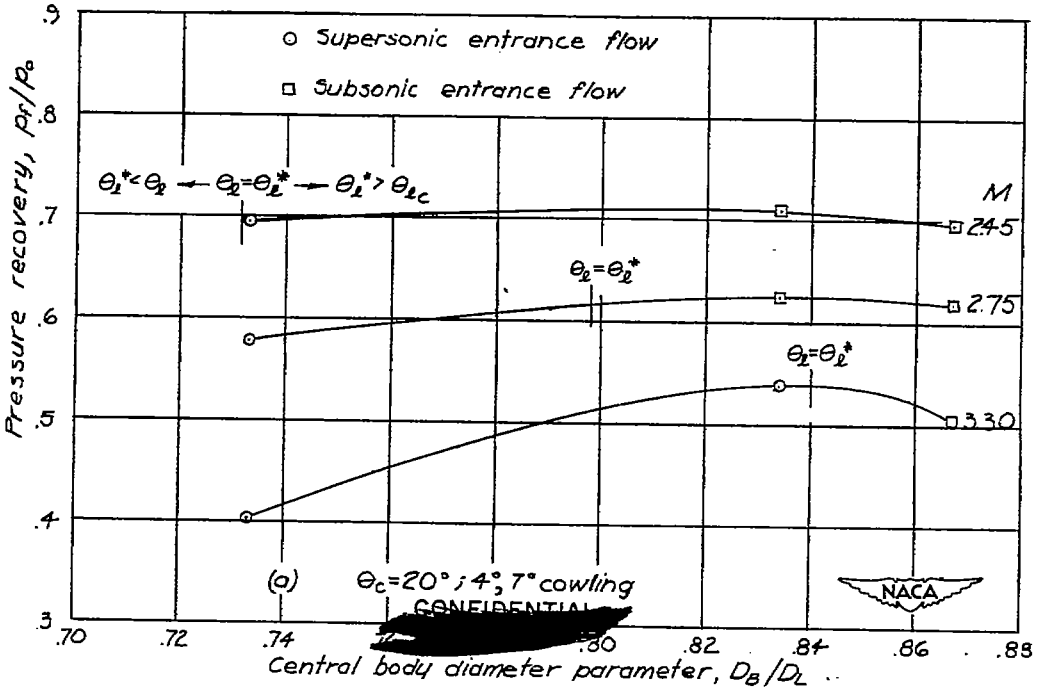

Figure 31.- Highest pressure recovery obtai[redacted] function of the central-body diameter ratio for M = 2.45. (The maximum pressure recovery obtained at M = 3.30 and M = 2.75 for the same cowling position parameter are also shown.)

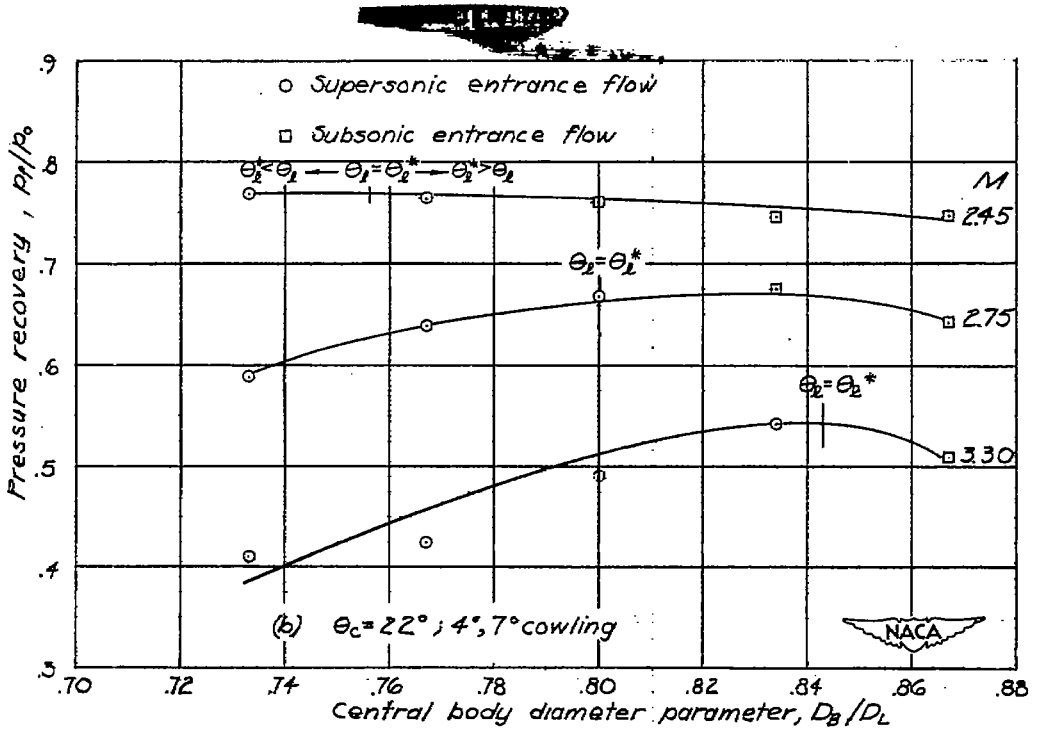

Figure 31.- Continued.

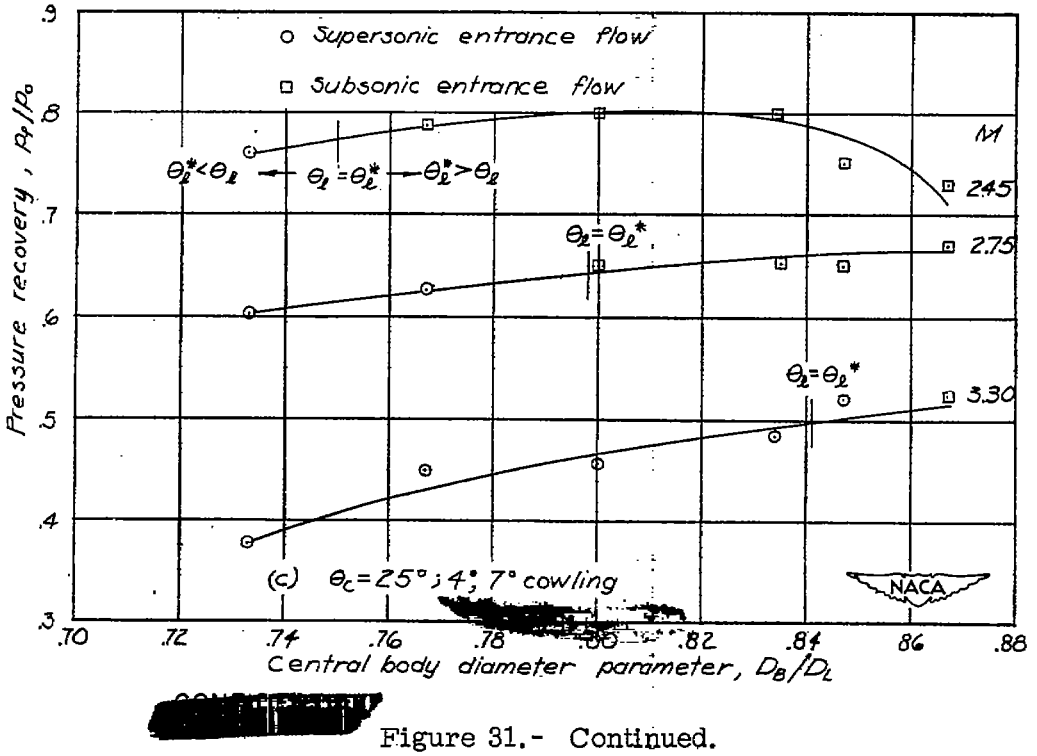

Figure 31.- Continued.

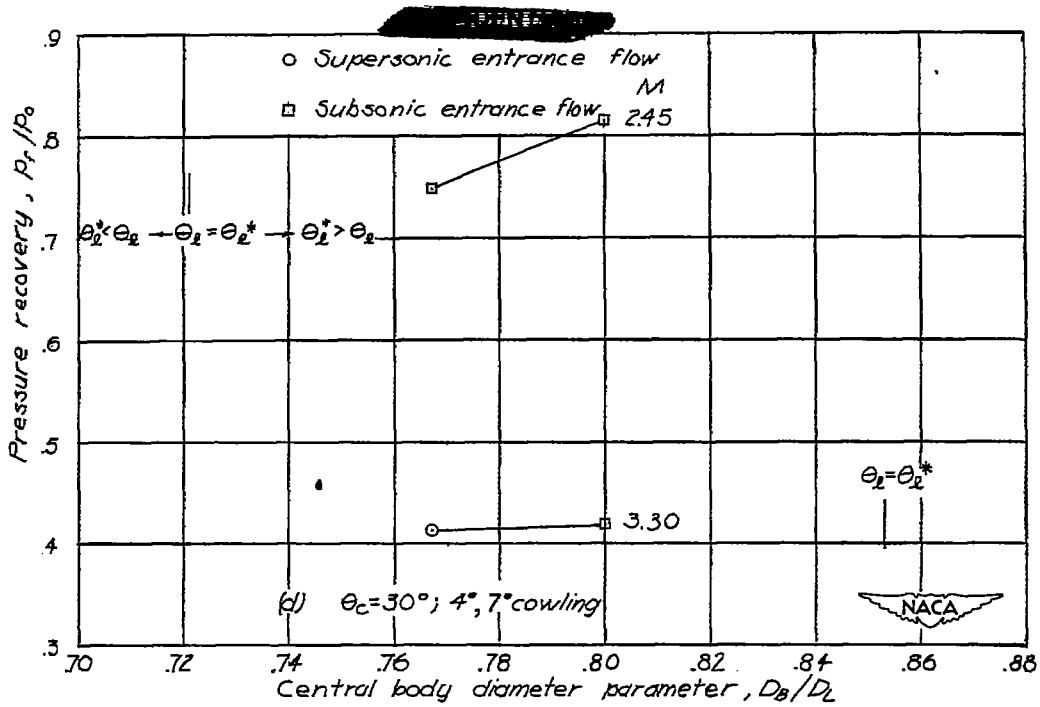

Figure 31.- Concluded.

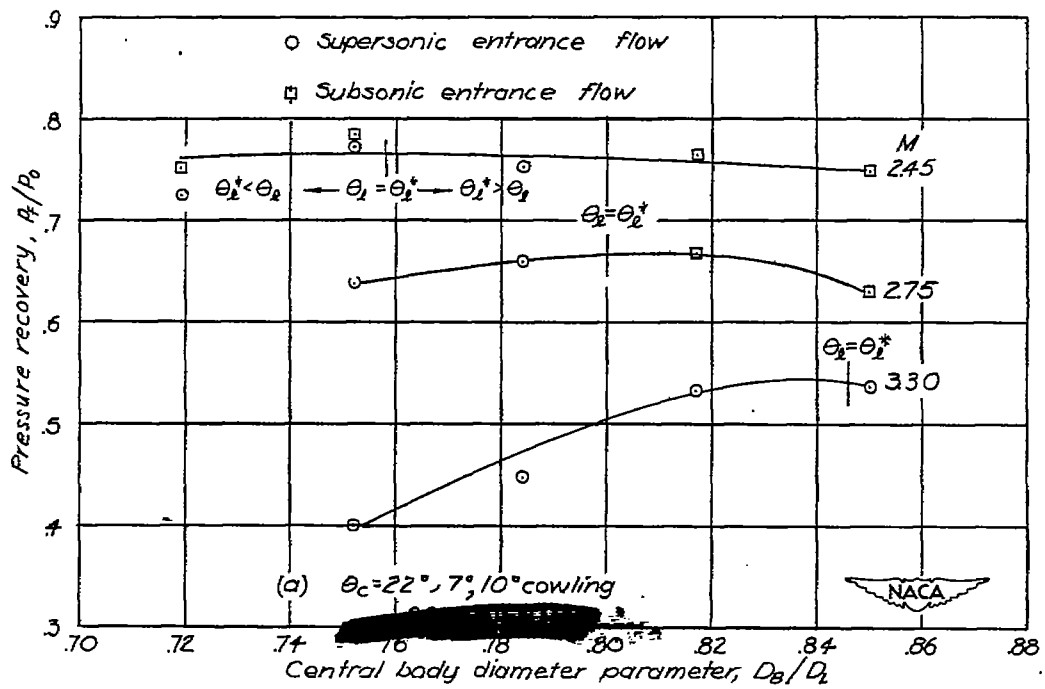

Figure 32.- Highest pressure recovery obtained as a function of the central-body diameter ratio for M = 2.45. (The maximum pressure recovery obtained at M = 3.30 and M = 2.75 for the same cowling position parameter are also shown.)

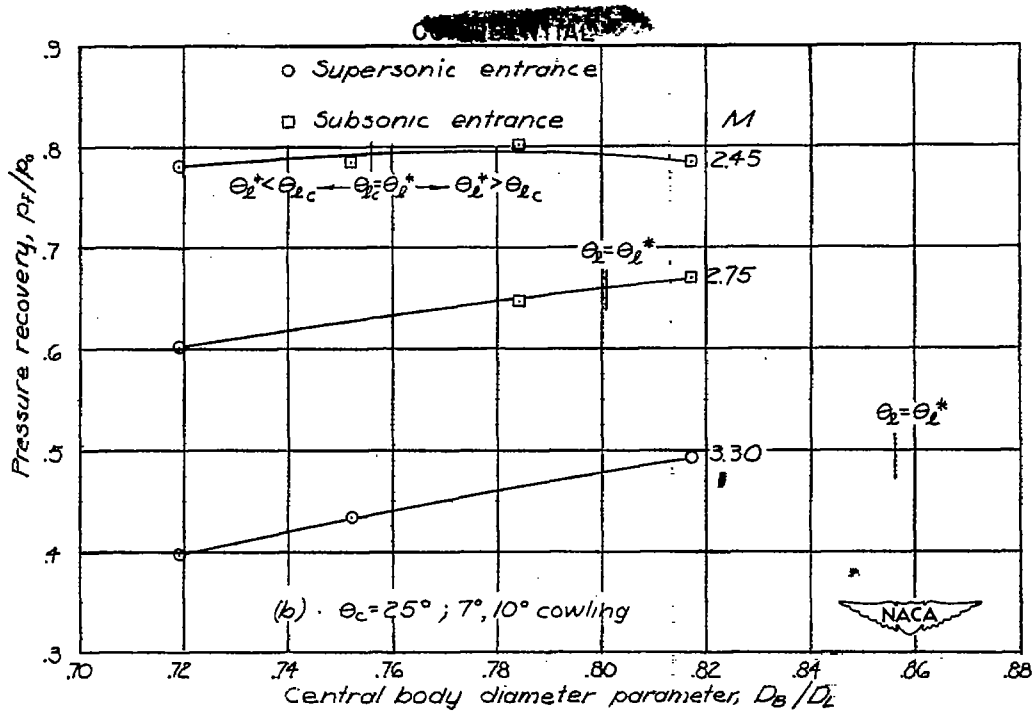

Figure 32.- Continued.

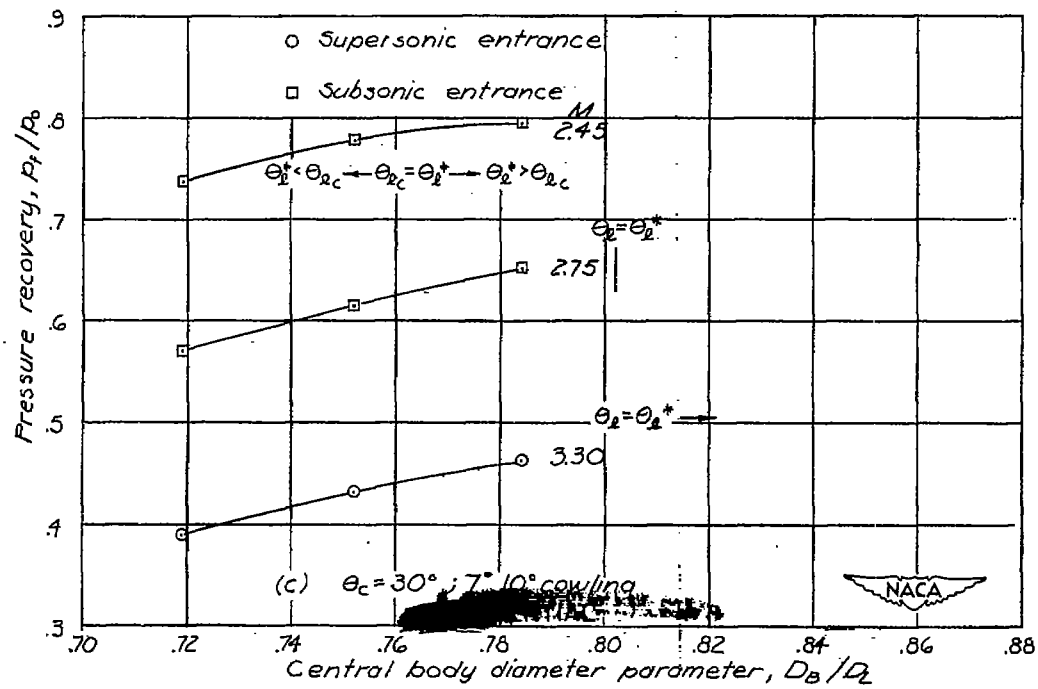

Figure 32.- Concluded.

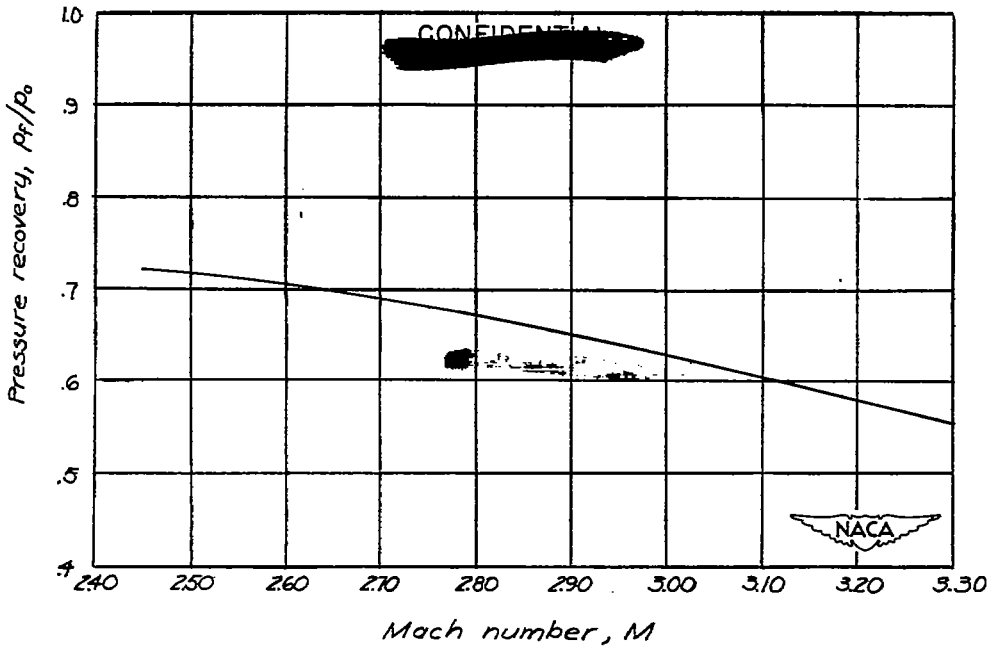

Figure 33.- Typical variation of pressure recovery with Mach number (model having $\theta_c = 22^\circ, 4^\circ, 7^\circ$ cowling, $\theta_l = 32.2^\circ$, and $D_B/D_L = 0.834$).

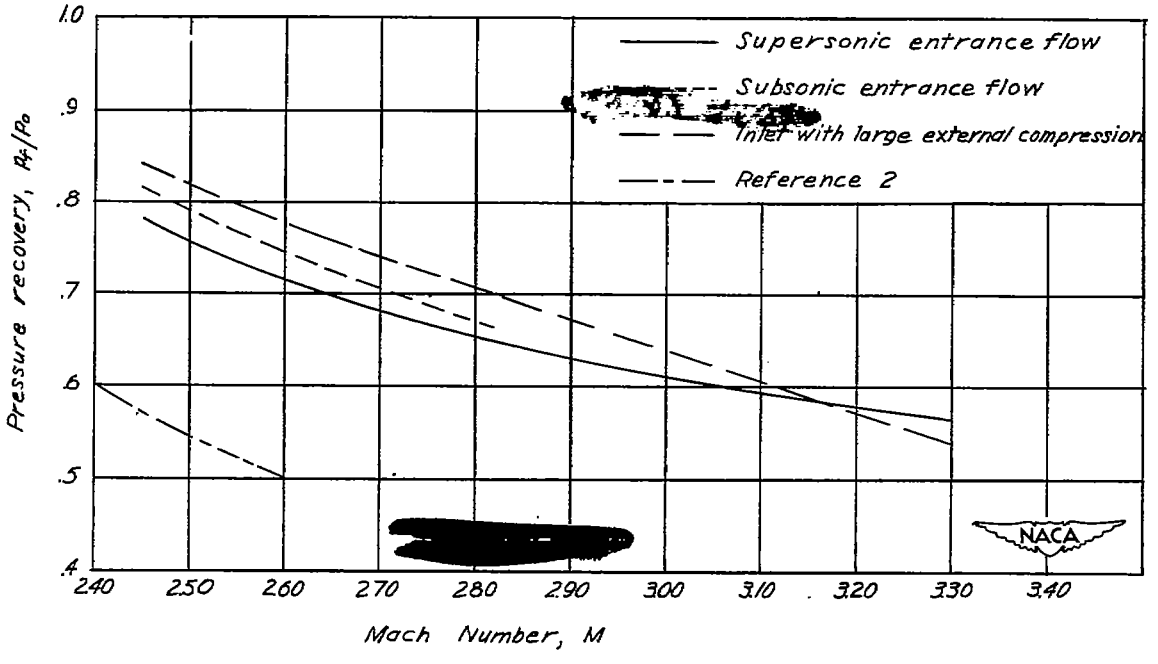

Figure 34.- Optimum pressure recovery obtained from all the configurations tested.

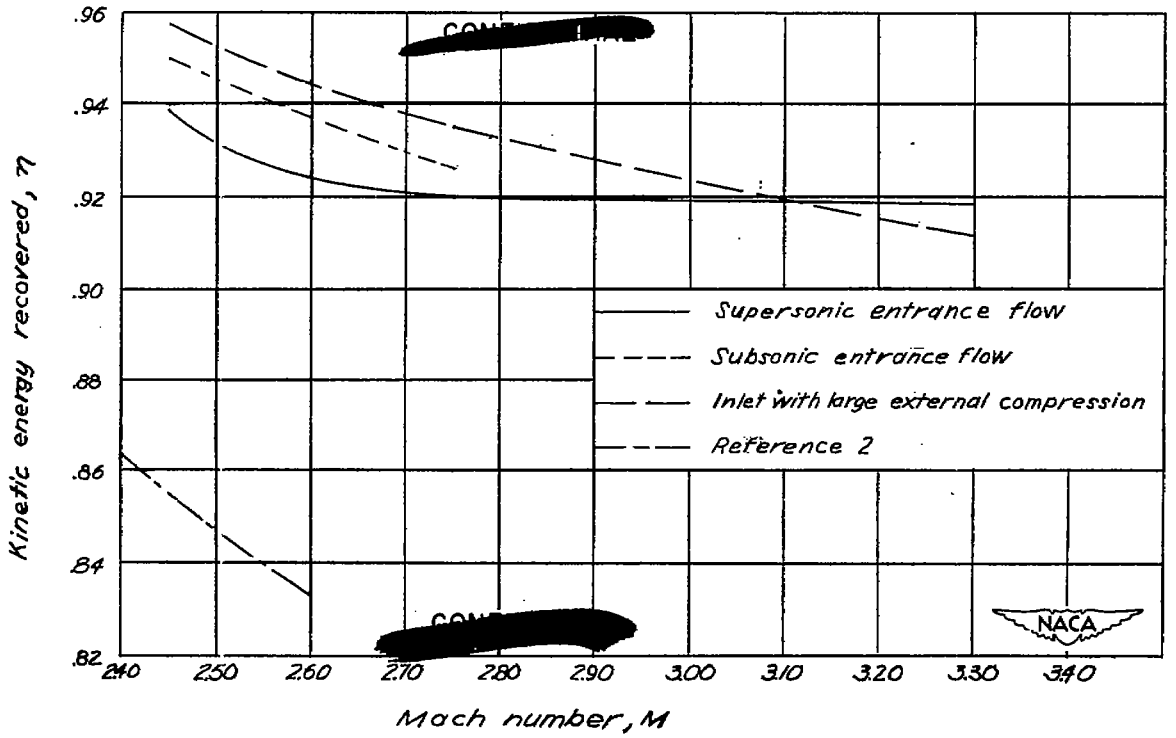

Figure 35.- Optimum kinetic energy recovery obtained from all the configurations tested.

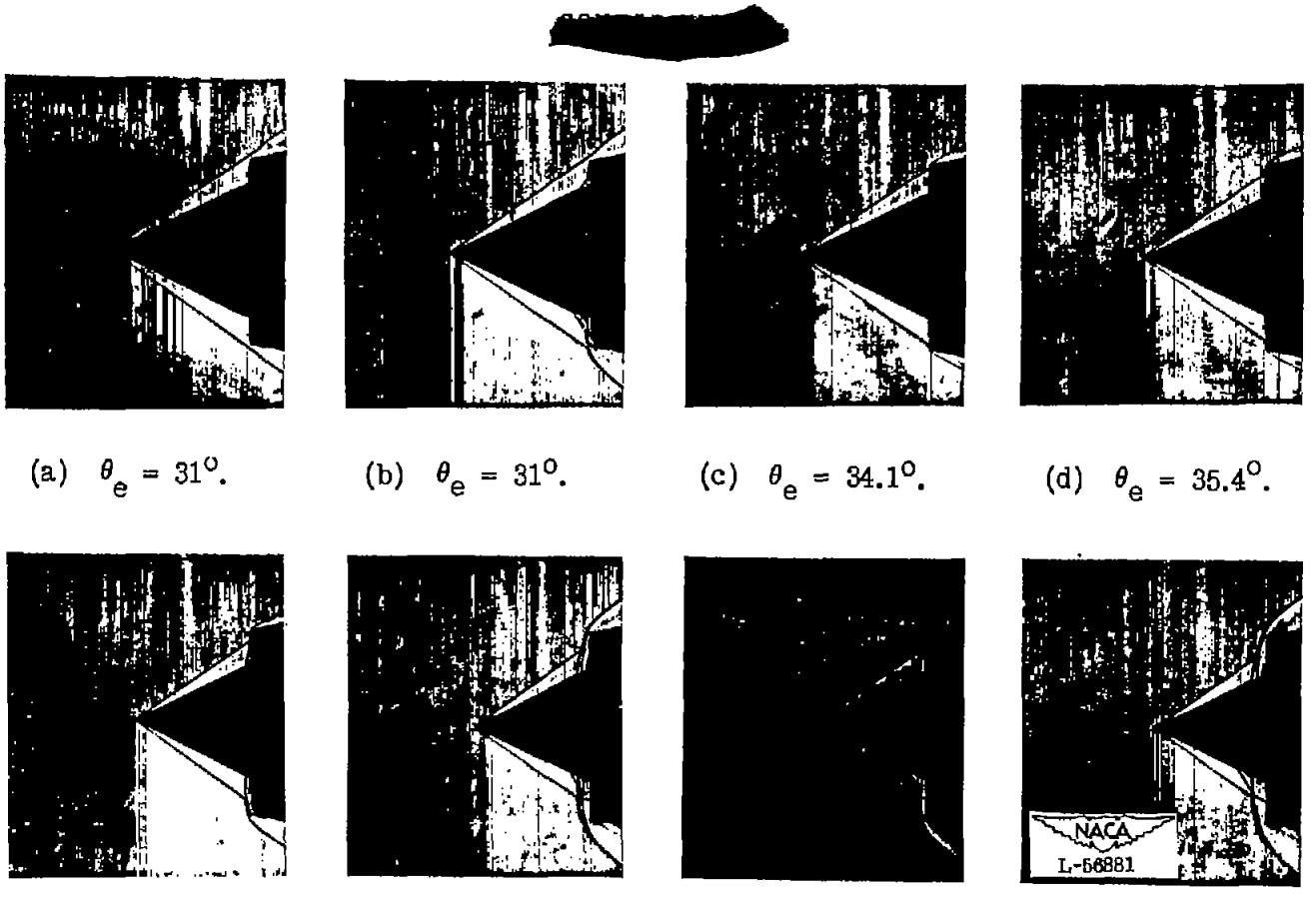

(a) $\theta_e = 31^\circ$. (b) $\theta_e = 31^\circ$. (c) $\theta_e = 34.1^\circ$. (d) $\theta_e = 35.4^\circ$.

(e) $\theta_e = 35.9^\circ$. (f) $\theta_e = 35.9^\circ$. (g) $\theta_e = 36.6^\circ$. (h) $\theta_e = 36.6^\circ$.

Figure 36.- Shadowgraphs of inlet configuration for $\theta_c = 25^\circ$, the 7°, 10° cowling and $D_B/D_L = 0.817$ for different values of θ_e for M = 3.30. (The corresponding values of pressure recovery are given in fig. 19(d).)

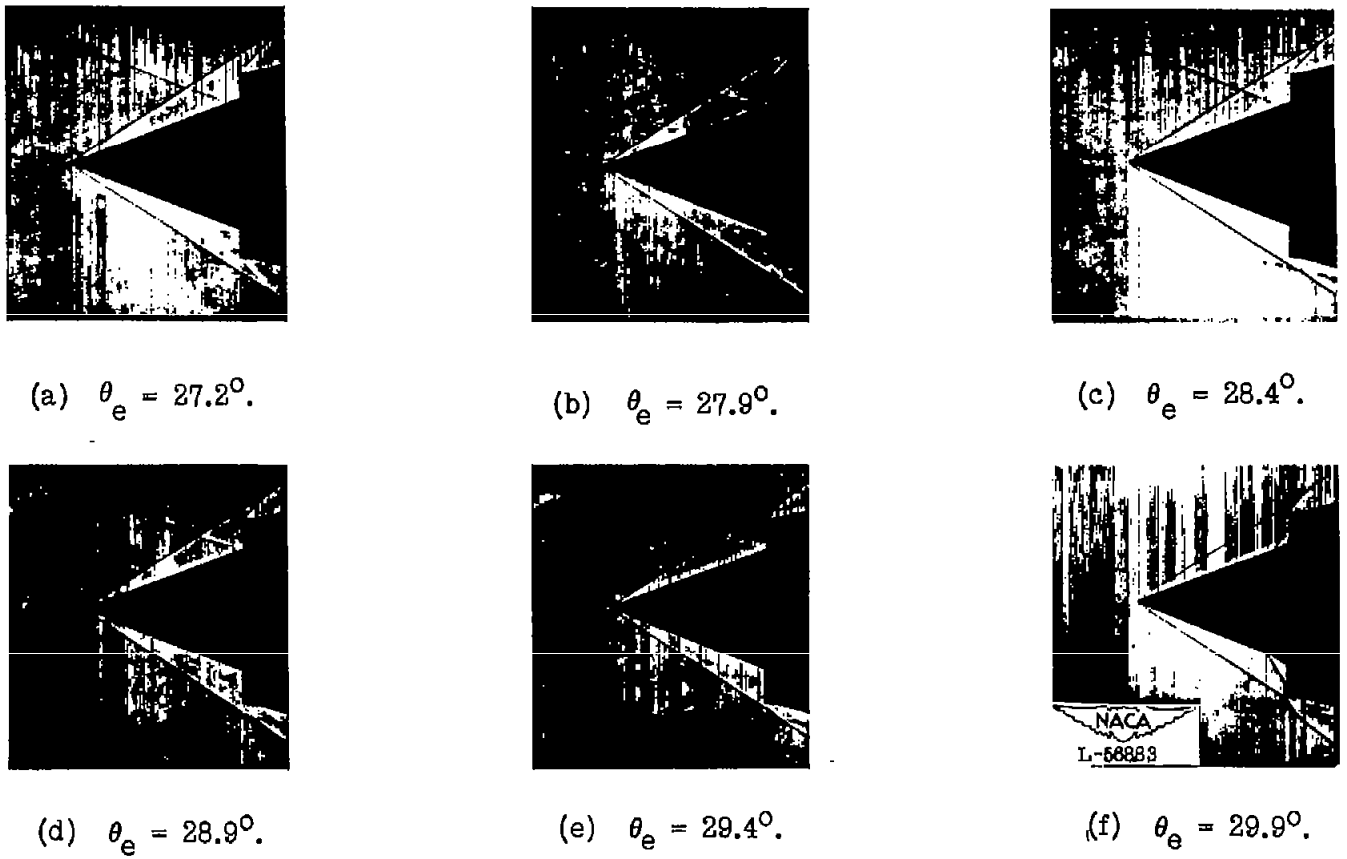

(a) $\theta_e = 27.2^\circ$.

(b) $\theta_e = 27.9^\circ$.

(c) $\theta_e = 28.4^\circ$.

(d) $\theta_e = 28.9^\circ$.

(e) $\theta_e = 29.4^\circ$.

(f) $\theta_e = 29.9^\circ$.

Figure 37.- Shadowgraphs of inlet configuration for $\theta_c = 20^\circ$, the 7°, 10° cowling and $D_B/D_L = 0.817$ for different values of θ_e for $M = 2.75$. (The corresponding values of pressure recovery are given in fig. 13(b).)

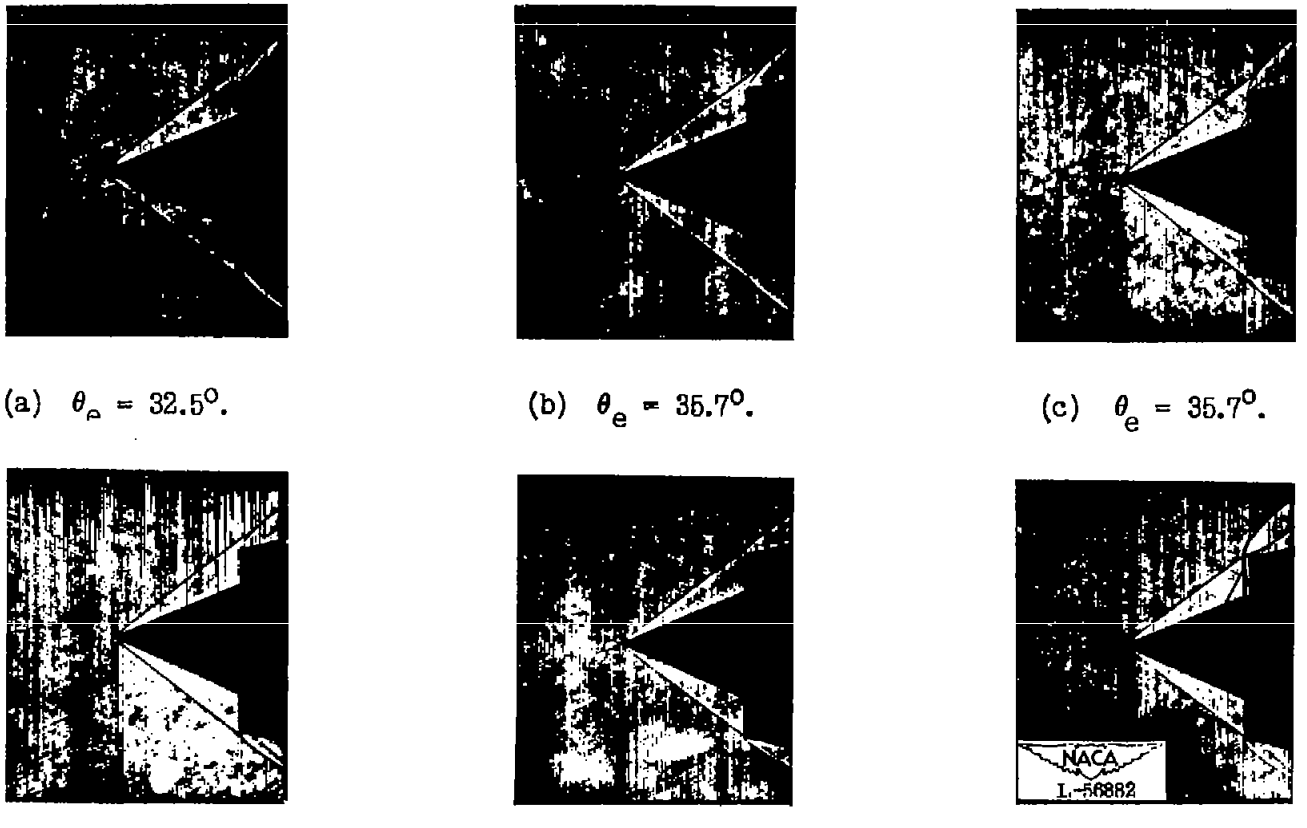

(a) $\theta_e = 32.5^\circ$.

(b) $\theta_e = 35.7^\circ$.

(c) $\theta_e = 35.7^\circ$.

(d) $\theta_e = 34.4^\circ$.

(e) $\theta_e = 35.1^\circ$.

(f) $\theta_e = 35.1^\circ$.

Figure 38.- Shadowgraphs of inlet configuration for $\theta_c = 22^\circ$, the 7°, 10° cowling and $D_B/D_L = 0.752$ for different values of θ_e for $M = 2.45$. (The corresponding values of pressure recovery are given in fig. 16(b).)

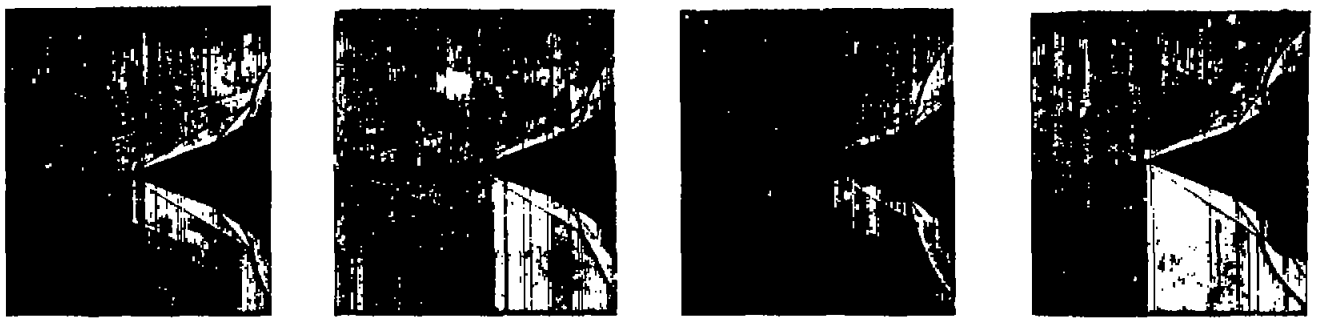

(a) $\theta_e = 28.9^\circ$; $M = 3.30$.

(b) $\theta_e = 30^\circ$; $M = 3.30$.

(c) $\theta_e = 30.3^\circ$; $M = 3.30$.

(d) $\theta_e = 30.5^\circ$; $M = 2.75$.

Inlet with large external compression

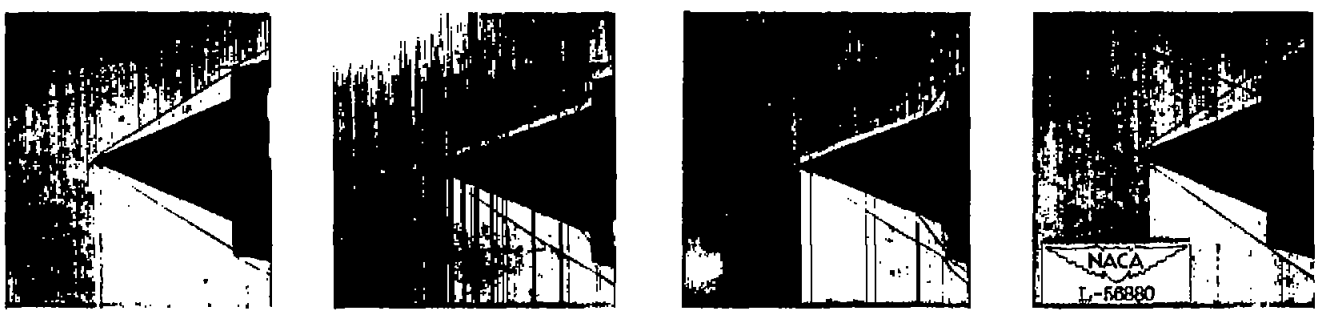

(e) $\theta_e = 31.4^\circ$; $M = 3.30$; $\theta_c = 22^\circ$; 7°, 10° cowling.

(f) $\theta_e = 31.4^\circ$; $M = 3.30$; $\theta_c = 20^\circ$; 4°, 7° cowling.

(g) $\theta_e = 30^\circ$; $M = 3.30$; $\theta_c = 20^\circ$; 4°, 7° cowling.

(h) $\theta_e = 32.9^\circ$; $M = 3.30$; $\theta_c = 22^\circ$; 7°, 10° cowling.

Figure 39.- Shadowgraphs of inlet configurations with large and small internal compression at $M = 3.30$ and $M = 2.75$.